DISSERTATIONES
TECHNOLOGIAE
UNIVERSITATIS
TARTUENSIS
92

RAUNO SEDRIK

Synthesis and investigation of polymers from different cyclic bio-based monomers

DISSERTATIONES TECHNOLOGIAE UNIVERSITATIS TARTUENSIS
92

DISSERTATIONES TECHNOLOGIAE UNIVERSITATIS TARTUENSIS
92

RAUNO SEDRIK

Synthesis and investigation of polymers from different cyclic bio-based monomers

UNIVERSITY OF TARTU
Press
1632

Institute of Technology, Faculty of Science and Technology, University of Tartu, Estonia

This dissertation was accepted for the commencement of the degree of Doctor of Philosophy in Engineering of Bioactive Compounds on 23.01.2025 by the Joint Council of the Doctoral Program of Engineering and Technology of the University of Tartu.

Supervisors: Lauri Vares, PhD
Associate Professor of Organic Chemistry
Institute of Technology, Faculty of Science and Technology
University of Tartu, Estonia

Patric Jannasch, PhD
Visiting Professor
Institute of Technology, Faculty of Science and Technology
University of Tartu, Estonia
Professor of Polymer Technology
Department of Chemistry, Faculty of Science
Lund University, Sweden

Reviewer: Dzmitry Kananovich, PhD
Senior Research Scientist
Division of Chemistry, Department of Chemistry and Biotechnology School of Science Tallinn University of Technology, Estonia

Opponent: Jonathan Potier, PhD
Associate Professor of Organic Chemistry
Department of Chemistry, Faculty of Sciences
University of Lille, France

Commencement: Auditorium 121, Nooruse 1, Tartu, Estonia, at 13.15 on February 19th, 2025

Publication of this thesis is granted by the Institute of Technology, Faculty of Science and Technology, University of Tartu.

ISSN 2228-0855 (print)
ISBN 978-9916-27-797-3 (print)
ISSN 2806-2620 (pdf)
ISBN 978-9916-27-798-0 (pdf)

University of Tartu Press
www.tyk.ee

ABSTRACT

The current demand for plastics is increasing rapidly; therefore, the need for sustainable feedstock for the polymer industry is also critical. Fossil feedstock is currently dominating because of low prices due to years of optimization and large-scale production. On the other hand, using naphtha as a carbon source comes with high CO_2 emissions that contribute to global warming.

Alternatively, bio-based feedstocks can alleviate this problem by contributing to a more circular carbon economy that should rival its fossil counterpart. Sadly, most bio-based polymers do not have good enough properties compared to mainstream polymers, like polyethylene (PE), polypropylene (PP), and polystyrene (PS), and therefore lack a competitive edge on the polymer market.

In this thesis, several bio-based compounds, such as citric acid, isosorbide, and vanillic acid, are converted into (meth)acrylate monomers. The obtained monomers are further converted into thermoplastic polymers using free radical polymerization and base-catalyzed thiol-arylate polymerization. Additionally, chemical recycling possibilities and life-cycle analysis are investigated.

TABLE OF CONTENTS

LIST OF PUBLICATIONS

This thesis is based on the following publications. The articles are referred to in the text using Roman numerals:

I. **Sedrik, R**.; Bonjour, O.; Laanesoo, S.; Liblikas, I.; Pehk, T.; Jannasch, P.; Vares, L. Chemically Recyclable Poly(β-Thioether Ester)s Based on Rigid Spirocyclic Ketal Diols Derived from Citric Acid. *Biomacromolecules* **2022**, *23*, 2685–2696.

II. Matt, L.; **Sedrik, R**.; Bonjour, O.; Vasiliauskaité, M.; Jannasch, P.; Vares, L. Covalent Adaptable Polymethacrylate Networks by Hydrazide Crosslinking Via Isosorbide Levulinate Side Groups. *ACS Sustain. Chem. Eng.* **2023**, *11*, 8294–8307.

III. de Souza, N. R. D.; Matt, L.; **Sedrik, R**.; Vares, L.; Cherubini, F. Integrating Ex-Ante and Prospective Life-Cycle Assessment for Advancing the Environmental Impact Analysis of Emerging Bio-Based Technologies. *Sustain. Prod. Consum.* **2023**, *43*, 319–332.

IV. **Sedrik, R**.; Bonjour, O.; de Souza, N. R. D.; Ismagilova, A.; Tamsalu, I.; Kisand, V.; Cherubini, F.; Jannasch, P.; Vares, L. Aromatic Polymethacrylates from Lignin-Based Feedstock: Synthesis, Thermal Properties, Life-Cycle Assessment and Toxicity. *ChemSusChem* **2024**, e202401239.

V. **Sedrik, R**; Mitrovich, I; Bonjuor, O; Jannasch, P; Vares, L. High-T_g Poly(meth)acrylates from Indolines. (unfinished manuscript).

Articles not included in the thesis.

VI. Laanesoo, S.; Bonjour, O.; **Sedrik, R**.; Tamsalu, I.; Jannasch, P.; Vares, L. Combining Isosorbide and Lignin-Related Benzoic Acids for High-T_g Polymethacrylates. *Eur. Polym. J.* **2024**, *202*, 112595.

VII. Tarasova, E.; Savale, N.; Trifonova, L.; Krasnou, I.; Reile, I.; Kudrjašova, M.; Mere, A.; Kaljuvee, T.; Mikli, V.; **Sedrik, R**.; Krumme, A. Effect of Green Co-Solvents on Properties and Synthesis of Cellulose Esters in Superbase Ionic Liquid. *Cellulose* **2024**, 31.

Author contributions

Paper I: Performed half of the monomer synthesis and polymerization experiments. Conducted degradation experiments and prepared the first draft of the manuscript and supporting information.

Paper II: Performed half of the thermal analysis measurements. Performed additional measurements and analysis of polymers after initial review. Contributed to the preparation of the manuscript.

Paper III: Provided a part of the experimental data needed for life-cycle assessment and participated in the preparation of the manuscript and supporting information.

Paper IV: Performed all the monomer synthesis and polymerization experiments. Performed some of the thermal analysis measurements. Prepared the first draft of the manuscript and supporting information.

Paper V: Performed all the monomer synthesis and polymerization experiments. Prepared the first draft of the manuscript.

Paper VI: Performed and supervised some initial experiments and participated in the preparation of the manuscript and supporting information.

Paper VII: Performed GPC measurements.

ABBREVIATIONS

2-MeTHF	2-methyltetrahydrofuran
5-IMA	isosorbide-5-methacrylate
AIBN	azobisisobutyronitrile
butA	butyl acrylate
Đ	polydispersity index
DBU	1,8-diazabicyclo[5.4.0]undec-7-en
DMA	dynamic mechanical analysis
DMAP	4-dimethylaminopyridine
DMF	dimethylformamide
DMSO	dimethyl sulfoxide
DSC	differential scanning calorimetry
ESI	electron spray ionization
Et	ethyl
EtOAc	ethyl acetate
FRP	free radical polymerization
FTIR	Fourier's transformation infrared spectroscopy
GVL	γ-valerolactone
GWP	global warming potential
HQ	hydroquinone
HRMS	high-resolution mass-spectrometry
LCA	life-cycle analysis
LCB	lignocellulosic biomass
Me	methyl
M_n	number average molecular mass
MTBE	methyl *tert*-butyl ether
MTT	3-(4,5-Dimethyl-2-thiazolyl)-2,5-diphenyl-2H-tetrazolium bromide
M_w	weight average molecular mass
MW	molecular weight
p-TsOH	*para*-toluenesulfonic acid
PE	polyethylene
PET	polyethylene terephthalate
r-PET	recycled polyethylene terephthalate
PLA	polylactic acid
(P)MMA	(poly)methyl methacrylate
PS	polystyrene
NMR	nuclear magnetic resonance spectroscopy
RAFT	reversible addition-fragmentation chain transfer polymerization

SEC	size-exclusion chromatography
$T_{d,95\%}$	thermal degradation temperature at 5% mass loss
T_g	glass-transition temperature
TGA	thermogravimetric analysis
THF	tetrahydrofuran
TMP	trimethylolpropane
TRL	technology readiness level
UV	ultraviolet light

INTRODUCTION

Plastics are polymeric materials consisting of one or more polymers and some additives, which enhance the material's properties or act as fillers to reduce the cost.[1] The term plastics is also sometimes used as a synonym for thermoplastics, but this is not recommended.[2]

Polymers are defined as substances composed of macromolecules. The repeating units in a polymer chain, are formed by monomers that undergo polymerization.[1] The term polymer comes from the Greek language: *polys* meaning "many" and *meros* meaning "part".[2,3] Polymers can be divided into three main categories: *thermoplastics*, which become liquid at elevated temperatures; *elastomers*, which are crosslinked rubbery polymers that can be elastically extended many times their original length; and *thermosets*, which are also crosslinked polymers where the crosslinking severely inhibits chain movement, thereby making these materials rigid. In the context of this work, the focus is primarily on thermoplastics, with some sidesteps into thermosets.

Modern society consumes many plastic products, which generates a lot of waste from manufacturing and transporting these products, while plastic packaging is also used for all kinds of other commodities.[4] The energy and raw materials used are primarily of fossil feedstock – a non-renewable material that will run out eventually. The other byproduct of the consumption of fossil fuels is the liberation of carbon that has been stored for millions of years, leading to excess carbon emissions. A part of that problem is also in the plastic industry, which primarily uses fossil fuels as starting material. While fossil-based plastics have generally excellent properties for their use, their end-of-life is met with complications in reuse and recycling.

A significant problem that has arisen with ever-increasing plastic usage is waste management. Most plastics are inherently stable and will not degrade in nature for hundreds of years. The primary end-of-life paths for polymer materials are landfilling, mechanical recycling, and incineration. The only somewhat viable option from those three is mechanical recycling, but it comes with the downside of worsening the material properties when reused. This is due to polymer chain degradation after multiple heating cycles caused by oxidation, heat, and could already be present before the recycling process.[5,6] Additionally, different polymers are collected and are hard to separate during recycling. It results in a material that is a mixture of various polymers and is characteristically also something in the middle. The eventual outcome is called down-cycling, which means that the material is used in less demanding applications every cycle when there is more than one cycle.

Bio-based polymers can reduce excess emissions using renewable feedstock that contributes to carbon capture via photosynthesis as an alternative to fossil materials. However, just using bio-based starting material is not the solution to all the plastics-related problems. Not all bio-based polymers are inherently biodegradable, which leads to issues similar to those of common plastics – waste

accumulation and carbon emission. Effective biodegradability, which can alleviate the waste problem, but still releases CO_2, usually requires specific conditions and microorganisms.[7] The solution to this problem would be designing polymers in a way that allows their recycling without losing performance, contributing to a circular economy.

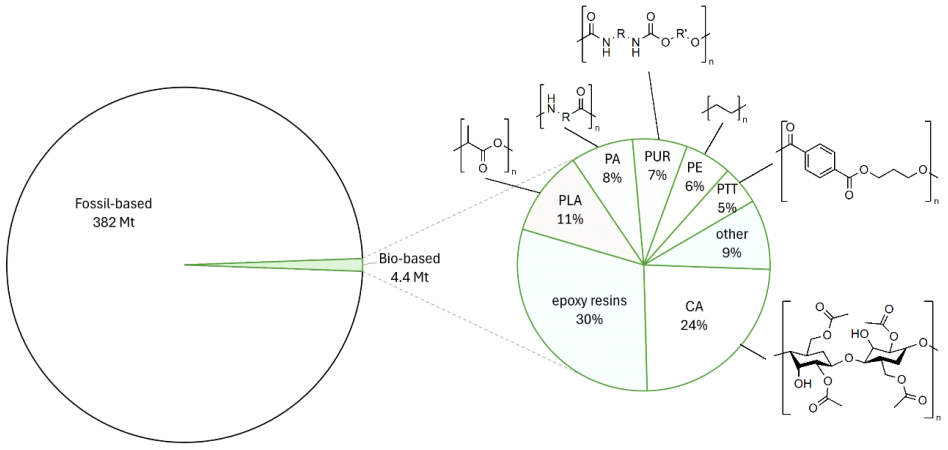

Figure 1. Global plastics production in 2022, bio-based plastics expanded on the right by production volume percentage. CA – cellulose acetate, PLA – polylactic acid, PA – polyamides, PUR – polyurethanes, PE – polyethylene, PTT – polytrimethylene terephthalate.[8]

In 2023, still, only slightly over 1% of the globally manufactured polymers were comprised of bio-based polymers – 4.4 million tons compared to 382 million tons of fossil-based polymers (Figure 1). It has to be noted that some of the polymers included in the graph are only partially bio-based. At the same time, the growth of the bio-based polymer market has been 17% compared to the overall growth of about 3%.[8]

Bio-based polymers have been commercially available for more than 100 years but are often inferior to their fossil-based counterparts. This is due to their structure, which includes oxygen linkages, which are less stable compared to C-C bonds, and can therefore lead to worse mechanical and thermal properties: lower thermal stability, chemical resistance, and glass-transition temperatures. For example, PLA, the best-known bio-based polymer, only has a glass-transition temperature of about 55 °C.[9,10] This means the material may lose its shape and purpose if something hotter comes into contact with it. This is one of the main challenges in bio-based polymer engineering – how do we use sustainable feedstock, which is in some ways inherently "weaker," to obtain materials that are competitive or even better performing than conventional commercial plastics? At the same time, the functionality of bio-based materials can be leveraged as an advantage for modification and, therefore, surpassing fossil materials.[11]

Another critical aspect of developing new materials is their impact on nature. This is calculated using life-cycle assessment (LCA), which evaluates parameters such as, e.g., global warming (CO_2 emissions), eutrophication and acidification of the environment, and land use throughout the whole process from obtaining the raw material to the product's end-of-life.

In this thesis, the primary focus was placed on using structures obtainable from different types of biomass and converting them into cyclic monomers and corresponding polymers (Scheme 1). In the first approach (Paper I), a condensation reaction between citric acid and a diketone, followed by ketalization via glycerol or trimethylolpropane (TMP), was used to obtain a multicyclic rigid structure. This was further converted into diacrylates, which were used in polymerization with a selection of dithiols to obtain poly(β-thioether ester)s. Additionally, the hydrolytic degradation of the created ketal units was tested. The second path (Paper II) utilized isosorbide, which was regioselectively functionalized with methacrylate and levulinate units, copolymerized with methyl methacrylate (MMA), and, after that, crosslinked with dihydrazides. The reversibility of the obtained network structures was also studied through the cleavage of crosslinking bonds. The third pathway (Paper III–IV) used lignin-derived carboxylic acids in a simple two-step conversion into methacrylate monomers, which were then used in a free-radical polymerization process. The fifth approach (Paper V) converted heterocyclic indoles and indolines into poly(meth)acrylates.

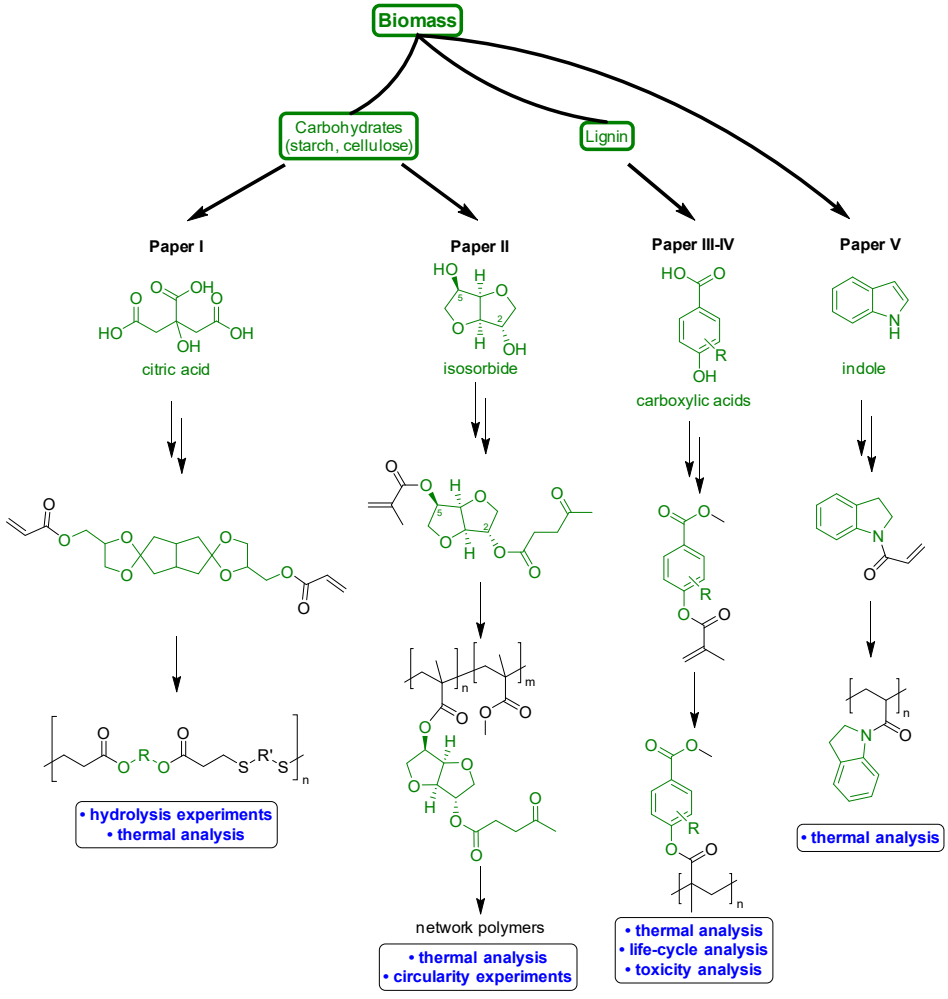

Scheme 1. Outline of the four papers included in the thesis. Green colour shows the parts obtained from biomass.

1. LITERATURE OVERVIEW

1.1 Bio-based polymers

A biopolymer is a substance formed from a specific type of biomacromolecule; biodegradability refers to the polymers' degradation via biological activity.[1] There are some common misconceptions about different "bio"-terms, such as biopolymer, biodegradability, and bio-based polymer. All these concepts are not inherently connected – bio-based polymers are not inherently biodegradable, but biopolymers, which are naturally occurring polymers, such as DNA, polysaccharides, lignin, etc., are always biodegradable.[1,12,13] At the same time, even fossil-based polymers can be biodegradable if designed appropriately. The same principle applies to bio-based polymers. Biodegradability also does not always mean that the material is degradable in natural environments; it most likely is degradable in an industrial setting under specific conditions.[13–16]

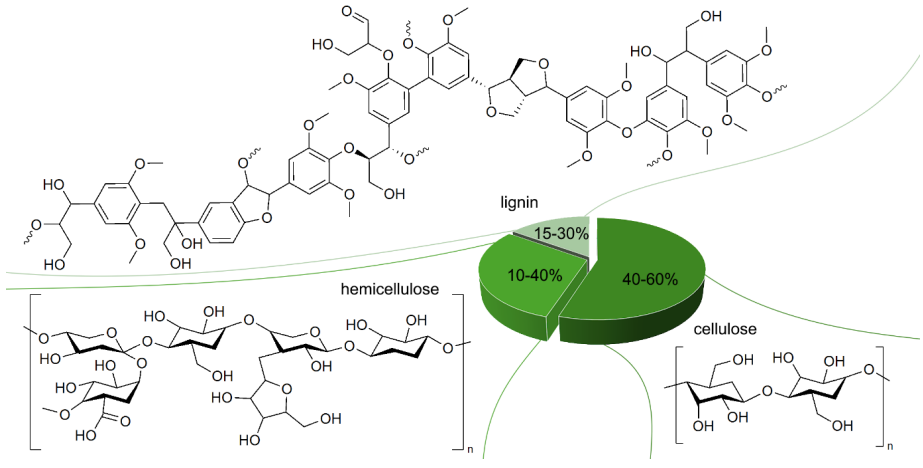

Figure 2. Composition of lignocellulosic biomass with structures of the different components.

Bio-based polymers are polymers derived from biomass, such as, e.g., cellulose and lignin. They can be obtained by directly modifying the biopolymers or created from already depolymerized material to obtain new monomers converted into subsequent polymers.[1] Due to the large availability, bio-based polymers should be mostly based on lignocellulosic biomass (LCB) instead of, e.g., starch, which is obtained from agricultural feedstock.[17,18] LCB comprises 40–60% cellulose, 10–40% hemicellulose, and 15–30% lignin.[17] Cellulose is mainly used to manufacture paper, while hemicellulose and lignin are often treated as waste products.

The main challenge with bio-based polymers is competing with other commercially used plastics. This is due to the oxygen linkages such as ester and acetal bonds, which are less stable compared to C-C bonds in carbohydrate polymers. These types of bonds can make the material less thermally or environmentally

stable and, therefore, unfit for use in some applications. Another major factor for their low competitiveness is their price – fossil-based polymer production has been optimized for a long time and is thus cheap and efficient, benefiting from large-scale manufacturing processes.

Bio-based polymers can also be direct replacements for fossil-based materials, e.g., PE from sugarcane. In this case, the only difference is the starting material. On the other hand, new polymers from bio-based feedstock should be designed to obtain materials with even better characteristics compared to the existing ones.

1.1.1 Carbohydrates from biomass

The most accessible source of biomass is poly- and monosaccharides, e.g., glucose and starch, which are primarily obtained from different agricultural crops. Most of these crops are also used to produce food, therefore making this type of biomass a direct competitor of the food industry. For example, bioethanol has been produced from corn or sugarcane for over 20 years.[19] Many platform chemicals can be obtained from glucose via biocatalytic or chemical methods (Figure 3).[20] For example, citric acid is obtained from glucose via fermentation.[21] Sorbitol can be further converted into chemicals like lactic acid, which is used to make polylactic acid (PLA); glycerol, which is widely used in medicine and cosmetics; and isosorbide.[20]

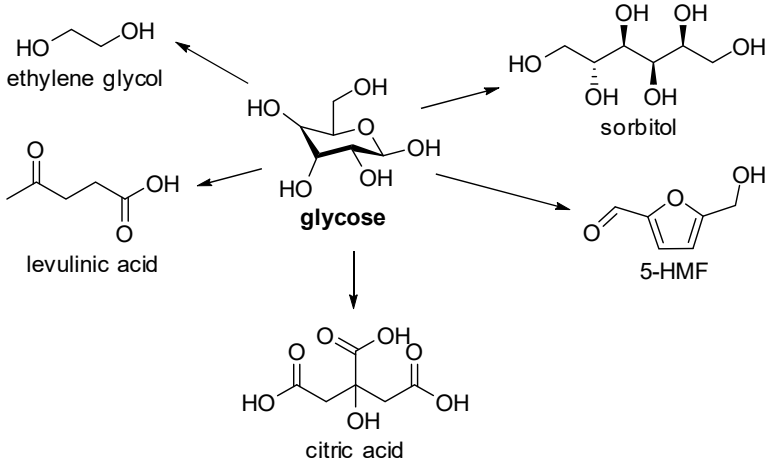

Figure 3. Common compounds obtained from glucose.

Alternatively, glucose can be obtained from cellulose depolymerization, which is complicated due to it being a highly crystalline, hydrogen-bonded and water insoluble material.[22,23] Conventional acidic hydrolysis methods are effective, but the used acid cannot be recovered efficiently, or is impossible in the case of H_2SO_4.[20,24] Some success has been found utilizing heterogeneous porous carbon-based catalysts for cellulose depolymerization.[25]

Cellulase enzymes are able to break down cellulose into glucose effectively.[25,26] Still, enzymatic breakdown of cellulose is roughly 100 times slower compared to starch, which highlights the difficulty of cellulose depolymerization.[27]

1.1.2 Isosorbide

Isosorbide is a bicyclic diol that is comprised of two *cis*-fused tetrahydrofuran rings, forming a V-shaped rigid structure.[28] It is produced from sorbitol via dehydration.[29] Sorbitol can be obtained from either cellulose or starch. Isosorbide is produced on an industrial scale and thus has been a promising building block for bio-based polymers, besides being used in the pharmaceutical and cosmetics industry.[28,30]

Unlike its stereoisomers, isoidide, and isomannide, isosorbide has two hydroxyl groups with different reactivity in the 2 (*exo*) and 5 (*endo*) positions, respectively (Figure 4). This opens up a possibility to selectively modify just one of these groups based on differences in reactivity and steric effects.[31] Our group has recently developed a method using enzymatic esterification to modify isosorbide hydroxyl groups regioselectively.[32]

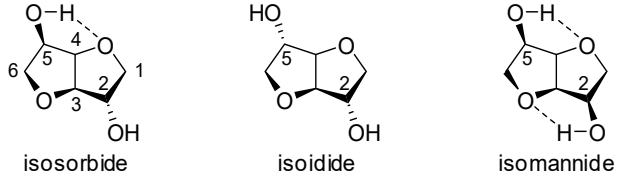

Figure 4. Structures of isosorbide and its isomers isoidide and isomannide. Dashed lines show intramolecular hydrogen bonding.

1.1.3 Isosorbide-based polymers

The first review on the use of isosorbide to produce polyesters, polycarbonates, and polyurethanes was published in 1992.[33] This included the isosorbide unit in the main chain of the polymer structure. However, isosorbide can also be introduced as a side chain when the hydroxyl groups are modified separately. For example, isosorbide polymethacrylates have been prepared by our group[32,34,35] and others.[36,37] Isosorbide monomethacrylates with different substituents were polymerized via free radical polymerization by our group.[32] Both poly(isosorbide-5-methacrylate) and poly(isosorbide-2-methacrylate) had T_g values of 167 °C at M_n = 105 kg/mol and at M_n = 65 kg/mol, respectively. Both polymers had thermal degradation temperatures at about 240 °C. Further studies using alkyl side chains of increasing length showed that these isosorbide polymethacrylates exhibit liquid crystallinity with long side chains.[34] Another study, using aromatic side chains, reached a similarly high T_g of 168 °C using para-nitrile substituted benzyl substituent in the 2-OH of isosorbide.[35] In contrast, Nonque et al. studied

a mixed system of exo/endo isosorbide methacrylates for polymerization and achieved a T_g of 175 °C at M_n = 80 kg/mol. Similarly, a mixture of endo/exo isosorbide acetates studied by Gallagher et. al. had T_gs about 130 °C with MW-s up to 30 kg/mol.[37]

1.1.4 Lignin

Lignin is a part of LCB and is the second most abundant biopolymer on the planet after cellulose. It acts as a binder between cellulose and hemicellulose, giving antioxidant properties due to its phenolic structure. Lignin is primarily obtained as a waste from pulp mills as a part of black liquor, which is mainly used as fuel to lower the operation costs of the mills. About 50 million tons of lignin is produced by paper and pulp mills globally annually, while only a small percentage is converted to value-added chemicals.[38]

The lignin structure varies based on the source of biomass. The three main units in lignin are hydroxyphenyl (H), guaiacyl (G), and syringyl (S), which have 0, 1, and 2 methoxy groups, respectively, attached to the aromatic ring (Figure 5). These units are mainly found in grassy plants, softwood, and hardwood, respectively, while the G-unit is the most common overall.

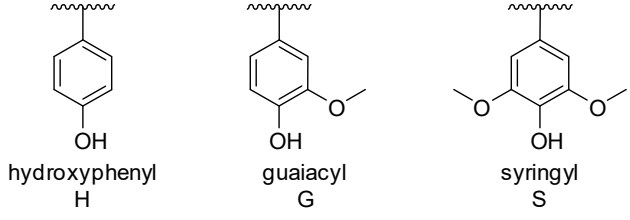

Figure 5. Structure of the central lignin units.

1.1.5 Lignin depolymerization and production

Lignin depolymerization is inherently difficult due to its recalcitrance and complex structure, which varies even between species.[39] This is explained by the different linkages between the aromatic rings, which have been described in literature.[40,41] As there are so many different types of bonds to cleave during depolymerization, it is challenging to target specific bonds selectively. The most common linkage in lignin structure is the *β-O-4* linkage (Figure 6).[41]

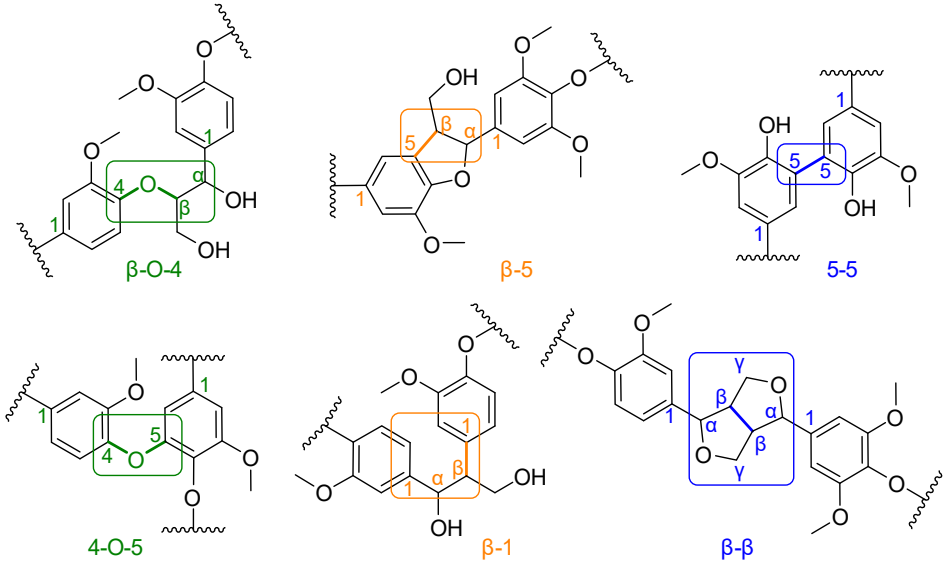

Figure 6. Some common linkages in lignin. Aromatic ring carbons marked with 1–6, side chain carbons with α, β, γ.

The heterogeneous structure leads to a wide variety of compounds that can be obtained from the depolymerization of lignin. Additionally, the method used leads to different products as well. The main methods for lignin depolymerization are chemical or biocatalytic.[42] While chemical methods, such as pyrolysis and oxidation, are more common, microorganism or enzyme-mediated processes have high potential in the future due to the environmental friendliness – using lower temperatures without any potentially harmful catalysts.[42,43]

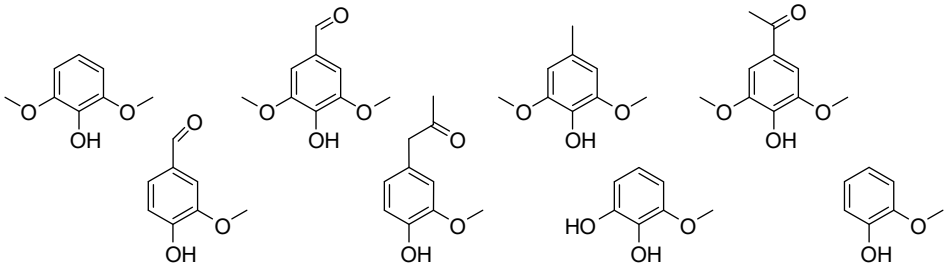

Figure 7. Some of the phenolic compounds that can be obtained from lignin depolymerization.

1.1.6 Lignin-based polymers

Lignin has been primarily used in polymer composites and blends, acting as a binder and additive.[44,45] Chemical modification of polymeric lignin is possible, but the resulting material will still be as heterogeneous as the lignin initially. Lignin modification is often achieved through the acylation or esterification of the hydroxyl groups, which make the modified lignin able to blend with common polymers somewhat.[46]

Another route towards viable homogeneous lignin-based materials is to chemically modify depolymerized lignin. This is often done through the functionalization of the free hydroxyl groups by adding polymerizable units. For example, Epps's group has done intensive research into lignin-derived polymethacrylates (Figure 8).[47–49] Using guaiacol, creosol 4-ethylguaiacol, and vanillin as starting materials, they achieved molecular weights around 50 kg/mol utilizing RAFT polymerization; the highest T_g, 136 °C, was achieved by vanillin methacrylate.[49] In another example, an even higher T_g was obtained with syringol using similar methods (205 °C).[47]

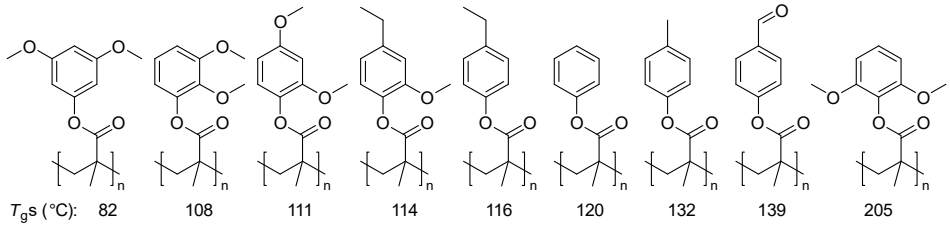

Figure 8. Different polymethacrylates from lignin-derived starting materials investigated by Epps et al. T_g values (°C) are depicted under the structures.

Free radical polymerization has been used to obtain nitrile-substituted lignin-based methacrylates with exceptionally high T_gs from 150 to 238 °C. these polymers were thermally stable up to over 300 °C due to the polarity of the nitrile group.[50] Similarly, Zhou et. al. managed to obtain thermoplastic polymers with a T_g of 180 °C from syringaldehyde methacrylate.[51] A somewhat more complex Lewis pair polymerization has been used to prepare vanillic acid based methacrylate with a T_g of 126 °C.[52]

1.1.7 N-heterocyclic aromatics

Heterocycles containing nitrogen, e.g., pyrroles, pyridines and indoles (Figure 9), are widely spread in nature and are used in the synthesis for pharmaceutics, dyes and agrichemicals.[53] Both pyrrole and indole have been polymerized to obtain conductive polymers that can be used in sensors, biomedical applications, batteries and supercapacitors.[54]

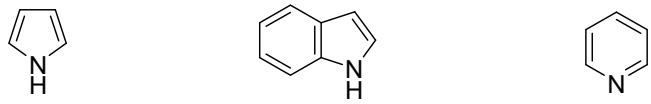

Figure 9. Some of the heterocyclic compounds found in nature.

Originally indole was discovered from the reduction process indigo. Later the process has been reversed – indole has been used as a precursor for making indigo dye. Large amounts of indole have been primarily produced by high-pressure crystallization of coal tar.[55,56] Recently, bio-based production of indole has been investigated, as indole is an intermediate in some metabolic pathways. One of the most promising pathways is tryptophan biosynthesis, which can be modified to release indole as an intermediate compound.[57]

1.2 Polymerization techniques

Polymers are formed by linking small monomer units to obtain large polymer molecules. This concept was introduced by Hermann Staudinger, who was awarded a Nobel Prize for his work on macromolecules in 1953.[58]

A common way to divide polymerizations is by polymer chain growth type: *step-growth* and *chain-growth* polymerization. The difference between the two comes from the addition mechanism. In step-growth polymerization, monomeric and oligomeric fragments can react with one another and each other to form larger chain fragments. These can undergo the same type of addition again, eventually forming larger chain fragments (Scheme 2a). Step-growth polymers achieve high molecular weight only at high conversion and take longer time to reach that point, following an exponential growth curve over conversion.[2,59]

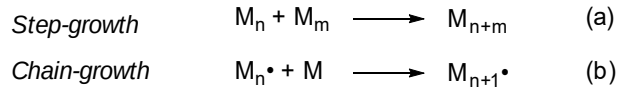

Scheme 2. Simplified growth mechanism formulas for step-growth (b) and chain-growth (a) polymerization (• symbolizes propagating reaction center).

In chain-growth polymerization, on the other hand, the polymer chain grows by the addition of new monomeric fragments to the reactive center, which is activated by an initiator. The reactive center can be an anion, cation, or a radical, which propagates along the chain to add new monomer fragments to the growing polymer chain (Scheme 2b). This leads to a more rapid growth in molecular weight as there are only large polymer fragments and monomers in the mixture at any point.[2,59] Earlier, a division into *condensation* and *addition* polymers was also used, but this was based on the composition structure of the polymers instead of the reaction mechanism.[59] As there are many different types of polymerization reactions, only the ones considered more relevant in the context of this thesis,

such as different types of radical polymerization and some crosslinking reactions, are described in more detail.

1.2.1 Radical polymerization

Radical polymerization is a type of chain-growth polymerization where the polymerization is carried by radicals.[60] It is the most versatile and commonly used polymerization type in the polymer industry.[2,61] The three stages in radical polymerization are initiation, propagation, and termination. During the initiation step, the initiator molecule first forms a radical either through homolysis or photolysis and then transfers to the monomer molecule. Homolysis is usually the result of heating, which causes a particular bond in the initiator to break, creating two radicals. These initiators commonly contain peroxide (–O–O–) or azo (–N=N–) linkages.[2,59] One of the most known radical initiators, azobisisobutyronitrile (AIBN), also contains an azo linkage and decomposes as shown on Scheme 3.

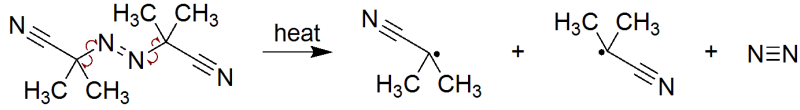

Scheme 3. The decomposition of AIBN into radicals.

UV-light can also cause the dissociation of the initiator, but this is less effective for typical radical initiators and is better used with photoinitiators, such as benzophenones and benzils. The advantage of photoinitiation is the ability to carry out the reactions at room temperature.[2,62]

After initiation, propagation involves rapid growth of the polymer chain. The initiator radical starts attacking monomers, adding to the polymer chain. The radical is transferred to the active center each time (Scheme 2a). Radical polymerization ends with termination, destroying the active center, and propagation cannot continue. There are two common mechanisms for termination: *combination* and *disproportionation*. In combination, two active centers couple to form a single polymer chain (Scheme 4a). Disproportionation leads to two terminated polymer chains – one active center takes the hydrogen atom from the other, leading to the other chain having an unsaturated bond in one end (Scheme 4b). It has been observed that combination is more common in vinyl monomer polymerizations, and disproportionation termination is dominant in MMA polymerizations, especially at higher temperatures.[2]

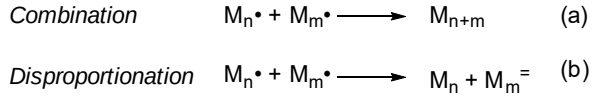

Scheme 4. Two of the most common termination mechanisms of radical polymerization (= marks an unsaturated bond).

Besides free radical polymerization (FRP), several controlled radical polymerization methods exist. The most common mechanisms are atom transfer radical polymerization (ATRP) and reversible addition-fragmentation chain transfer (RAFT), first reported in 1995 and 1998, respectively.[63–65]

Controlled radical polymerizations have the benefits of controlling polydispersity, chain length, tacticity, and monomer distribution in copolymers. This is achieved by the equilibrium of active and dormant polymer chains, resulting in homogeneous polymer structure and molecular weight distribution.[63]

1.2.2 Michael reaction in thiol-(meth)acrylate systems

The thiol-ene reaction, a subtype of the Michael addition reaction, involving a sulfur nucleophile, is also robust and efficient for step-growth polymerizations that can be initiated radically or by an anionic or cationic initiator.[66,67] UV-initiated thiol-ene reactions are not inhibited by oxygen as most other radical polymerizations.[68] This removes the need for an inert atmosphere for such thiol-ene reactions, further simplifying the setup. All these characteristics make it suitable to categorize as a "click" reaction.

The method is primarily used to make polymer networks using multifunctional thiols and alkenes or post-modification of linear polymers to create cross-linked systems.[66] These types of materials have been widely used in the medical sector.[69] Some examples of linear polymers have also been described.[70–73] Junkers et al. have prepared biodegradable thiol-acrylate polymers from 1,4-butanedithiol and 1,6-hexanediol diacrylate with M_n-s up to 10 kg/mol and T_g-s up to 53 °C, which were degraded via ester linkages.[73] Long et al. used isosorbide diacrylates with various flexible dithiols to create linear polymers with T_g-s from –9 to 15 °C and thermal stability around 300 °C.[71]

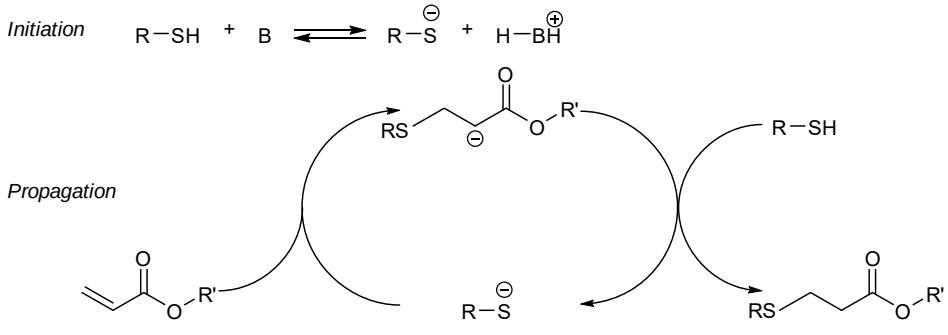

Scheme 5. Base-catalyzed thiol-acrylate addition mechanism.[74]

Base-catalyzed Michael addition reactions have higher efficiencies and fewer side reactions than radical thiol-ene reactions.[75] Weak organic bases such as primary amines, e.g., Et_3N and 1,8-diazabicyclo[5.4.0]undec-7-ene (DBU) or nucleophilic phosphines, can be used for initiating thiol-ene addition.[76] The reaction rate in base-catalyzed addition is closely related to the C=C bond –

higher electron density leads to lower reaction rates.[74] This order of reactivity is reversed in a radically initiated reaction. Additionally, steric effects reduce the reactivity even further.[68]

1.2.3 Crosslinking of polymers

Introducing covalent or ionic bonds, or weaker interactions, e.g., hydrogen bonding, between polymer chains is a viable option to enhance polymer properties like M_n, T_g, and durability.[2,77] This can be done by incorporating functional units utilized after polymerization to link the polymer chains or by using multifunctional units for polymerization. At low crosslink density, the rubbery polymer can be easily stretched, but recovers its initial form once released. Such polymers are called elastomers. High crosslink density is a common characteristic of a thermoset, which has a more rigid structure, and cannot be processed after initial formation.[2] Crosslinked polymers, also referred to as polymer networks, can be of high or low regularity, low or high crosslink density (Figure 10).[78]

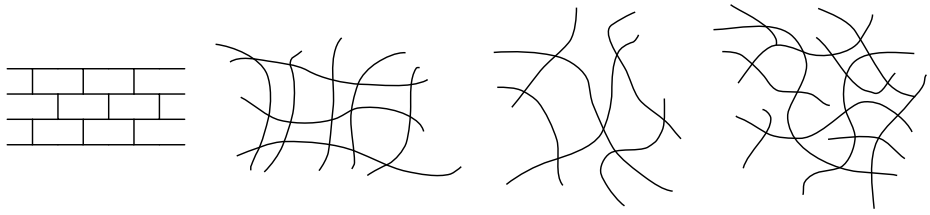

Figure 10. Simplified structures of crosslinked polymers with different regularity.

One of the earliest examples of crosslinking is the vulcanization of natural rubber using sulfur discovered by Charles Goodyear in 1839.[79] As mentioned in the previous chapter, thiol-ene chemistry is widely used to obtain network polymers.

1.2.4 Covalent adaptable networks

Covalent adaptable networks (CANs) are an excellent option for changing polymer properties by post-treatment.[80] They function similarly to regular crosslinked polymers but have the upside of reversible crosslinking, allowing recycling, reuse, or even healing of these materials.[80,81] The reversibility only occurs under specific conditions, e.g., UV radiation, certain pH values, or temperature.[82] The accepting functionality of a crosslinking bond must be incorporated into the polymer structure to allow possible crosslinking reactions. Such reversible crosslink materials could be used in composite materials, 3D printing, and electronic packaging materials to improve or make it possible to recycle those materials.[81]

One such reversible bond that can be utilized in CANs is the acylhydrazone linkage, which can be cleaved under acidic conditions.[81] A dihydrazide reacts with two carbonyl groups and forms an acylhydrazone bond, connecting two polymer chains (Scheme 6). Adipic hydrazide is widely investigated as a crosslinker with aldehydes and ketones and is considered safe for food contact applications.[83]

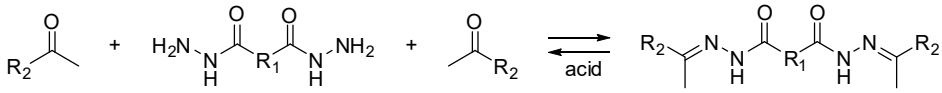

Scheme 6. Simplified mechanism of acylhydrazone bond formation and cleavage.

1.3 End-of-life of polymers

As already briefly discussed in the introduction, waste management is a significant plastic-related problem. Polymers, which are mostly inherently inert, do not decompose but pile up in nature. Most plastic waste globally reaches landfills or is incinerated for energy.[84]

In Europe, where the end-of-life of polymers is managed the best, about a quarter of plastic waste is landfilled, while the recycling rate is slightly higher, at 26.9%, and the rest, at 50%, is incinerated.[85] Significant improvements are still needed as landfilling pollutes the environment and incineration releases a large amount of CO_2 similarly to burning fossil fuels. Recycling is the only method that allows circularity of polymer materials by reusing and repurposing them in either similar or lower end applications (Figure 11).

Another not so favorable option is pyrolysis, which involves using high temperatures (over 400 °C) in an oxygen-free environment and catalysts to break down the polymer backbone into smaller fragments. This process is very energy-intensive and thus has a high associated cost. Pyrolysis can be suitable for hydrocarbon polymers such as PE, PP, or PS and yields low molecular weight hydrocarbon oils and gases, which can be used for producing fuels. Still, the feedstock needs fractionation to separate specific compounds.[86,87]

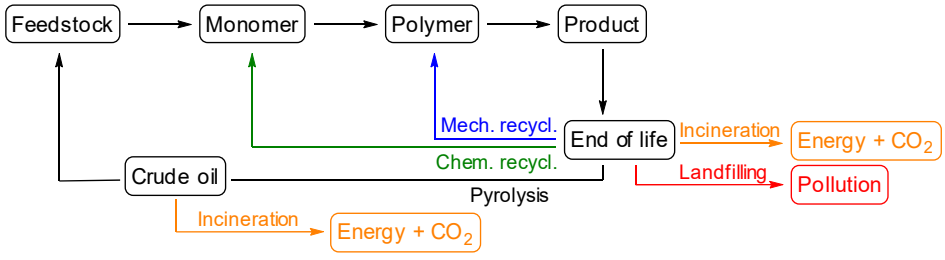

Figure 11. Different end-of-life possibilities of a plastic product.

1.3.1 Mechanical recycling

Mechanical recycling includes sorting, washing, and grinding waste material into small pieces, that are thereafter melted and formed into new products. It is still the most widely used form of recycling. Typically, however, this leads to the deterioration of the properties of the plastic in each of the cycles.[5] Mixed plastic waste streams are complex systems and obtaining type-separated waste plastics is complicated. As a result, the mechanically recycled material can be a mixture

of polymers; therefore, the properties will also be averaged over those fractions. Contamination with some foreign polymers can also lead to an additional loss in polymer properties through chemical processes that lead to the degradation of the primary polymer.

Mechanical recycling can be divided into two categories: primary and secondary recycling. Primary recycling refers to using recycled material the same way it was originally used. Usually, this process incorporates a some virgin feedstock to compensate for the loss of properties from mechanical recycling. The best example of primary recycling is PET bottles. However, recycled-PET (r-PET) also suffers from a loss of some thermal and mechanical properties due to the lowering of MW.[5,6] Secondary recycling refers to the down-cycling of materials – meaning the recycled material is used in a less demanding application, for example, recycled food-grade PET used for producing textile fibers.

1.3.2 Chemical recycling

Chemical recycling, sometimes called tertiary recycling, involves breaking chemical bonds in polymers to obtain either monomers or starting materials for the monomers followed by subsequent repolymerization.[5,88] The monomers obtained through this process are equivalent to virgin monomers and can be therefore used in the same application as the recycled material. Additionally, the monomer precursors can be used in other applications.[88] Currently, chemical recycling only contributes ca 0.1% of the total recycling rate in Europe.[85] There are several chemical recycling methods, but they are not widely used in the industry because of their high cost. This type of recycling is preferred since it allows the plastic materials to be re-obtained with their original properties.

An approach to pave a road for chemical recycling is to design polymers to allow cleavage of certain bonds, e.g., ester or acetal, to re-obtain the starting material by treating the polymer under specific conditions. Acetal units are known to degrade hydrolytically under acidic conditions and have been successfully incorporated into polymer backbones by some groups.[89–92] After that, the polymer can typically be obtained by repolymerization.

Enzymatic recycling has gained more interest lately. The main benefit of enzymatic degradation is the use of mild reaction conditions, usually in water, at around 37 °C.[93] This is beneficial since the need for high energy is a common problem for depolymerization methods. Additionally, avoiding the use of chemicals adds another ecological benefit. An efficient method to recycle PET was developed by Marty et al., which allows the depolymerization of at least 90% of PET into monomers in 10 hours.[94] They also repolymerized the obtained material to obtain the same properties as virgin PET, which indicates the viability of their method.

1.3.3 Importance of life cycle assessment

Life cycle assessment (LCA) is a method that allows the evaluation of the environmental impact of a process, including all the steps from obtaining and processing the starting material to the utilization of the product after its use. Such a cradle-to-grave approach gives the complete picture of a process and identifies critical hotspots that need improvement to lessen environmental impact.[95,96]

LCA of new and emerging materials with low technology readiness levels (TRL) is crucial to determine their potential applicability on a larger scale – non-favorable LCA results should lead to significant improvements in the production process or in worse cases to halt of development.[97] LCA methods allow theoretical scale-up of lab-scale methods to compare them with extensive industrial processes – known as *ex-ante* LCA.[98,99] Additionally, *prospective* LCA allows for the simulation of future trends by estimating socio-economic tendencies.[100] A fair comparison would not be possible without these two methods as early lab-scale methods are often inefficient and the materials are produced only in small quantities.[101]

Another fallback can be the lack of data on common chemicals and solvents that have yet to reach large-scale commercial production. While global warming potential (GWP) is the most common LCA parameter, other impact categories are equally important. For example, if we only measure GWP, many bio-based materials made from renewable feedstocks are superior to fossil materials, but different impact factors such as land use, acidification, and eutrophication can be less favorable.[102] For instance, bio-PE has a lower carbon footprint compared to fossil HDPE if renewable energy is used and transport emissions are minimized (–1.0 and 2.6 kg CO_2eq/kg for bio-PE and fossil-PE, respectively).[103] On the other hand, the land use of bio-PE makes it less advantageous, as the change from a forest to a sugar cane plantation leads to higher emissions by comparison (3.6 kg CO_2eq/kg). In addition, bio-PE has ca 10 times higher impacts in eutrophication and acidification.[104]

Similarly to early assessment of other environmental factors, measuring the toxicity of new materials is crucial to obtain information about how they affect the environment and humans.[105] Common polymers, e.g., PE, PP, and PS, have been evaluated via toxicology.[106] However, novel polymers such as those described in this thesis are usually neglected from a toxicology standpoint. From a green chemistry standpoint, any toxicity is unwanted.[107]

2. AIMS OF THE STUDY

The current thesis aims to find sustainable alternatives to commercial high-performance polymers from bio-based feedstock. Different lignocellulosic materials – citric acid and isosorbide from starch or cellulose sugars and building blocks from lignin – were used as the precursors of the synthesized monomers. Cyclic building blocks were selected because their structural rigidity may lead to improved material characteristics. A secondary focus was put on the design of the materials from a circular economy perspective, which entails incorporating some form of reversibility to allow chemical recycling of the materials. To achieve these aims, the work was divided into four parts:

1) synthesis of spirocyclic di(meth)acrylates, polymerization with dithiols into poly(β-thioether ester)s, investigation of structure-property relationship analysis, and chemical recycling possibilities (Paper I)
2) synthesis of isosorbide-2-levulinate-5-methacrylate, polymerization into homo- and copolymethacrylates and reversible crosslinking studies (Paper II)
3) synthesis of lignin-based aromatic methacrylates, their polymerization, and studies of their properties, life cycle, and toxicity (Paper III–IV)
4) synthesis of indole and indoline (meth)acrylates, polymerization into homo- and copolymers (Paper V)

3. RESULTS AND DISCUSSION

First the synthesis of spirocyclic monomers and respective polymers from citric acid feedstock is carried out. The thermal properties of the polymers and potential chemical recycling path are investigated. Next, isosorbide methacrylates with levulinic side chain are studied as covalent adaptable networks with hydrazide crosslinkers. Finally, lignin-based carboxylic acids are converted into methacrylate monomers and are thereafter polymerized and characterized. Additionally, their life cycle and toxicity are evaluated.

3.1 Poly(β-thioether ester)s from spirocyclic diols

PAPER I

This paper includes three parts: 1) spirocyclic di(meth)acrylate synthesis; 2) polymerization of the di(meth)acrylates with dithiols and their characterization; 3) investigation of the hydrolytic stability of the monomers and polymers.

3.1.1 Spirocyclic di(meth)acrylate synthesis

A method previously developed by our group[108] was used for spirocyclic diol synthesis to convert diketones **B** (*cis*-bicyclo[3.3.0]octane-3,7-dione) and **T** ([4.3.3]propellane-8,11-dione) into diols with either trimethylolpropane (TMP) or glycerol (Scheme 7). The diols were further converted into di(meth)acrylates, which were used in thiol-acrylate polymerizations.

The ketalization reaction was performed under reflux in toluene with TMP using *p*-TsOH as a catalyst. The crude product was purified via chromatography in petroleum ether and EtOAc, resulting in a mixture of the *cis* and *trans* isomers, which were not separated before the subsequent (meth)acrylation. This is because the isomers have similar retention factors, making their separation difficult – separation was only done for isomer analysis. Diols prepared from **B** – **tB** and **gB** were obtained in high yields of 91 and 92%, respectively. The tricyclic ketone **T** also worked well with TMP – the resulting **tT** was obtained with an 88% yield. Still, the reaction between **T** and glycerol proved to be more complicated, most likely due to the lower reactivity of **T** caused by steric hindrance. This was also observed in the reaction between **T** and TMP, as it took significantly longer compared to ketalization reactions involving **B**, 48, and 16 h, respectively.

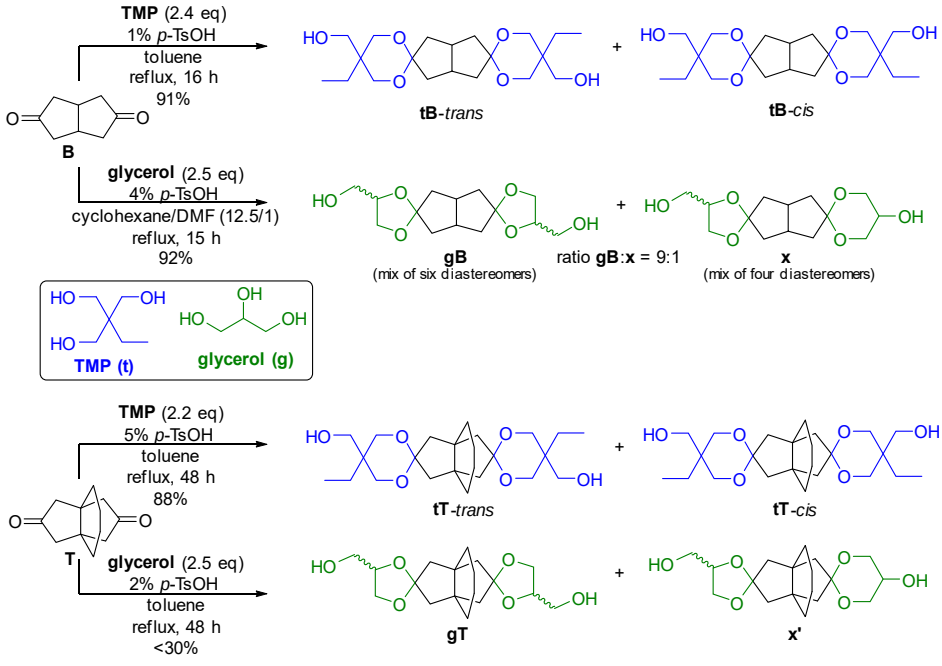

Scheme 7. Spirodiol synthesis from diketones **B** and **T**.

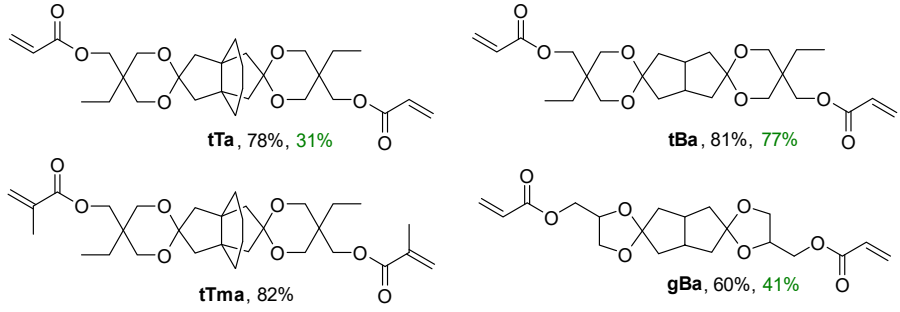

Figure 12. Spirocyclic di(meth)acrylate monomers with the obtained yields in CH_2Cl_2 (black) or 2-MeTHF (green), respectively.

The conversion from diols to (meth)acrylates was done using a conventional esterification reaction with (meth)acryloyl chloride in either CH_2Cl_2 or "greener" 2-MeTHF, using Et_3N as an acid scavenger. The yields in CH_2Cl_2 were, on average, higher compared to the yields obtained in 2-MeTHF, most likely due to higher solubility of starting material in CH_2Cl_2 (Figure 12). The tricyclic **tTa** had lower solubility in 2-MeTHF, which is the likely cause of the low yield. All products were purified using flash chromatography with EtOAc mixtures with petrol ether.

3.1.2 Polymerization and characterization of poly(β-thioether ester)s

Polymerizations were carried out in $CHCl_3$ or 2-MeTHF with 10% DBU, using a 1:1 ratio of dithiol and di(meth)acrylate. The reactions started at 0 °C and left stirring for 24 h. After the polymerization the reaction mixture was precipitated into MeOH, filtered and dried under vacuum. The dithiols used were 1,3-propanedithiol (PDT), 1,6-hexanedithiol (HDT), and 4,4'-thiobisbenzenedithiol (TBBT). The polymers were named as a combination of the (meth)acrylate and dithiol parts, e.g., **poly(tTa-PDT)**.

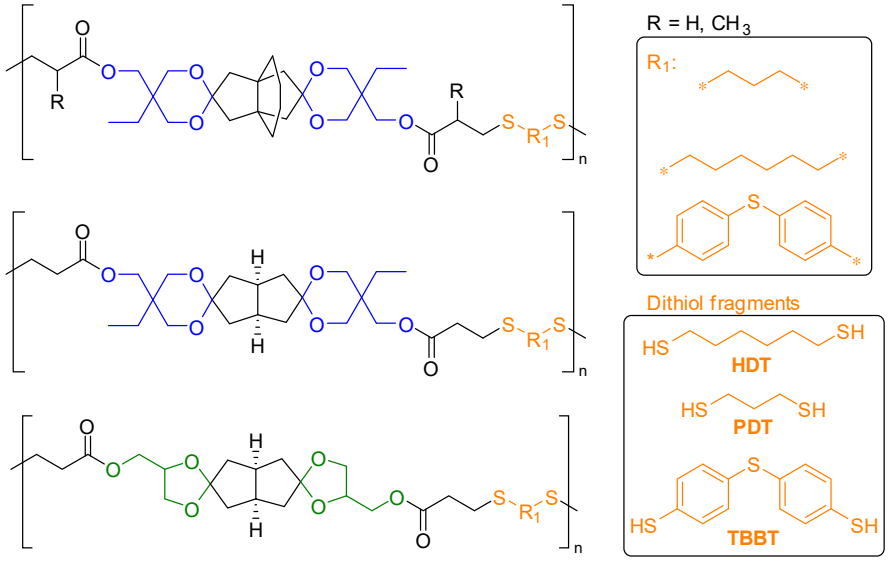

Figure 13. Polymer structures with different monomers. The TMP fragment is blue, the glycerol fragment is green, and dithiol fragments are shown separately in orange.

Initially, different organic bases were evaluated to find the most suitable one for polymerization. In a test reaction, monofunctional decanethiol was used in 5 eq. compared to **tTa**. The bases used for the test reaction were 1,8-Diazabicyclo[5.4.0]undec-7-ene (DBU), 1,4-diazabicyclo[2.2.2]octane (DABCO) or 1,5,7-triazabicyclo[4.4.0]dec-5-ene (TBD). The reactions were monitored by ^{1}H NMR spectroscopy using $CDCl_3$ as the solvent for 5 hours. After the first hour, similar conversions (ca 90%) were observed for DBU and TBD catalyzed reactions, but DABCO showed only a 25% decrease in acrylate signals, which can be explained by its lower pKa value. After 2 hours, there were no visible acrylate signals left in the reaction with DBU, while the test reaction using TBD did not show full conversion even after 5 hours, although the pKa-s DBU and TBD are similar.[109] Therefore, DBU was chosen as the base for the thiol-acrylate polymerizations.

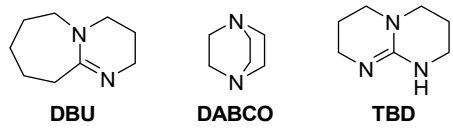

Figure 14. The structures of different organic bases were used to test the thiol-acrylate reaction.

Table 1. Results of thiol-acrylate polymerizations with different monomer combinations.

Entry	Polymer	M_n[a] (kg/mol)	M_w[a] (kg/mol)	$Đ$[a]	Yield[b] (%)	T_g (°C) DSC	T_g (°C) DMA	$T_{d,95\%}$ (°C)
1	Poly(gBa-HDT)	15	34	2.28	23	–16	–	324
2	Poly(tBa-HDT)	18	37	2.07	67	7	–	321
3	Poly(tTa-HDT)	27	99	3.61	70	27	22	320
4	Poly(tTma-HDT)	11	16	1.50	46	25	28	314
5	Poly(gBa-PDT)	15	29	1.92	70	–7	–	322
6	Poly(tBa-PDT)	26	48	1.82	77	15	–	320
7	Poly(tTa-PDT)	18	63	3.61	77	24	17	323
8	Poly(tTma-PDT)	14	37	2.59	68	32	27	315
9	Poly(tTa-TBBT)	22	39	1.75	77	40	35	317
10	Poly(tTma-TBBT)	12	30	2.45	46	46	36	282

[a]Measured by SEC in $CHCl_3$. [b]Isolated yield.

The results of the polymerization, molar distribution of the polymers, and thermal properties can be seen in Table 1. During the DSC measurements, an interesting effect was observed when different annealing temperatures were used. The polymers showed an increase in T_gs when the annealing was carried out at elevated temperatures (Figure 15). This change was explained by the crosslinking of residual (meth)acrylate end-groups. The crosslinking was also confirmed by the reduced solubility of some of the samples. Another possible explanation could be the opening of ketal rings at higher temperatures.

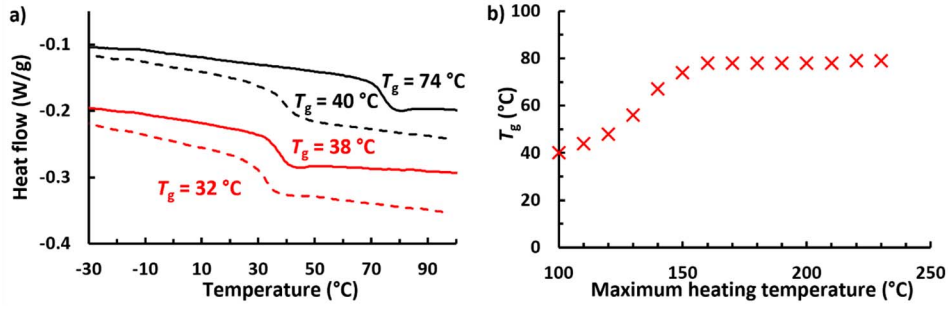

Figure 15. (a) DSC heating traces of **poly(tTa-TBBT)** (black) and **poly(tTma-PDT)** (red) recorded after annealing at 200 (solid lines) and 100 °C (dashed lines), respectively, showing the increase of T_g with the annealing temperature. (b) T_g measured by DSC analysis of **poly(tTa-TBBT)** after the sample had been heated to the given maximum temperature in the preceding heating scan.

The obtained M_ns were in the range 12–27 kg/mol, where the lower values were measured for the **gBa** and **tTma**-containing polymers. The low M_ns of the **gBa** polymers could be explained by the surprisingly lower polymerization rate of these polymers, which required a longer reaction time. The effect of the methacrylate groups on the M_n values could be explained by the lower reactivity compared to acrylates in Michael additions. The impact on the different components is indicated by the change in T_g values. Changes caused by the different dithiols correspond to their structure – the longer aliphatic HDT gives lower T_gs compared to shorter PDT and bis-aromatic TBBT as can be seen for **poly(tTa-HDT)** (27 °C), **poly(tTa-PDT)** (24 °C) and **poly(tTa-TBBT)** (40 °C) (Table 1, entries 3,7, and 9). The higher T_g of **poly(tTa-HDT)** can be explained by its higher M_n value. An expected increase in T_g can be seen when replacing the bicyclic **tBa** with tricyclic **tTa**, which increases the rigidity of the polymer chain, e.g., **poly(tBa-PDT)** (15 °C) and **poly(tTa-PDT)** (24 °C) (Table 1, entries 6,7). The polymers, including the **gBa** fragment, yielded the lowest T_gs, –16 and –7 °C, for **poly(gBa-HDT)** and **poly(gBa-PDT)** (Table 1, entries 1,5), respectively. The lower M_ns somewhat cause this, but likely also because the five-membered ketal ring has a lower rotational barrier compared to the six-membered ring of **tBa**. The polymers having dimethacrylate units showed slightly higher T_gs compared to the corresponding acrylate polymers due to more restricted chain mobility, e.g., 32 °C for **poly(tTma-PDT)** (Table 1, entry 8) compared to 24 °C for **poly(tTa-PDT)** (Table 1, entry 8). The thermal degradation temperatures of all the polymers were similar at around 300 °C.

3.1.3 Hydrolytic stability of the monomers and polymers

The hydrolytic stability of the monomers was investigated in 1:3 (v/v) solution of 10 mM aqueous trifluoroacetic acid (TFA) in CD_3CN at 20 °C and monitored by ^{1}H NMR. Both **tT** and **gB** were roughly 50% hydrolyzed after 8 hours. After 24 hours, 72 and 65% were hydrolyzed, respectively. Almost complete hydrolysis was observed after 1 week, resulting in a mixture of the initial diketones and triols – **TMP** and **T** for **tT** and glycerol and **B** for **gB**. It must be noted that **gB** is sensitive to HCl and water traces often present in $CDCl_3$, resulting in significant ketal bond hydrolysis after a few hours, and thus, DMSO-d_6 or CD_3CN and TFA as acid catalyst were used for NMR analysis of the compound.

Next, the hydrolytic stability of polymers was evaluated. The first experiments were conducted in aqueous solutions at pH = 0, 3, 8, 14 for 14 days at 37 °C. The samples were dried, weighed, and analyzed by SEC. No significant changes were observed in sample weight or molar mass under these conditions. As the hydrolysis in the aqueous environment was negligible, a 9:1 (v/v) mixture of acetone and 0.1 M HCl was used at 50 °C for 72 hours. The following SEC analysis showed a significant MW decrease (M_n was down to ca 1500 g/mol), and diketone signals were also visible in the ^{1}H NMR spectra. Finally, harsher conditions were used, and the 0.1 M HCl was replaced by 1 M aq. HCl in otherwise identical conditions. Faster degradation occurred, and the polymer samples dissolved after

just a few hours. After one week, about 60 mol% of diketone T was detected in the **poly(tTma-PDT)** sample. However, the glycerol-containing **poly(gBa-PDT)** degraded even faster, as it fully dissolved under 2 hours and after 4 hours showed complete hydrolysis in the ^{1}H NMR spectra, as seen in Figure 16. These results conclude that these polymers are stable in aqueous environments from pH 0 to 14 but can be hydrolyzed in acidic aqueous acetone.

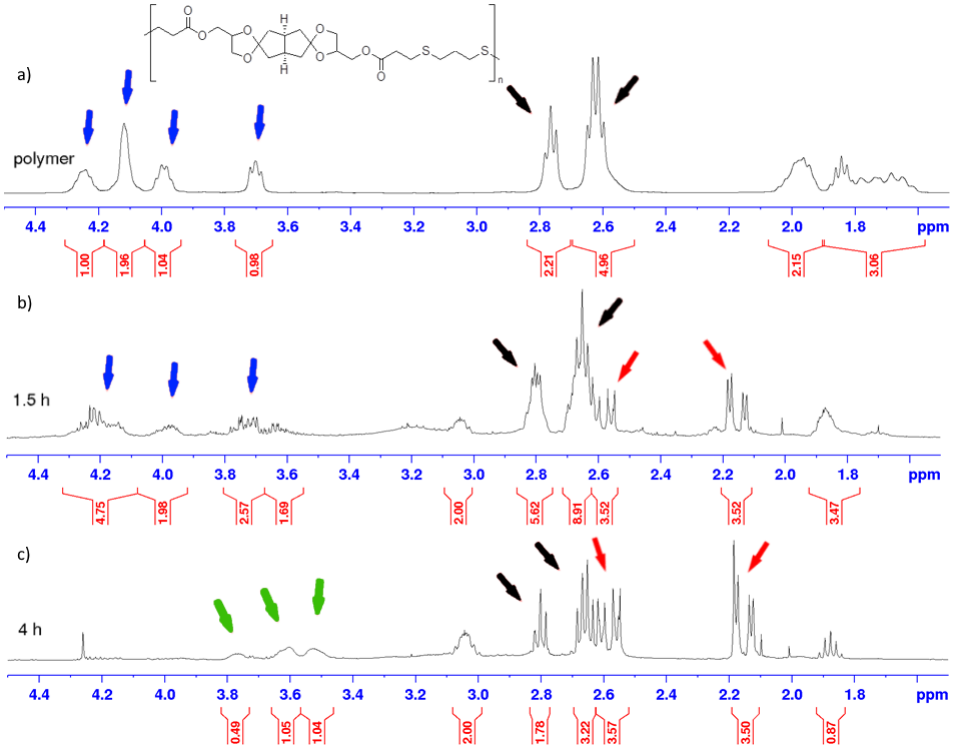

Figure 16. **Poly(gBa-PDT)** hydrolysis in 10% 1 M aqueous HCl in acetone monitored by ^{1}H NMR analysis. Red arrows indicate the formation of diketone signals, and blue arrows indicate the disappearance of the signals from the dioxalane ring. Green arrows point at the appearance of glycerol signals, and black arrows show the signals from the PDT fragment.

3.2 Isosorbide polymethacrylate networks via levulinate side group crosslinking using dihydrazides

PAPER II

This paper consists of three main parts: 1) synthesis of isosorbide 5-methacrylate-2-levulinate monomer and subsequent (co)polymerization with MMA; 2) crosslinking reaction using the obtained linear polymethacrylates and two dihydrazides; 3) investigation of the reversibility of the acylhydrazone bonds in the polymer network. The molecular weights and thermal properties were studied in all parts to determine the structure-property relations.

3.2.1 Enzymatic synthesis of isosorbide 5-methacrylate-2-levulinate monomer and (co)polymerization with MMA

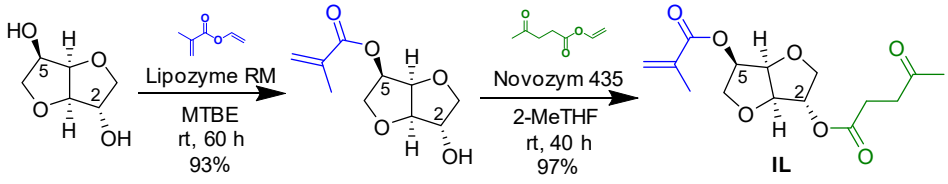

Scheme 8. Synthesis pathway for 5-methacrylate-2-levulinate isosorbide (**IL**).

Isosorbide 5-methacrylate was prepared using a method previously developed by our group.[32] The use of vinyl methacrylate with Lipozyme RM biocatalyst allows selective esterification of the 5-OH position. To carry out the second step, vinyl levulinate was first prepared using a palladium catalyzed method described in the literature.[110] The crude vinyl levulinate was filtered, washed with petroleum ether, and distilled.

Next, the esterification with vinyl levulinate was carried out similarly to the first step, but Novozym 435 was used a biocatalyst for the esterification instead. Isosorbide 5-methacrylate-2-levulinate (**IL**) was obtained in 97% yield without chromatographic separation (Scheme 8). Next, the **IL** monomer was used in free radical copolymerizations with MMA to vary the number of pendant ketone groups. Homopolymers of **IL** and MMA were prepared for comparison, while the copolymers comprised 20–95 mol% of MMA (Table 2). The ratio between MMA and **IL** was determined from ^{1}H NMR spectra and varied 1–3% from the targeted ratio. The T_gs of the copolymers correspond well to their composition – more MMA giving higher values. The degradation temperatures for the **PIL** and copolymers are from 203 to 222 °C, while $T_{d,95\%}$ for PMMA is higher. This is due to the thermal instability of the **IL** monomer inherited from the isosorbide bicycle.

Table 2. Polymerization and thermal data of the linear polymethacrylates.

Entry	Poly-methacrylate	Conversion (mol%)[a]		Monomer ratio (mol%)[b]		M_n (kg/mol)[c]	$Đ$[c]	T_g (°C)[d]	$T_{d,95\%}$ (°C)[d]
		MMA	IL	MMA	IL				
1	PMMA	72	–	100	0	31	1.5	127	246
2	P(MMA$_{95}$-IL$_5$)	68	78	95	5	32	1.6	115	206
3	P(MMA$_{90}$-IL$_{10}$)	73	78	90	10	49	1.6	95	206
4	P(MMA$_{80}$-IL$_{20}$)	57	72	81 (80)	19	37	1.6	96	222
5	P(MMA$_{60}$-IL$_{40}$)	63	82	57 (60)	43	27	1.6	89	203
6	P(MMA$_{40}$-IL$_{60}$)	59	82	37 (40)	63	20	1.7	75	217
7	P(MMA$_{20}$-IL$_{80}$)	58	75	21 (20)	79	16	1.6	77	209
8	PIL	–	81	0	100	42	2.0	74	210

[a]Determined by ^{1}H NMR data of crude polymer. [b]Determined from ^{1}H NMR data of dried polymer. [c]Measured by SEC in $CHCl_3$.

3.2.2 Crosslinking of linear polymers with dihydrazides

The linear polymers were crosslinked via the levulinic ketone groups using two dihydrazides with different lengths – malonic dihydrazide (**mdh**) with three carbons and adipic dihydrazide (**adh**) with six carbons (Scheme 9).

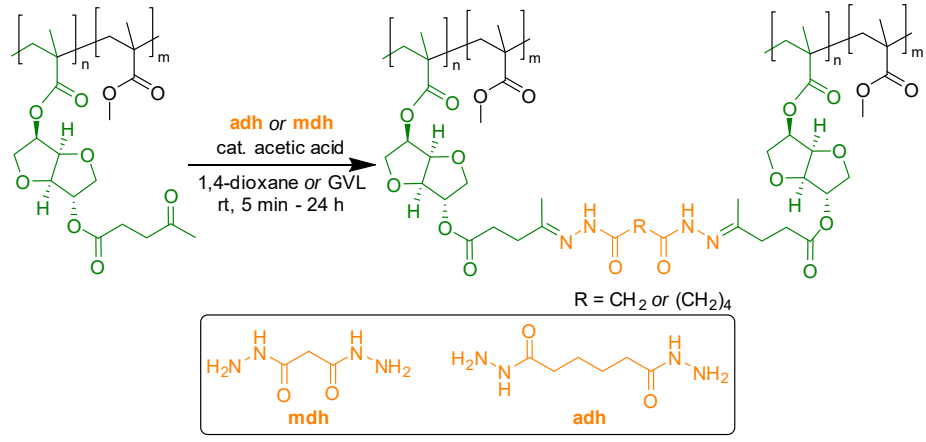

Scheme 9. The crosslinking reaction between linear copolymers using dihydrazides **mdh** and **adh** with a catalytic amount of acetic acid.

The amount of crosslinker used corresponded with half the number of ketone groups in the linear polymer, as one linker reacts with two polymer chains, e.g., for **P(MMA$_{20}$-IL$_{80}$)**, 40 mol% dihydrazide was used. For **PIL** and PMMA homopolymers, 5 and 10 mol% crosslinkers were used, respectively. The initial experiments were carried out in 4:1 mixture of 1,4-dioxane and water, commonly used in crosslinking reactions with hydrazides.[111,112] As 1,4-dioxane is an

unfavorable solvent from a green chemistry perspective, we looked for alternatives. GVL was used in subsequent reactions, as it dissolved the material similarly to 1,4-dioxane and is considered a green solvent.[113] The crosslinking reaction for **P(MMA$_{80}$-IL$_{20}$)-adh$_{10}$** was tested in both solvents, but no significant changes in thermal properties were observed (Table 3, Entries 7–8).

All the samples were insoluble in tested solvents, confirming the crosslinking. This was further proved by FTIR analysis of the samples, which showed C=N bonds present in all the crosslinked samples. Swelling ratios of the polymer networks were also analyzed. Still, no clear correlation was found between crosslinker amount and swelling ratios, most likely due to M_n differences between the linear copolymers. The gel content was over 90% for all the crosslinked polymers.

The crosslinked polymer networks showed higher degradation temperatures compared to their linear counterparts. The increases were up to 80 °C, which indicates the significant effect of crosslinking on the thermal stability of the material. Similarly to the linear polymers, the polymer networks showed a multistep degradation. Expectedly, the crosslinking increased T_gs compared to linear polymers. Inconsistencies of the T_g values of crosslinked polymers with increased amounts of crosslinker can be explained by the M_n differences of the linear starting material. As expected, the networks incorporating the shorter **mdh** achieved higher T_gs than those using **adh**, as seen in Table 3 (white and green lines, respectively) and Figure 17. The most significant difference was seen for **P(MMA$_{20}$-IL$_{80}$)**, where the crosslinked variant with **mdh** reached a 41 °C higher T_g compared to **P(MMA$_{20}$-IL$_{80}$)-adh$_{40}$** (entries 14–15).

Table 3. Reaction conditions and thermal data for crosslinked polymers with both crosslinkers.

Entry	Crosslinked polymer[a]	Solvent[b]	Reaction time	$T_{d,95\%}$ (°C)[c]	T_g (°C)[d]	Swelling ratio[e]
1	PMMA-adh$_{10}$	GVL:H_2O	24 h	273	126	*n.d.*[f]
2	PMMA-mdh$_{10}$	GVL:H_2O	24 h	281	127	*n.d.*[f]
3	P(MMA$_{95}$-IL$_5$)-adh$_{2.5}$	GVL:H_2O	19 h	286	125	*n.d.*[f]
4	P(MMA$_{95}$-IL$_5$)-mdh$_{2.5}$	GVL:H_2O	10 h	264	130	4.5
5	P(MMA$_{90}$-IL$_{10}$)-adh$_5$	1,4-dioxane:H_2O	5 min	282	109	3.2
6	P(MMA$_{90}$-IL$_{10}$)-mdh$_5$	GVL:H_2O	5 min	230	123	3.6
7	P(MMA$_{80}$-IL$_{20}$)-adh$_{10}$*	1,4-dioxane:H_2O	5 min	285	129	*n.d.*[f]
8	P(MMA$_{80}$-IL$_{20}$)-adh$_{10}$	GVL:H_2O	5 min	283	117	1.9
9	P(MMA$_{80}$-IL$_{20}$)-mdh$_{10}$	GVL:H_2O	5 min	235	133	2.3
10	P(MMA$_{60}$-IL$_{40}$)-adh$_{20}$	1,4-dioxane:H_2O	5 min	265	125	2.9
11	P(MMA$_{60}$-IL$_{40}$)-mdh$_{20}$	GVL:H_2O	5 min	223	165	3.9
12	P(MMA$_{40}$-IL$_{60}$)-adh$_{30}$	1,4-dioxane:H_2O	5 min	279	138	3.2
13	P(MMA$_{40}$-IL$_{60}$)-mdh$_{30}$	GVL:H_2O	5 min	229	166	2.7
14	P(MMA$_{20}$-IL$_{80}$)-adh$_{40}$	1,4-dioxane:H_2O	5 min	276	129	2.3
15	P(MMA$_{20}$-IL$_{80}$)-mdh$_{40}$	GVL:H_2O	5 min	236	170	3.0
16	PIL-adh$_5$	GVL:H_2O	30 min	273	72	6.6
17	PIL-mdh$_5$	GVL:H_2O	30 min	251	92	3.2

[a]The name of the crosslinked polymer is presented as **P(MMA$_x$-IL$_y$)-adh$_z$** or **P(MMA$_x$-IL$_y$)-mdh$_z$** in which ***z*** corresponds to the concentration of **adh** or **mdh** in mol%, respectively. [b]Solvent mixture with a 4:1 (v:v) ratio. [c]Determined by TGA at 5% weight loss under N_2. [d]Determined by DSC. [e]Determined in THF. [f]*n.d.* – not determined.

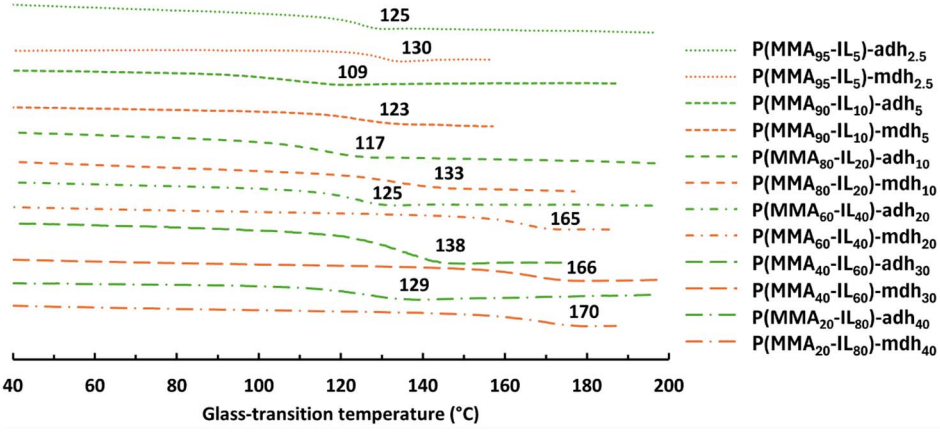

Figure 17. DSC curves of **adh** (green lines) and **mdh** (orange lines) crosslinked polymers. T_g values provided on the DSC curves.

Additionally, different amounts of **adh**, from 2.5 to 10 mol%, were used to crosslink **P(MMA$_{80}$-IL$_{20}$)** to see how it influences thermal properties. As expected, a higher crosslinker amount slightly increased degradation temperature and T_g due to increased chain restriction of the polymer network (Table 4).

Table 4. Crosslinked networks of P(MMA$_{80}$-IL$_{20}$) using different amounts of **adh** as crosslinker.

Entry	Crosslinked polymer[a]	Reaction time	$T_{d,95\%}$ (°C)[b]	T_g (°C)[c]
1	P(MMA$_{80}$-IL$_{20}$)-adh$_{2.5}$	24 h	275	102
2	P(MMA$_{80}$-IL$_{20}$)-adh$_5$	24 h	277	107
3	P(MMA$_{80}$-IL$_{20}$)-adh$_{10}$	5 min	283	117

[a]The name of the crosslinked polymer is presented as **P(MMA$_x$-IL$_y$)-adh$_z$** or **P(MMA$_x$-IL$_y$)-mdh$_z$** in which **z** corresponds to the concentration of **adh** or **mdh** in mol%, respectively. [b]Determined by TGA at 5% weight loss under N_2. [c]Determined by DSC.

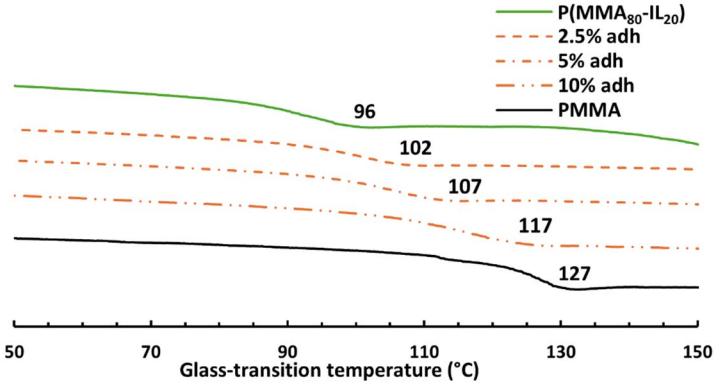

Figure 18. DSC curves of **P(MMA$_{80}$-IL$_{20}$)** with different amounts of **adh** crosslinker. Linear **P(MMA$_{80}$-IL$_{20}$)** and PMMA are added for comparison. T_gs are depicted on the respective curves.

3.2.3 De-crosslinking and re-crosslinking of dihydrazide crosslinked polymers

Next, the reversibility of the acylhydrazone bonds in the crosslinked polymer networks was tested in a 9:1 mixture of acetone and water with pH = 1 and pH = 4. The de-crosslinking reaction was monitored using ^{1}H NMR spectroscopy until no further changes were seen and the sample was fully dissolved. At pH = 1, the de-crosslinking was fast, taking less than 20 minutes, but at pH = 4, the reaction took significantly longer – up to 38 days. FTIR spectra of the dried samples confirmed the breaking of C=N bonds.

Table 5. Reaction time, molecular weight, and thermal data of polymers after de-crosslinking.

Entry	Crosslinked copolymer	Reaction time	De-crosslinked polymethacrylate[a]	M_n (kg/mol)[b]	$Đ^b$	$T_{d,95\%}$ (°C)[c]	T_g (°C)[d]
1	P(MMA$_{80}$-IL$_{20}$)-adh$_{10}$	20 min	*de$_1$*-P(MMA$_{80}$-IL$_{20}$)-adh$_{10}$	31	1.6	246	90
2	P(MMA$_{80}$-IL$_{20}$)-adh$_{10}$	12 days	*de$_4$*-P(MMA$_{80}$-IL$_{20}$)-adh$_{10}$	27	1.8	267	90
3	P(MMA$_{40}$-IL$_{60}$)-adh$_{30}$	20 min	*de$_1$*-P(MMA$_{40}$-IL$_{60}$)-adh$_{30}$	15	2.0	246	92
4	P(MMA$_{40}$-IL$_{60}$)-adh$_{30}$	17 days	*de$_4$*-P(MMA$_{40}$-IL$_{60}$)-adh$_{30}$	14	2.2	248	57
5	P(MMA$_{80}$-IL$_{20}$)-mdh$_{10}$	12 min	*de$_1$*-P(MMA$_{80}$-IL$_{20}$)-mdh$_{10}$	31	1.8	242	109
6	P(MMA$_{40}$-IL$_{60}$)-mdh$_{30}$	38 days	*de$_4$*-P(MMA$_{40}$-IL$_{60}$)-mdh$_{30}$	11	2.4	247	86

[a]de$_1$ and de$_4$ correspond to using pH = 1 and pH = 4, respectively. [b]Determined by SEC in THF using poly(ethylene oxide) standards. [c]Determined by TGA at 5% weight loss under N_2. [d]Determined by DSC.

The de-crosslinked polymers in Table 5 showed very similar molecular weights compared to the linear polymers **P(MMA$_{80}$-IL$_{20}$)** and **P(MMA$_{40}$-IL$_{60}$)** used to prepare the crosslinked polymers (Table 2, entries 4,6). On the other hand, the $T_{d95\%}$ and T_g values were slightly higher compared to the initial linear polymers, most likely due to some hydrazone linkages remaining attached to one levulinic ketone group. The de-crosslinked polymers were subsequently re-crosslinked using the same method as for initial crosslinking. The resulting crosslinked polymers were again compared to the first batch of polymer networks. The thermal data of the re-crosslinked polymers corresponded with the previously obtained values, and the T_g values even reached slightly higher values. This circular pathway confirms the reversibility of the acylhydrazone crosslinking reaction and thus enables the chemical recycling of these polymers.

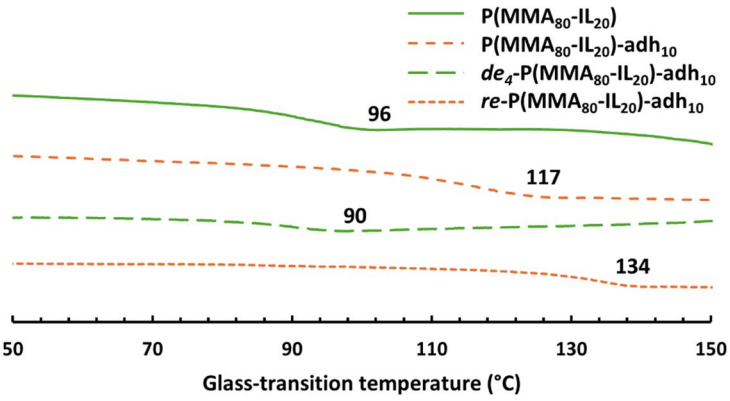

Figure 19. DSC curves of **P(MMA$_{80}$-IL$_{20}$)**, after crosslinking **P(MMA$_{80}$-IL$_{20}$)-adh$_{10}$**, de-crosslinking and re-crosslinking. T_gs are depicted on the respective curves.

3.3 Creating a combined framework for a life-cycle assessment method for emerging technologies

PAPER III

This paper includes three main parts: 1) the development of an LCA framework combining ex-ante and prospective LCA methods for emerging bio-based technologies; 2) the application of the said method to two bio-based polymers – isosorbide methacrylate and vanillic acid derived methacrylate polymers, which are compared with fossil counterparts – PMMA, PS, and PC; 3) results of the analysis.

3.3.1 Integrating ex-ante and prospective LCA methods

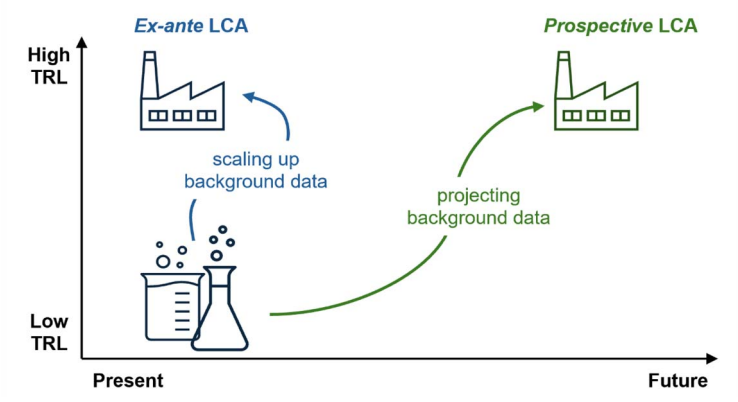

Figure 20. Visual representation of ex-ante and prospective LCA differences in time scale.

The development of an integrated ex-ante and prospective LCA approach was divided into three phases. Phase I includes the identification of fossil counterparts to the specific bio-based polymer to reach a fair reference point. As for bio-based polymers that are the equivalent of fossil-based materials with just bio-based feedstock, it is straightforward. However, for new materials, a one-to-one comparison is more complicated, as the new material can have some added benefits, such as, for example, enhanced thermal properties or recyclability. Next, the functional unit has to be defined to allow comparison on the same scale. Finally, system boundaries must be determined – the theoretical factory should be viable where planned – not surpassing the potential amount of locally available feedstock. A complete cradle-to-grave approach should be considered similarly, considering the likely carbon emissions and other impacts based on the local energy production matrix. The previous steps lead to value chain design, which considers all the last considerations.

Phase II consists of the different stages of ex-ante LCA – scaling up the process. First, a process description is designed by taking lab-scale experimental procedures and turning them into an inventory with specific amounts of reagents, solvents, energy usage, etc. All irrelevant steps for an industrial process, e.g., some purification steps, are removed from the description. Next, a flowchart is designed for the industrial plant, highlighting all the equipment, machinery, and inputs needed for all steps. Then, potential process synergies are identified. These include recovery and reuse of solvents and reagents plus heat recovery. After that, the process yields are projected to be close to stochiometric values and closer to theoretical maximum yields, and side streams are considered with the improved yields from the last step. These side streams include co-products, fugitive emissions, and residues. Co-products that have commercial value can help alleviate the environmental impacts by taking a part of the overall impact. In contrast, emissions have a negative effect and can pinpoint potential hotspots for improvement of the process. Finally, all process steps are scaled up individually and summed up to obtain final impact values for ex-ante LCA.

Phase III combines the steps of prospective LCA by looking at the future. It considers different factors, such as economic, environmental, and social changes, specifically energy production, the transportation sector, and various policies, e.g., the Paris Agreements.[114] The PREMISE software package has the resources to allow the LCA inventories to be projected into the future.[115] Finally, an uncertainty analysis of key contributors is conducted for a more robust and fair result.

3.3.2 Applying the combined methodology to a case study

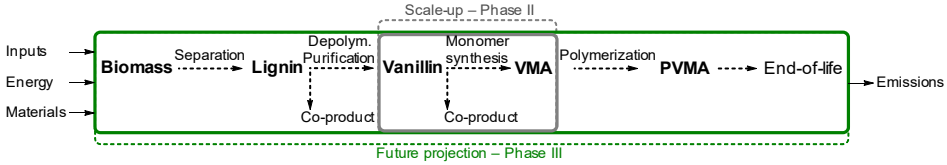

Scheme 10. An example of a simplified biorefinery setup for the production setup of **PVMA** from biomass.

An idealized biorefinery system (Scheme 10) is used to estimate the environmental impacts of two different bio-based polymers: isosorbide polymethacrylate (**PIMA**), vanillic acid derived polymethacrylate (**PVMA**) compared to their commercial counterparts – polystyrene (PS), PMMA and polycarbonate (PC). Four different synthesis pathways were evaluated for **IMA**: in the first step, either vinyl methacrylate or methacrylic anhydride was used; in the second step, either acetic anhydride or vinyl acetate. A functional unit of 1 kg was used in the calculations, meaning everything, e.g., the amount of solvent used or starting material used, is calculated based on 1 kg of polymer produced.

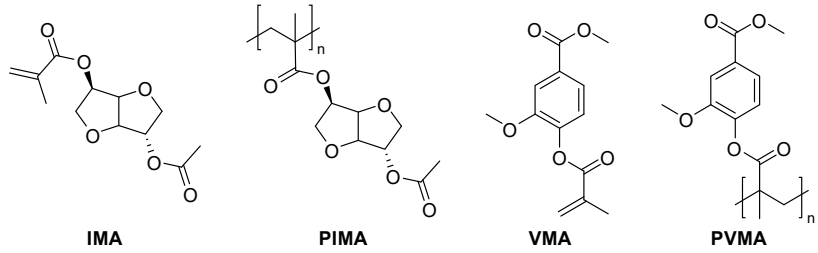

Figure 21. Structures of the two bio-based methacrylate monomers and polymers, isosorbide-derived methacrylate (**P**)**IMA** and vanillic acid derived methacrylate (**P**)**VMA**, investigated in the LCA study.

Impacts from biomass pretreatment are allocated among cellulose, hemicellulose, and lignin-based on a mass basis. Impacts from monomers production are allocated among monomers and co-products on a mass basis.

The LCA inventory is obtained following the Phase II procedure in section 3.3.1. Three different locations are used for calculations: the European Union average, Norway, and Estonia. This corresponds to different biomass compositions, renewable energy availability, and transport distances between materials and the plant, which mainly impact CO_2 emissions. Wood residue combustion is used in heat reactors as the only impact comes from their collection and transport. Each synthesis step from biomass to the starting material of the laboratory processes is taken from a database with the corresponding impact factors. Unfortunately, we had to exclude vanillin conversion to vanillic acid due to a lack of data. The lab-scale scale-up is done in a two-way discussion between the chemists

and LCA analysts to ensure the usage of relevant assumptions during the process. Thus, a 97% recovery rate was selected to recover primary solvents; some washing steps were removed. Additionally, 100% yields were assumed to highlight a best-case scenario. The polymerization step is estimated to use similar conditions to commercial styrene and MMA polymerization at 1.0 kg CO_2-eq/kg polymer. Incineration was selected as the end-of-life treatment, as it is most common for durable plastics such as PMMA, PS, and PC. Climate change impacts are calculated using the IPCC[116] 100-year Global Warming Potential (GWP), freshwater eutrophication, ozone depletion, marine eutrophication, fossil depletion, and human toxicity are calculated using ReCiPe 2016.[117]

Prospective LCA uses the PREMISE 1.2.5 package to transform the current database into future scenarios. Historical patterns were also taken into account to extrapolate current trends. Also, the climate change mitigation targets of the three countries were considered. The primary changes for future scenarios include more efficient and cleaner energy production, transportation, and usage of bio-based chemicals.

3.3.3 Results of the analysis

The application of ex-ante LCA leads to 91 and 97% reductions in climate change impacts for **PIMA** and **PVMA**, respectively, using the EU average electricity mix. The most significant factor in this change is the recovery of the primary solvents during the reaction.

Using the prospective LCA assumptions, the climate change impact of **PVMA** and **PIMA** was reduced by 31, 30, and 42% in the EU, Norway, and Estonia, respectively, in 2035. In 2050, the impacts were reduced by an additional 21, 8 and 25% (Figure 22). Fossil counterparts used for comparison are already highly optimized processes and, therefore, do not change over time. From a 10–15-year perspective, both **PVMA** and **PIMA** show the potential to have lower impacts compared to PMMA, PS, and PC.

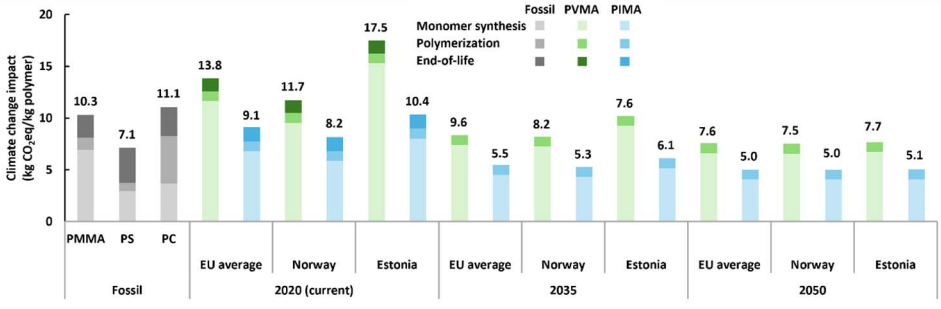

Figure 22. Climate change impacts of **PVMA** and **PIMA** based on different energy mixes (EU average, Norway, Estonia) projected for 2020 (present), 2035, and 2050. Fossil-based PMMA, PS, and PC are used as comparisons.

Other environmental impacts investigated include fossil depletion, freshwater and marine eutrophication, human toxicity, and ozone. After applying the combined ex-ante and prospective LCA method, **PIMA** shows lower impacts in all categories besides marine eutrophication compared to PC, which has the worst impacts of the fossil polymers in all categories besides marine eutrophication. This is caused by using enzymes in the synthesis and can be reduced by their reuse. **PVMA** has higher impacts than PIMA in most categories but is still lower than PC in all categories besides ozone depletion. One of the reasons for this is the use of NaOH during lignin processing. Compared to PMMA, both bio-based polymers have higher impacts on freshwater eutrophication and ozone depletion but lower impacts on marine eutrophication and fossil depletion; human toxicity impacts are similar for all three. To compete against PMMA, energy usage needs to be more efficient, and the process needs to include the methacrylic co-products. Additionally, **PVMA** needs a more efficient lignin depolymerization process to be genuinely competitive.

This combined framework still has room for improvement since the data needed to carry out in-depth analyses can be missing, especially for less used and emerging chemicals. The ex-ante LCA is done with assumptions that can vary in actual scale-up, leading to underestimation in, e.g., energy usage. Still, as it only contributes to roughly 10% of the overall impacts, it is not a significant factor. This study cannot estimate the availability of biomass for the chemical sector as there are other competing sectors, such as transportation and aviation, where biomass might not even be the optimal solution to reducing environmental impacts.

3.4 Lignin-based aromatic polymethacrylates

PAPER IV

This paper includes three main parts: 1) two-step conversion of three lignin-derived carboxylic acids into polymethacrylates; 2) polymerization and copolymerization with methyl methacrylate (MMA) and the characterization of these polymers; 3) life-cycle assessment and toxicology measurements.

3.4.1 Monomer synthesis

Three carboxylic acids – *p*-hydroxybenzoic acid (**B**), vanillic acid (**V**), and syringic acid (**S**), were first converted into methyl esters via the acid functionality using conventional acidic esterification under reflux in MeOH (Scheme 11). Trans-esterification using MMA was tested to obtain the methacrylate monomers, but this resulted in low yields. Next, methacrylic anhydride was used for the methacrylation. Still, the yields remained moderate, 48–73%, due to a considerable number of byproducts containing di- and oligomers from condensation reactions and possibly some products from side reactions in the aromatic ring. Thus, chromatographic separation was needed to obtain pure products. Finally, when

anhydride was replaced by methacryloyl chloride, the desired monomers **BMA**, **VMA,** and **SMA** were obtained without chromatography in 93, 90, and 92% yields, respectively. In this case, the usual chlorinated solvents were successfully replaced by bio-based 2-MeTHF without a significant impact on the yield.

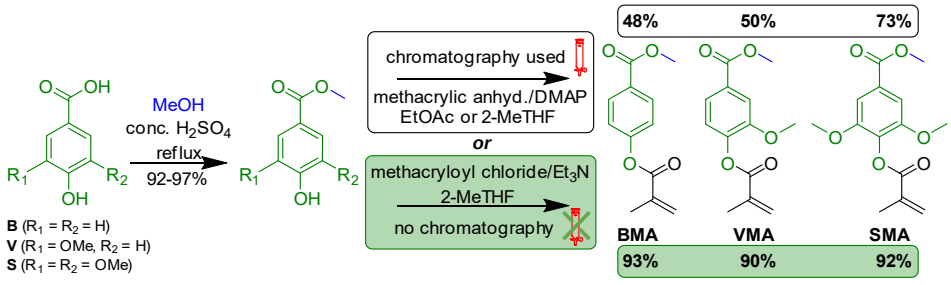

Scheme 11. Synthesis of the methacrylate monomers **BMA**, **VMA,** and **SMA** using two different methods.

3.4.2 Homopolymerization of methacrylates and copolymerization with MMA

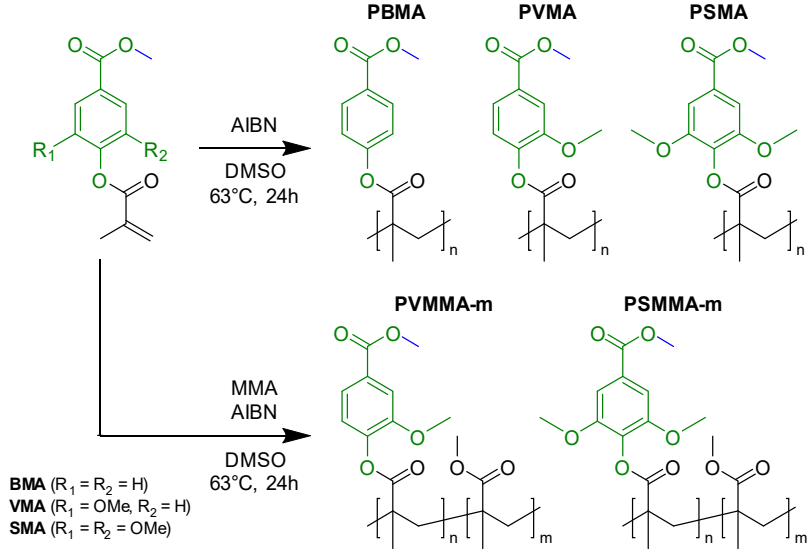

Scheme 12. Polymerization and copolymerization of methacrylate monomers in DMSO.

At first, different solvents, such as EtOAc, toluene, $CHCl_3$, DMSO, γ-valerolactone (GVL), and 2-MeTHF, were evaluated as the polymerization medium. EtOAc gave lower yields on average than other solvents and also resulted in vastly different M_n values for the three monomers, ranging from 16 to 48 kg/mol (Table 6, entries 4, 9, 14). Similar inconsistencies between the monomers were observed using GVL (M_n from 14 to 94 kg/mol) (Table 6, entries 2, 10, 13) and

toluene (8 to 38 kg/mol) (Table 6, entries 3, 6, 7). Using toluene, the amount of AIBN had to be reduced to 0.1 mol% to achieve masses over 30 kg/mol (Table 6, entry 7). 2-MeTHF was also tested, but the molecular weight obtained was relatively low at 15 kg/mol (Table 6, entry 11). Bio-based GVL afforded a high M_n of 94 kg/mol for PSMA, but was difficult to remove during drying. Polymerizations in DMSO were the most consistent, yielding M_ns over 50 kg/mol for all three monomers. Thus, DMSO was selected for all subsequent polymerizations.

Table 6. Polymerization in different solvents.

Entry	Polymer	Solvent	M_n[a] (kg/mol)	$Đ$[a]	Isolated yield (%)
1	PBMA	DMSO	62	3.6	71
2	PBMA	GVL	14	2.1	64
3	PBMA	Toluene	19	2.3	67
4	PBMA	EtOAc	48	2.4	45
5	PVMA	DMSO	53	3.8	81
6	PVMA	Toluene	8	1.8	40
7	PVMA	Toluene[b]	38	2.9	47
8	PVMA	Chloroform	36	2.5	50
9	PVMA	EtOAc	48	2.6	57
10	PVMA	GVL	48	3.7	87
11	PVMA	2-MeTHF	15	2.5	76
12	PSMA	DMSO	53	4.1	67
13	PSMA	GVL	94	2.1	59
14	PSMA	EtOAc	15	2.1	31
15	PSMA	Chloroform	50	1.9	55

[a]Measured by SEC in THF. [b]0.1 mol% of AIBN used.

The homopolymers had rather wide molecular weight distribution ranging from 3.1 to 3.6, which can be caused by the use of DMSO, as observed by Nonque et al.[36] The thermal degradation temperatures of the polymers were high, between 277–313 °C. The T_gs were all over 100 °C, i.e., 106 and 128 °C for **PBMA** (Table 7, entry 1) and **PVMA** (Table 7, entry 3) respectively, and in the case of **PSMA**, reaching as high as 197 °C (Table 7, entry 4). A higher MW sample **PBMA-2** reached a significantly higher T_g than **PBMA**, suggesting that the M_n at infinite molar mass using Flory-Fox equation is about 160 °C. An apparent increase in T_gs was observed with an increasing number of methoxy groups attached to the aromatic cycle. This indicates that the additional groups limit the movement of the polymer chain. The large temperature window between T_g and $T_{d95\%}$ for all the polymers makes their melt processing potentially viable.

Table 7. Polymerization and thermal data of aromatic polymethacrylates prepared in DMSO.

Entry	Polymer	AIBN (mol%)	MMA content (mol%)		M_n[b] (kg/mol)	$Đ$[b]	Isolated yield (%)	T_g[c] (°C)	$T_{d,95\%}$[d] (°C)
			Target	Obtained[a]					
1	PBMA	0.500	–	–	62	3.6	71	106	277
2	PBMA-2	0.500	–	–	121	3.1	77	133	280
3	PVMA	0.500	–	–	60	3.6	84	128	313
4	PSMA	0.500	–	–	54	3.6	46	197	307
5	PVMMA-25	0.125	25	22	236	1.9	91	134	292
6	PVMMA-50	0.250	50	44	93	2.6	78	127	281
7	PVMMA-75	0.375	75	74	69	2.7	79	125	271
8	PSMMA-75	0.375	75	69	54	2.8	83	139	258

[a]Determined from ^{1}H NMR spectra. [b]Measured by SEC in THF. [c]Measured using DSC. [d]Thermal degradation temperature at a 5% mass loss.

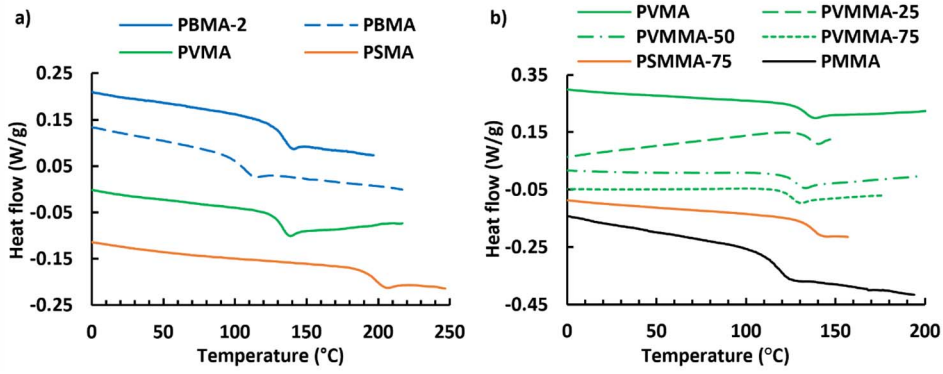

Figure 23. DSC curves of the polymethacrylate homopolymers (a) and copolymers with MMA (b).

In addition to homopolymers, copolymers containing 25–75 mol% MMA were prepared with **VMA** and **SMA** (Table 7, entries 5–8) with the aim of improving the thermal properties of PMMA. The actual ratio between MMA and **VMA**/**SMA** was determined from ^{1}H NMR spectra of the dried copolymer samples, and it was found to differ by up to 6% compared to the target values. As the amount of AIBN was increased when a higher amount of MMA was used, the M_ns of the copolymers decreased. The copolymers also had slightly lower polydispersity values, likely due to MMA's high reactivity. Degradation temperatures for all copolymers were relatively high, from 258 to 292 °C. The copolymers with **VMA** exhibited similar T_gs: 134, 127 and 125 °C for **PVMMA-25**, **PVMMA-50** and **PVMMA-75** (Table 7, entries 5–7), respectively, compared to homopolymer **PVMA** (128 °C). This is because the obtained T_g value for the MMA control sample, polymerized under the same conditions, was 124 °C, i.e., higher than the

usually reported value of 105 °C. The differences in T_g values of the **PVMMA** series are due to M_n differences. Compared to **PVMMA-75**, **PSMMA-75** reached a higher T_g of 139 °C, making **SMA** more desirable to use as a T_g-raising component in MMA. Finally, the rheological properties of **PVMA** and **PSMMA-75** were investigated. Both samples showed high stability in the melt state and thus were deemed melt-processable and potential candidates for an extensive range of applications.

3.4.3 Life cycle and cytotoxicity assessment

Besides the polymer properties, the effect of the polymers on the environment is also essential. That is why a LCA analysis was carried out for monomers **VMA** and **SMA**. The evaluated categories, 100-year global warming potential (GWP 100), terrestrial acidification, and freshwater eutrophication, are especially relevant for bio-based polymers. Both monomer synthesis pathways were investigated using methacrylic anhydride (**-anh**) or methacryloyl chloride (**-acl**). Obviously, at the lab-scale, the impacts of the synthesis procedure are very high, but using the methodology developed in Paper III allows a fairer comparison with industrial processes.

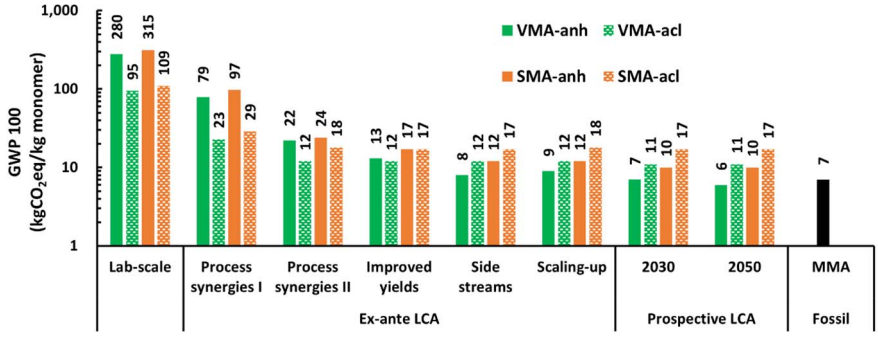

Figure 24. 100-year global warming potential of monomers **VMA** and **SMA**, using both synthesis pathways **anh** and **acl**, compared to fossil MMA.

After ex-ante LCA, the impacts were reduced by about 90% in all three categories. The effect on GWP 100 can be seen on Figure 24. The main contributor to high impacts were solvents, which should be recovered during the process, reducing the impacts significantly. Additionally, the **acl** method reached higher impact values because the production of 2-MeTHF currently has higher environmental impacts than EtOAc used in the **anh** method. Thus, the lowest environmental impacts were calculated for **VMA-anh**, which were close to the values of MMA for GWP 100 but somewhat higher for terrestrial acidification and freshwater eutrophication (Figure 25). It must be noted that the production of MMA has been optimized for decades and is highly efficient, having a comparatively low environmental impact.

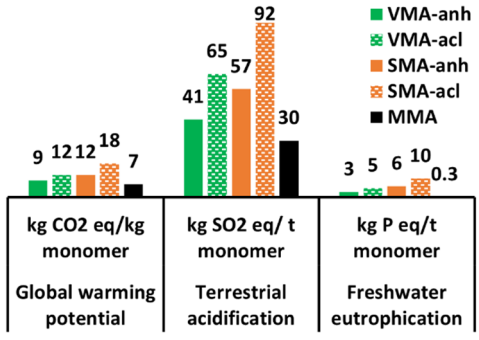

Figure 25. The environmental impacts of ex-ante LCA for **VMA** and **SMA** using two different methods (**anh** and **acl**) compared to MMA.

Finally, the cytotoxicity of the methacrylate monomers and polymers was evaluated on the HeLa cell line using MTT assay during 24 and 48 hours, respectively. The observed cell viabilities were significantly higher for polymers in all concentrations compared to monomers (Figure 26). This was expected because of the high reactivity of methacrylate groups towards living organisms. Again, the results obtained for **PVMA** were similar to the values for PMMA, a polymer widely used in medical applications. As such, **PVMA** can be considered non-toxic, while **PBMA** and **PSMA** have low toxicity.

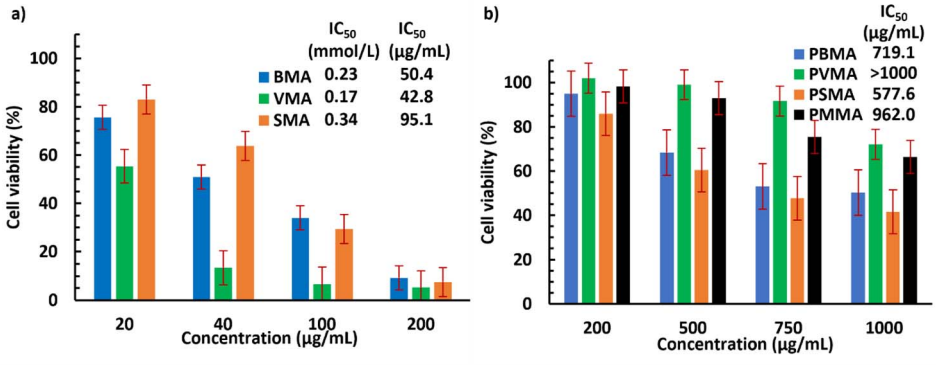

Figure 26. Cell viability of HeLa cells after exposure to the methacrylate monomers during 24 h (a) and polymers during 48 h (b).

3.5 Indoline polyacrylates and copolymers

PAPER V

This project investigates naturally occurring heterocyclic compounds – indole and its derivative, indoline, as building blocks for high-T_g polymer materials.

3.5.1 Synthesis of indole and indoline (meth)acrylates

Initially, four different monomers: indole acrylate (**NdA**) and methacrylate (**NdMA**), indoline acrylate (**NdlA**) and methacrylate (**NdlMA**), were considered for obtaining poly(meth)acrylates (Figure 27).

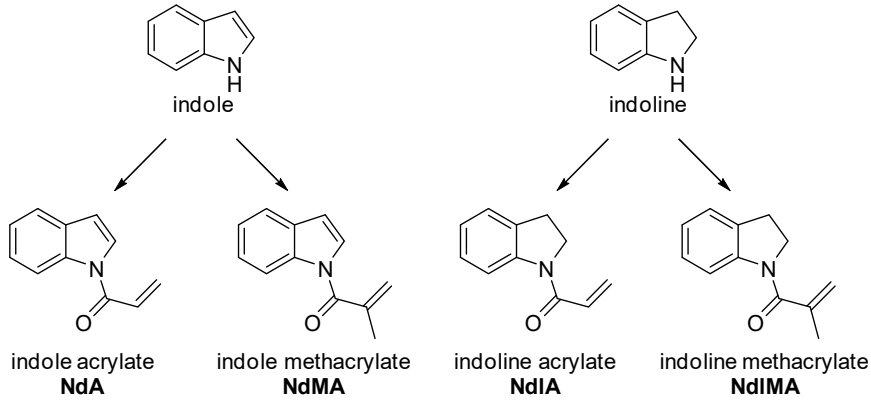

Figure 27. Potential (meth)acrylates obtainable from indole and indoline.

A literature method was used to synthesize **NdlA** (Scheme 13).[118] In this chromatography-free method, the indoline acrylate was precipitated into cold saline water. An 87% yield was obtained for indoline acrylate.

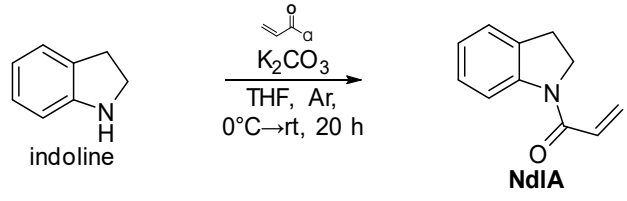

Scheme 13. Synthesis procedure for indoline acrylate.

Synthesis of indole (meth)acrylates was significantly more difficult. Very low conversions were achieved using a similar method to the one used for indoline. Acylation with methacrylic anhydride did not work at all and some insoluble particles formed. Finally, dehydrogenation of indoline acrylate with 2,3-dichloro-5,6-dicyano-1,4-benzoquinone (DDQ) was tested, which gave a yield of 34% after chromatographic purification (Scheme 14).[118]

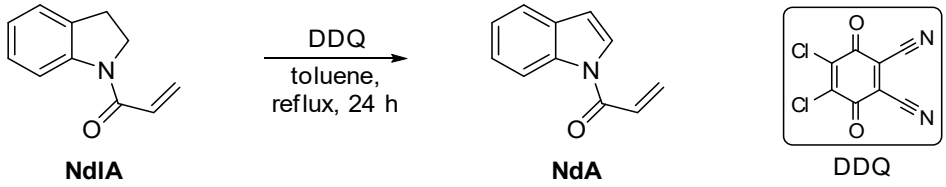

Scheme 14. Dehydrogenation of indoline acrylate into indole acrylate.

3.5.2 Polymerization of indole and indoline (meth)acrylates

Free radical polymerization using AIBN was used for all the polymerization reactions. Different solvents were tested, and DMSO worked the best on average. Using $CHCl_3$ as the solvent did not yield a polymer (Table 8, entry 5); in 2-MeTHF resulted in a low M_n (Table 8, entry 4). These test polymerizations were carried out using **NdlA** monomer. but indoline methacrylate and indole acrylate did not polymerize under the same conditions at all or gave very low conversions. This may be explained by the additional double bond in the heterocycle of indole, which can stabilize the molecule.[59]

Table 8. Homopolymerizations of the heterocyclic (meth)acrylates using 0.5 mol% AIBN.

Entry	Monomer	Solvent	M_n[a] (kg/mol)	$Đ$[a]	Isolated yield (%)	T_g[b] (°C)	$T_{d,95\%}$[c] (°C)
1	NdlA	toluene	17	2.2	75	169	365
2	NdlA	DMSO	28	3.3	79	173	379
3	NdlA[d]	DMSO	34	2.8	71	172	383
4	NdlA	2-MeTHF	4	1.9	65	*n.d.*	*n.d.*
5	NdlA	$CHCl_3$	*no polymerization*		*n.d.*	*n.d.*	*n.d.*
6	NdMA	DMSO	*no polymerization*		*n.d.*	*n.d.*	*n.d.*
7	NdA	DMSO	*no polymerization*		*n.d.*	*n.d.*	*n.d.*
8	NdlMA	DMSO	*no polymerization*		*n.d.*	*n.d.*	*n.d.*

[a]Determined by DSC. [b]Measured using DSC. [c]Determined by TGA at 5% mass loss. [d]0.25 mol% AIBN was used. *n.d.* – not determined.

The measured T_g-s were high – up to 173 °C, which made the polymers quite brittle. Additionally, the degradation temperatures are exceptionally high – from 365 to 383 °C, leaving room for a wide processing window.

3.5.3 Copolymerization with different commercial (meth)acrylates

First, copolymerization was tested using indole methacrylate with MMA to increase the reactivity by adding MMA. Unfortunately, these tests were unsuccessful, as the 1^H spectrum of the first test (Table 9, entry 1) did not show polymerization. The second test with indoline methacrylate (Table 9, entry 2) only had PMMA signals in the polymer sample, which meant that the heterocyclic monomer was not included in the polymer chain.

Next, to add more variability in T_gs (glass transition temperatures), MMA and butyl acrylate (butA) were used in copolymerizations with indoline acrylate. The obtained M_ns were in the range of 50 to 82 kg/mol.

Table 9. Copolymerizations of heterocyclic (meth)acrylates with MMA and butA using 0.5 mol% AIBN.

Entry	Polymer	Monomer ratio (mol%)[a]		M_n[c] (kg/mol)	$Đ$[c]	Isolated yield (%)	T_g[d] (°C)	Calc. T_g[e] (°C)	$T_{d,95\%}$[f] (°C)
		Feed	Actual[b]						
1	P(NdMA$_{50}$MMA$_{50}$)[g]	50%	–	–	–	*n.d.*	*n.d.*	*n.d.*	*n.d.*
2	P(NdlMA$_{75}$MMA$_{25}$)[h]	75%	0%	–	–	*n.d.*	*n.d.*	*n.d.*	*n.d.*
3	P(NdlA$_{75}$MMA$_{25}$)	75%	69%	65	2.9	65	166	161	390
4	P(NdlA$_{50}$MMA$_{50}$)	50%	51%	62	3.3	73	153	149	388
5	P(NdlA$_{25}$MMA$_{75}$)	25%	21%	53	3.3	78	140	136	376
6	P(NdlA$_{75}$butA$_{25}$)	75%	74%	50	3.0	83	124	117	371
7	P(NdlA$_{50}$butA$_{50}$)	50%	52%	82	2.7	71	78	62	368

[a]Percentage value depicts the heterocyclic monomer. [b]Determined by ^{1}H NMR of the crude polymer. [c]Measured by SEC in THF. [d]Measured using DSC. [e]Calculated from the feed ratio of monomers using T_g values for both components. [f]Determined by TGA at 5% weight loss under N_2. [g]No polymerization. [h]Only PMMA in dried polymer spectrum. *n.d.* – not determined.

All the copolymers had a similar thermal decomposition temperature to the homopolymers ranging from 365 to 390 °C (Table 9). The T_gs of the copolymers with both MMA and butA matched the predicted values (Table 9, entries 3–5 and 6,7, respectively). The DSC results show that depending on the added commercial polymer, a wide range of copolymers with T_gs ranging from 78 to 166 °C could be obtained.

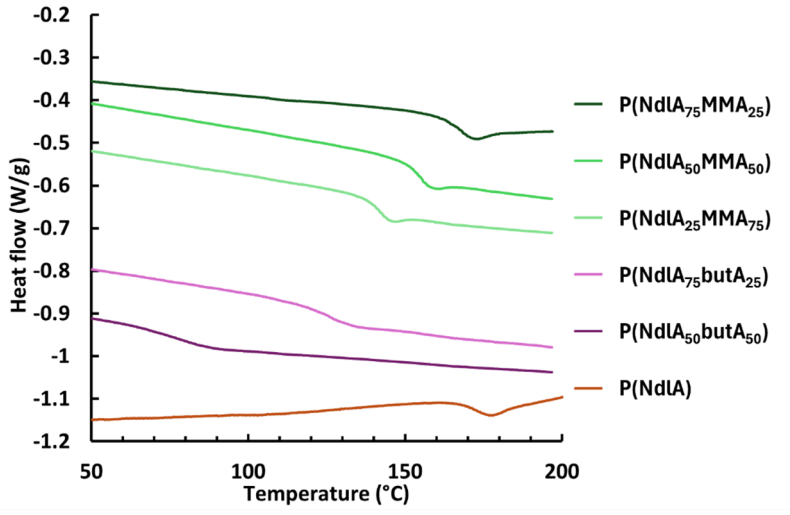

Figure 28. DSC graphs of indoline homopolymer and copolymers.

4. MATERIALS, METHODS, AND EXPERIMENTAL DETAILS

Detailed descriptions of materials and methods used, experimental and analytic procedures, and other information can be found in papers I–IV.

Additional experiments that are not included in publications, and additional topics that may not result in publications, are described in the following chapters. All the reagents and solvents were used as received, if otherwise not specified.

A 400 MHz Bruker spectrometer was used for NMR analysis of the compounds at 400 and 101 MHz for ^{1}H and ^{13}C, respectively. Residual solvent signals were used for calibration (7.26 ppm and 77.16 ppm for $CDCl_3$). Silica gel 60 (0.040−0.063 mm, 230−400 mesh) was used for flash chromatography.

4.1 Synthesis of indoline acrylate

This synthesis was carried out using a modified procedure from the literature.[118] Indoline (2.0 mL, 2.1 g, 15.6 mmol) was dissolved in 30 mL of THF, K_2CO_3 (4.36 g, 31.5 mmol) was added, and the flask was flushed with argon and capped with a septum. The mixture was cooled using an ice bath, and acryloyl chloride (1.56 g, 1.37 mL, 17.2 mmol) was added for 10 minutes. The reaction mixture was stirred for 4 hours and precipitated into 120 mL of ice-cold water. Next, NaCl (2.0 g) was added, and the solution was stirred for 30 minutes to assist with the precipitation of the product. The solids were filtered, washed with distilled water, and dried under vacuum. Indoline acrylate (2.11 g) was obtained as a white powder with a 79% yield.

^{1}H NMR (400 MHz, $CDCl_3$): δ 8.33 (br d J_{HH} = 7.5 Hz, 1H), 7.23 (m, 2H), 7.07 (t, J_{HH} = 7.4 Hz, 1H), 6.56 (m, 2H), 5.82 (d, J_{HH} = 9.9 Hz, 1H), 4.20 (t, J_{HH} = 8.2 Hz, 2H), 3.25 (m, 2H). (Figure A1)

^{13}C NMR (100 MHz, $CDCl_3$): δ 163.9, 142.9, 131.6, 129.1, 129.0, 127.7, 124.6, 124.1, 117.6, 48.1, 28.1. (Figure A2)
The NMR spectra matched the ones in the literature.[118]

4.2 Synthesis of indole acrylate

This synthesis was carried out using a modified procedure from the literature.[118]

Indoline acrylate (1.78 g, 10.2 mmol) was dissolved in 40 mL of toluene, DDQ (2.85 g, 12.5 mmol) was added, and the mixture was refluxed for 22 hours. After cooling down, 40 mL of EtOAc was added, and the organic phase was washed with 25 mL of water and 25 mL of brine consecutively. Then, it was dried on $MgSO_4$ and concentrated under reduced pressure. Next, the product was purified

via flash chromatography (5% EtOAc in petroleum ether) to obtain 602 mg of the product (34% yield).

^{1}H NMR (400 MHz, $CDCl_3$): δ 8.50 (d J_{HH} = 8.3 Hz, 1H), 7.57 (d J_{HH} = 7.8 Hz, 1H), 7.52 (d J_{HH} = 3.8 Hz, 1H), 7.37 (td J_{HH} = 8.3 Hz, 1.3 Hz, 1H), 7.30 (d J_{HH} = 7.4 Hz, 1.0 Hz, 1H), 6.97 (dd J_{HH} = 16.7 Hz, 10.3 Hz, 1H), 6.68 (m, 2H), 6.04 (dd J_{HH} = 10.5 Hz, 1.5 Hz, 1H). (Figure A3)

^{13}C NMR (100 MHz, $CDCl_3$): δ 164.0, 135.9, 132.1, 130.7, 128.0, 125.2, 124.7, 124.1, 121.0, 116.9, 109.5. (Figure A4)
The NMR spectra matched the ones in the literature.[118]

4.3 Free radical polymerization of (meth)acrylates

The monomer was dissolved in DMSO at a 100 mg/mL concentration, and 0.5 mol% of AIBN was added as a solution in the solvent. After that, the mixture was degassed with argon for 1 hour, and the tube was sealed with a cap and put into a preheated oven at 63 °C. After 24 hours, the tube was removed from the oven and cooled to room temperature. The reaction mixture was precipitated into MeOH (100 ml per 100 mg of monomer). The precipitate was filtered, washed with MeOH, and dried in a vacuum oven at 80 °C over 48 hours. The dried sample was weighed and ready for the different analyses.

4.4 Thermal analysis of the polymers

Thermogravimetric analysis (TGA) was performed using TA Instruments TGA Q500 apparatus to determine the thermal stability of the polymers under an N_2 flux of 60 mL/min. Samples were kept isothermally at 100 °C for up to 20 min to remove solvent residues. After equilibration at 30 °C, the temperature was increased to 600 °C at a heating rate of 10 °C/min. The thermal decomposition temperature ($T_{d,95\%}$) was determined at 5% weight loss.

Differential scanning calorimetry (DSC) was carried out using a TA Instruments DSC Q2000 differential scanning calorimeter. Dried samples were transferred to aluminum pans and sealed. The samples were first heated to 150–250 °C, depending on their respective onset of decomposition, at a rate of 10 °C/min. After an isothermal period of 5 min, the samples were cooled to –50 °C followed by a 5 min isothermal period. Finally, the samples were heated to the original temperature at 10 °C/min. T_g values were evaluated from the thermograms as the middle point between the onset and offset temperatures of the glass transitions.

CONCLUSIONS

The conclusions that can be made from this thesis:

- The prepared poly(β-thioether ester)s were chemically hydrolysable, leading to potential recycling paths of these polymers
- The reversibility of the crosslinks in the isosorbide levulinate network polymers was confirmed and the circularity of the crosslinking was shown
- Lignin-based polymethacrylates had very high glass-transition temperatures, low toxicity and favourable life-cycle assessment results
- Indoline polyacrylates exhibited very high glass-transition temperatures and exceptionally high thermal stability

The results obtained in this thesis indicate that biomass is a viable starting material for high-performance polymers. Additional studies into the recyclability, toxicity and life cycle of the polymers showed that the obtained materials are competitive compared to fossil-based counterparts and can even exceed their properties in some aspects.

SUMMARY

The rapid increase in plastic consumption, primarily based on fossil resources, is not sustainable. Therefore, we need alternative feedstocks to create plastics that do not negatively impact the environment through carbon emissions, but may contribute to a circular carbon economy. Designing new polymers with recyclability or (bio)degradability in mind is a promising pathway to alleviate the impact of plastic waste and reach a sustainable future.

This thesis investigated different biomass-based structures to evaluate them as replacements for everyday polymers in more demanding applications. The main feature of the monomers prepared in this thesis is their cyclic nature, which should lead them to better polymer properties, e.g., enhanced glass transition temperatures. Additionally, other aspects of the polymers were investigated to find improvements over common plastics. These aspects included the recyclability and reuse of the polymer material, as well as their overall environmental impact and toxicity to the environment.

In the first article, a citric acid derived starting material was converted to a cyclic diketone, which was further modified to obtain 4- and 5-cyclic structures via ketalization with trimethylolpropane and glycerol, respectively. The obtained diols were converted to di(meth)acrylates and polymerized with different dithiols in the presence of an organic base. Four different di(meth)acrylates and three different dithiols were used to obtain a wide range of polymers with molecular weights from 11 to 27 kg/mol. All the polymers had high thermal stability, from 282 to 324 °C. The polymers containing glycerol fragments were the softest, with T_gs, from –16 to –7 °C. Both of the other diacrylates gave higher T_gs from 7 to 46 °C, the highest one was achieved using bis-aromatic dithiol and dimethacrylate. Additionally, it was found that the polymers contained a small amount of acrylate end-groups, which could be used to crosslink the material. After heat treatment, a noticeable increase in T_g from 40 to 74 °C was observed for one of the higher T_g diacrylate polymers, which confirmed the finding. In addition to thermal characteristics, the degradability of these spirocyclic structures was studied. First, the spirodiol was hydrolyzed under acidic conditions to break the ketal linkages and obtain the diketone and the triol. A similar experiment was conducted for the polymers, which showed a lower rate of hydrolysis. Still, for the glycerol-containing material, after 4 hours, complete hydrolysis of the ketal bonds was observed. These experiments indicated the potential of chemical recycling for the polymers containing our spirocyclic backbone.

The second paper investigated a covalent adaptable polymer network system based on isosorbide levulinate polymethacrylates and dihydrazide crosslinkers. First, isosorbide 5-methacrylate was prepared via enzymatic catalysis. Then levulinic acid was attached to the via vinyl levulinate enzymatically. Copolymers with varying amounts of MMA were prepared to investigate different crosslink densities. The molecular weights of the copolymers were in the range 16 to 49 kg/mol. Thermal degradation temperatures for the homo- and copolymers

were slightly over 200 °C, while the T_gs range from 74 °C of the isosorbide levulinate homopolymer to 127 °C obtained for PMMA. Next, the linear copolymers were crosslinked with two dihydrazides with different chain lengths to obtain network polymers. The network structures significantly increased their thermal stability, ranging from 223 to 264 °C for the shorter linker and 265 to 286 °C for the more flexible crosslinker. Likewise, the increase in T_g values was also significant, up to 170 °C for the network with the shorter linker and highest crosslink density. There was also a clear trend of increasing T_g value with increasing crosslinker amount. Finally, the reversibility of the crosslink reaction was investigated. The networks were successfully de-crosslinked, which could be observed via FTIR spectroscopy, and, after that, re-crosslinked. The T_gs of the de- and re-crosslinked samples also confirmed the reactions. The circular nature of these networks makes them particularly interesting as reusable materials.

The third paper focused on developing an LCA method based on combining two different LCA methodologies. The goal was to create a framework for assessing new and emerging processes to industry standards on a fair basis. The work included an early case study on the vanillic monomer from the fourth article and isosorbide 5-methacrylate, comparing them to their commercial counterparts PS, PMMA, and PC. The study started with gathering lab-scale experimental data and then using ex-ante LCA methods to propose a scaled-up bioreactor procedure for the synthesis pathways. These steps brought an emerging technology to a similar technology readiness level to widespread processes. Next, the obtained data was projected into the future by using predicted improvements in Estonia, Norway, and the EU up to 2050. The main change in this phase included more efficient transportation, energy production, and a wider spread of bio-based technologies. The current results for the isosorbide polymer were comparable to those of their fossil counterparts. However, the lignin-based polymer still had somewhat higher impacts, partially due to the inefficiencies in lignin depolymerization. The future predictions show that both polymers had a lower climate change impact than fossil PMMA, PS, and PC.

The fourth article started with monomeric units of lignin, more specifically, carboxylic acids, e.g., vanillic acid. These acids were converted into methacrylic monomers via two simple chemical esterification reactions. Firstly, the acid was converted into a methyl ester using methanol under acidic reflux. Secondly, the free hydroxyl group was methacrylated using either methacrylic anhydride or methacryloyl chloride. The second method with methacryloyl chloride resulted in higher yields and came with the benefit of not needing chromatography for monomer purification. Standard free radical polymerization using AIBN was used to polymerize the three monomers. Molecular weights around 54–121 kg/mol were obtained, and the thermal stability of the homopolymers was around 300 °C. The T_gs of the homopolymers increased with the additional methoxy groups attached to the aromatic cycle in the structure, ranging from 106 to 197 °C. Additional copolymerizations with MMA allowed for molecular weights of up to 236 kg/mol while not significantly impacting the T_g of the vanillic polymer, as the T_gs are very similar. Besides thermal characterization, life cycle assessment

and toxicology studies were carried out. Using the new methodology developed in the third article, the LCA study showed a promising result for the vanillic monomer in all inspected categories, achieving results comparable to highly optimized MMA production. Toxicology experiments showed no toxicity for the vanillic polymer and low toxicity for the other two polymers.

The fifth paper investigated indoles and indolines as starting materials for high-T_g poly(meth)acrylates. Indole and indoline were converted into corresponding (meth)acrylates using acyl chlorides. Free radical polymerizations were carried out, but only indole acrylate was the only one to give a homopolymer, while the other monomers did not polymerize. The obtained indole acrylate of 34 kg/mol had a T_g of 172 °C. Additionally, copolymerizations with MMA and butyl acrylate were carried out, which lead to copolymers with T_gs ranging from 78 to 166 °C. Both the homopolymer and copolymers had exceptionally high thermal stability from 368 to 390 °C.

This thesis confirms that it is possible to obtain polymer materials with excellent thermal properties from various bio-based structures. Additionally, other aspects of the materials, such as recyclability, life cycle assessment, and toxicity, were studied to obtain additional information, reinforcing these materials' viability as future replacements for fossil polymers even further.

SUMMARY IN ESTONIAN

Tsüklilise struktuuriga biopõhiste monomeeride ja vastavate polümeeride süntees ning analüüs

Peamiselt fossiilsetel ressurssidel põhineva plasti tarbimise kiire kasv ei ole jätkusuutlik. Seetõttu on vajalik leida alternatiivsed lähteressursid, mis ei oleks keskkonnale negatiivse mõjuga ja mis oleks osa süsiniku ringmajandusest. Uute polümeeride loomisel tuleb rõhku panna ka nende taaskasutusele ja (bio)lagunemisele, et vähendada plastjäätmetega seotud probleeme ja jõuda jätkusuutliku tulevikuni.

See töö uuris erinevaid biomassist saadavaid struktuure, et leida alternatiive nõudlikes rakendustes kasutatavatele plastidele. Käesolevas töös kasutatud monomeeride põhiomaduseks on nende tsükliline struktuur, mis peaks parendama nende materjalide omadusi, näiteks tõstma klaasistumistemperatuuri (T_g). Lisaks uuriti saadud polümeeride teisi omadusi, mis võiksid võrdluses laiatarbeplastikutega anda eeliseid, näiteks taaskasutatavus, keskkonnajalajälg ja toksilisus keskkonna suhtes.

Esimeses artikli alguspunktiks oli sidrunhape, millest valmistati tsükliline diketoon. Järgmiseks kasutati trimetüloolpropaani (TMP) ja glütserooli, et ketaliseerida diketoonid vastavalt 4- ja 5-tsüklilisteks dioolideks. Saadud dioolidele lisati (met)akrülaadi rühmad, mille kaudu need polümeriseeriti orgaanilise aluse juuresolekul erinevate ditioolidega. Kokku kasutati nelja erinevat di(met)akrülaati ja kolme ditiooli, et saada hulk polümeere molekulmassidega 11 kuni 27 kg/mol. Kõigil saadud polümeeridel oli kõrge termiline stabiilsus – 282 kuni 324 °C. Glütserooli sisaldavad polümeerid olid kõige pehmemad, T_g varieerus vahemikus –16 kuni –7 °C. TMP-d sisaldavad polümeerid olid kõrgema T_g-ga 7 kuni 46 °C. Neist kõrgeim saavutati bis-aromaatset ditiooli ja viietsüklillist dimetakrülaati sisaldavas polümeeris. Lisaks sellele leiti, et polümeerid sisaldavad vähesel määral akrülaadi jääkgruppe, mille kaudu saab antud materjale ristsidestada. Ühe kõrgema T_g-ga polümeeri puhul kinnitati seda teooriat kui selle materjali kuumutamisel tõusis T_g 40 °C-lt 74 °C-ni. Peale polümeeride termiliste omaduste uuriti ka spirotsüklite lagunemist. Kõigepealt katsetati happelises keskkonnas spirodiooli lagunemist, mis andis tulemusena tagasi algse diketooni ja triooli. Sarnane katse viidi läbi ka polümeeridega, kuid lagunemise kiirus oli märgatavalt aeglasem. Siiski leiti, et glütserooli sisaldavas polümeeris lagunesid nelja tunniga kõik spirotsüklid. Need lagundamiskatsed viitavad spirotsüklilisi struktuure sisaldavate materjalide keemilise taaskasutamise võimalikkusele.

Teine artikkel uuris kovalentseid adaptiivseid polümeerivõrgustikke, mis koosnesid isosorbiidi levulinaadi polümetakrülaatidest ja neid siduvatest dihüdrasiididest. Alustuseks sünteesiti ensümaatilisel meetodil isosorbiid-5-metakrülaat, mille vabale hüdroksüülrühmale kinnitati levulinaat, kasutades samuti ensümaatilist meetodit vinüüllevulinaadiga. Järgmiseks kopolümeriseeriti saadud monomeer mitmes vahekorras metüülmetakrülaadiga (MMA), et oleks võimalik

uurida erineva ristseostatuse määraga materjale. Saadud kopolümeeride molekulmassid olid vahemikus 16 kuni 49 kg/mol, termilise lagunemise temperatuurid üle 200 °C. T_g-d olid vahemikus 74 °C isosorbiidi levulinaadi homopolümeeril kuni 127 °C polümetüülmetakrülaadil (PMMA). Järgmiseks seoti saadud lineaarsed polümeerid kahe erineva ahelapikkusega dihüdrasiidiga ja saadi ristsidestatud polümeervõrgustikud. Võrreldes lineaarsete polümeeridega, tõusis saadud võrgustike termiline stabiilsus oluliselt ja oli vahemikus 223 kuni 264 °C lühema linkeri kasutamisel ja 265 kuni 286 °C pikemat linkerit kasutades. Samuti tõusis saadud materjalide T_g, mis ulatus kõrgeima ristseostatuse määraga ja lühema linkeri puhul koguni 170 °C-ni. Oodatult tõusis T_g väärtus kõrgema ristseotusastme korral. Lõpuks uuriti ka saadud võrgustikest lineaarsete polümeeride tagasi saamist. Ristsidemed õnnestus lagundada ja seda kinnitas ka infrapunaspektroskoopia analüüs. Seejärel oli võimalik saadud lineaarsed polümeerid algset meetodit kasutades uuesti ristsidestada. Saadud polümeeride ja võrgustike T_g väärtused kinnitasid samuti reaktsioonide toimumist. Antud materjalide ringlus lineaarsest polümeerist polümeervõrgustikuks ja tagasi teeb need taaskasutatavate materjalidena eriti huvipakkuvaks.

Kolmandas artiklis töötati välja uus meetod elutsüklianalüüsi (LCA) tegemiseks, milleks ühendatakse kaks LCA metodoloogiat. Töö eesmärgiks oli luua meetod, millega saaks adekvaatselt võrrelda uusi ja arenevaid protsesse suureskaalaliste tööstusprotsessidega. Võrdluses oli neljanda artikli vaniljehappest saadud monomeer, isosorbiid-5-metakrülaat ning nendega sarnased turul saadaolevad polümeerid: polüstüreen (PS), PMMA ja polükarbonaat (PC). Kõigepealt koguti laborikatsete andmed ning kasutades *ex-ante* LCA meetodit loodi teoreetiline skaleeritud süntees bioreaktoris. Nende arvutuste abil oli võimalik saada reaalsete tööstusprotsessidega võrreldav meetod. Järgmiseks projitseeriti saadud tulemused tulevikku, kasutades Eesti, Norra ja Euroopa keskmisi andmeid aastani 2050. Selles etapis arvestati järgmisi peamisi muutuseid: transpordi tõhususe kasv, puhtam energia tootmine ja laiem biotoormel põhinevate tehnoloogiate levik. Saadud tulemuste põhjal oli isosorbiidi polümeer võrreldav kaubanduslike polümeeridega. Kuid ligniini-põhine vaniljehappest saadud polümeer oli kõrgemate keskkonnanäitajatega, mis on osaliselt seotud ka ligniini depolümeriseerimise protsessi ebaefektiivsusega. Tuleviku perspektiivis olid mõlemate biopõhiste polümeeride keskkonnamõjud madalamad kui fossiilsetel (PS, PMMA ja PC).

Neljanda artikli alguspunktiks olid ligniinist saadavad monomeersed ühendid, täpsemalt karboksüülhapped nagu vaniljehape. Need happed muudeti kahe lihtsa esterdamisreaktsiooni kaudu metakrülaatmonomeerideks. Esimeses etapis lisati happerühmale happekatalüütiliselt metanool, et saada vastav metüülester. Järgmiseks lisati vabale hüdroksüülrühmale metakrülaat, kasutades metakrüülanhüdriidi või metakrüloüülkloriidi. Metakrüloüülkloriidi kasutav meetod osutus paremaks, kuna produkti sai puhastada kromatograafiat kasutamata ning ka saagised olid anhüdriidi meetodist kõrgemad. Saadud monomeeride polümeriseerumiseks kasutati tavalist vabaradikaalpolümerisatsiooni, kasutades termilist initsiaatorit AIBN. Saadud polümeeride molekulmassid olid vahemikus 54–121 kg/mol ning

need olid termiliselt stabiilsed kuni *ca* 300 °C-ni. Sõltuvalt aromaatse tsükli küljes olevate metoksürühmade arvust kasvas polümeeride T_g 106 °C-lt 197 °C-ni. MMA-ga tehtud kopolümeerid olid molekulmassidega kuni 236 kg/mol, kuid vaniljehappest saadud polümeeri T_g väärtust MMA lisamine ei mõjutanud, kuna nende T_g-d on väga lähedased. Lisaks uuriti ka saadud polümeeride elutsüklit ja toksikoloogiat. Kolmandas artiklis loodud metodoloogiat kasutades saadi vaniljehappe monomeerile kõigis kategooriates madalamad keskkonnamõjude väärtused kui optimeeritud MMA tootmisel. Toksikoloogiaeksperimentide tulemused näitasid, et vaniljehappest saadud polümeer ei ole toksiline ja teised kaks polümeeri on madala toksilisusega.

Viiendas artiklis kasutatakse kõrge T_g-ga polümetakrülaatide saamiseks lähteainena indooli ja indoliini. Kasutades atsüülkloriide valmistati mõlemast vastavad (met)akrülaadid. Jägmisena polümeriseeriti saadud monomeerid vabaradikaalpolümerisatsiooni meetodil, kuid ainult indoliini akrülaadist saadi homopolümeer, kuna teised monomeerid ei polümeriseerunud. Saadud homopolümeeri molekulmass oli 34 kg/mol ja T_g 172 °C. Lisaks viidi läbi kopolümerisatsioonid MMA ja butüülakrülaadiga-ga ning saadi kopolümeerid T_g väärtustega 78 kuni 166 °C. Kõigi saadud polümeeride termiline stabiilsus oli väga kõrge vahemikus 368 kuni 390 °C.

Käesolev väitekiri tõestab, et biopõhistest struktuuridest on võimalik sünteesida suurepäraste termiliste omadustega polümeere. Lisaks uuriti saadud materjalide taaskasutust, viidi läbi elutsüklianalüüs ning analüüsiti nende polümeeride toksikoloogiat. Tulemused kinnitavad, et käesolevas töös välja töötatud materjalid on perspektiivsed asendamaks tulevikus fossiilsetest allikatest saadavaid polümeere.

REFERENCES

(1) Vert, M.; Doi, Y.; Hellwich, K.-H.; Hess, M.; Hodge, P.; Kubisa, P.; Rinaudo, M.; Schué, F. Terminology for Biorelated Polymers and Applications (IUPAC Recommendations 2012). *Pure Appl. Chem.* **2012**, *84*, 377–410. https://doi.org/10.1351/PAC-REC-10-12-04.

(2) Young, R. J.; Lovell, P. A. *Introduction to Polymers*, 3rd Editio.; CRC Press, **2011**. https://doi.org/10.1201/9781439894156.

(3) Jensen, W. B. The Origin of the Polymer Concept. *J. Chem. Educ.* **2008**, *85*, 624. https://doi.org/10.1021/ed085p624.

(4) Stegmann, P.; Daioglou, V.; Londo, M.; van Vuuren, D. P.; Junginger, M. Plastic Futures and Their CO2 Emissions. *Nature* **2022**, *612*, 272–276. https://doi.org/10.1038/s41586-022-05422-5.

(5) Rahimi, A. R.; Garciá, J. M. Chemical Recycling of Waste Plastics for New Materials Production. *Nat. Rev. Chem.* **2017**, *1*, 1–11. https://doi.org/10.1038/s41570-017-0046.

(6) Ragaert, K.; Delva, L.; Van Geem, K. Mechanical and Chemical Recycling of Solid Plastic Waste. *Waste Manag.* **2017**, *69*, 24–58. https://doi.org/10.1016/j.wasman.2017.07.044.

(7) Mülhaupt, R. Green Polymer Chemistry and Bio-Based Plastics: Dreams and Reality. *Macromol. Chem. Phys.* **2013**, *214*, 159–174. https://doi.org/10.1002/macp.201200439.

(8) Skoczinski, P.; Carus, M.; Tweddle, G.; Ruiz, P.; Hark, N.; Zhang, A.; de Guzman, D.; Ravenstijn, J.; Käb, H.; Raschka, A. *Bio-Based Building Blocks and Polymers – Global Capacities, Production and Trends 2023–2028*; Hürth, Germany, **2024**. https://doi.org/10.52548/VXTH2416.

(9) Södergård, A.; Stolt, M. Properties of Lactic Acid Based Polymers and Their Correlation with Composition. *Progress in Polymer Science (Oxford)*. **2002**, pp 1123–1163. https://doi.org/10.1016/S0079-6700(02)00012-6.

(10) Nguyen, H. T. H.; Qi, P.; Rostagno, M.; Feteha, A.; Miller, S. A. The Quest for High Glass Transition Temperature Bioplastics. *J. Mater. Chem. A* **2018**, *6*, 9298–9331. https://doi.org/10.1039/c8ta00377g.

(11) Cywar, R. M.; Rorrer, N. A.; Hoyt, C. B.; Beckham, G. T.; Chen, E. Y. X. Bio-Based Polymers with Performance-Advantaged Properties. *Nat. Rev. Mater.* **2021**, *7*, 83–103. https://doi.org/10.1038/s41578-021-00363-3.

(12) Vieira, M. G. A.; Da Silva, M. A.; Dos Santos, L. O.; Beppu, M. M. Natural-Based Plasticizers and Biopolymer Films: A Review. *Eur. Polym. J.* **2011**, *47*, 254–263. https://doi.org/10.1016/j.eurpolymj.2010.12.011.

(13) Sivan, A. New Perspectives in Plastic Biodegradation. *Curr. Opin. Biotechnol.* **2011**, *22*, 422–426. https://doi.org/10.1016/j.copbio.2011.01.013.

(14) *Handbook of Biodegradable Polymers*; Lendlein, A., Sisson, A., Eds.; Wiley, **2011**. https://doi.org/10.1002/9783527635818.

(15) Nair, L. S.; Laurencin, C. T. Biodegradable Polymers as Biomaterials. *Prog. Polym. Sci.* **2007**, *32*, 762–798. https://doi.org/10.1016/j.progpolymsci.2007.05.017.

(16) Ghatge, S.; Yang, Y.; Ahn, J. H.; Hur, H. G. Biodegradation of Polyethylene: A Brief Review. *Appl. Biol. Chem.* **2020**, *63*. https://doi.org/10.1186/s13765-020-00511-3.

(17) O'dea, R. M.; Willie, J. A.; Epps, T. H. 100th Anniversary of Macromolecular Science Viewpoint: Polymers from Lignocellulosic Biomass. Current Challenges and Future Opportunities. *ACS Macro Lett.* **2020**, *9*, 476–493. https://doi.org/10.1021/acsmacrolett.0c00024.
(18) Isikgor, F. H.; Becer, C. R. Lignocellulosic Biomass: A Sustainable Platform for the Production of Bio-Based Chemicals and Polymers. *Polym. Chem.* **2015**, *6*, 4497–4559. https://doi.org/10.1039/C5PY00263J.
(19) Goldemberg, J. Ethanol for a Sustainable Energy Future. *Science (80-.).* **2007**, *315*, 808–810. https://doi.org/10.1126/science.1137013.
(20) Yabushita, M.; Kobayashi, H.; Fukuoka, A. Catalytic Transformation of Cellulose into Platform Chemicals. *Appl. Catal. B Environ.* **2014**, *145*, 1–9. https://doi.org/10.1016/j.apcatb.2013.01.052.
(21) Soccol, C. R.; Vandenberghe, L. P. S.; Rodrigues, C.; Pandey, A. New Perspectives for Citric Acid Production and Application. *Food Technol. Biotechnol.* **2006**, *44*, 141–149.
(22) Zhang, Y. P.; Ding, S.; Mielenz, J. R.; Cui, J.; Elander, R. T.; Laser, M.; Himmel, M. E.; McMillan, J. R.; Lynd, L. R. Fractionating Recalcitrant Lignocellulose at Modest Reaction Conditions. *Biotechnol. Bioeng.* **2007**, *97*, 214–223. https://doi.org/10.1002/bit.21386.
(23) Klemm, D.; Heublein, B.; Fink, H. P.; Bohn, A. Cellulose: Fascinating Biopolymer and Sustainable Raw Material. *Angew. Chemie - Int. Ed.* **2005**, *44*, 3358–3393. https://doi.org/10.1002/anie.200460587.
(24) Rinaldi, R.; Schüth, F. Acid Hydrolysis of Cellulose as the Entry Point into Biorefinery Schemes. *ChemSusChem* **2009**, *2*, 1096–1107. https://doi.org/10.1002/cssc.200900188.
(25) Shrotri, A.; Kobayashi, H.; Fukuoka, A. Cellulose Depolymerization over Heterogeneous Catalysts. *Acc. Chem. Res.* **2018**, *51*, 761–768. https://doi.org/10.1021/acs.accounts.7b00614.
(26) Fukuoka, A.; Dhepe, P. L. Catalytic Conversion of Cellulose into Sugar Alcohols. *Angew. Chemie – Int. Ed.* **2006**, *45*, 5161–5163. https://doi.org/10.1002/anie.200601921.
(27) Zhang, Y. H. P.; Lynd, L. R. Toward an Aggregated Understanding of Enzymatic Hydrolysis of Cellulose: Noncomplexed Cellulase Systems. *Biotechnol. Bioeng.* **2004**, *88*, 797–824. https://doi.org/10.1002/bit.20282.
(28) Fenouillot, F.; Rousseau, A.; Colomines, G.; Saint-Loup, R.; Pascault, J. P. Polymers from Renewable 1,4:3,6-Dianhydrohexitols (Isosorbide, Isomannide and Isoidide): A Review. *Prog. Polym. Sci.* **2010**, *35*, 578–622. https://doi.org/10.1016/j.progpolymsci.2009.10.001.
(29) Zhang, J.; Li, J. B.; Wu, S. Bin; Liu, Y. Advances in the Catalytic Production and Utilization of Sorbitol. *Ind. Eng. Chem. Res.* **2013**, *52*, 11799–11815. https://doi.org/10.1021/ie4011854.
(30) Scott, A. Roquette Embraces Biobased Materials. *Chem. Eng. News* **2012**, *90*, 16–17. https://doi.org/10.1021/cen-09027-bus2.
(31) Flèche, G.; Huchette, M. Isosorbide. Preparation, Properties and Chemistry. *Starch – Stärke* **1986**, *38*, 26–30. https://doi.org/10.1002/star.19860380107.
(32) Matt, L.; Parve, J.; Parve, O.; Pehk, T.; Pham, T. H.; Liblikas, I.; Vares, L.; Jannasch, P. Enzymatic Synthesis and Polymerization of Isosorbide-Based Monomethacrylates for High- Tg Plastics. *ACS Sustain. Chem. Eng.* **2018**, *6*, 17382–17390. https://doi.org/10.1021/acssuschemeng.8b05074.

(33) Braun, D.; Bergmann, M. 1,4:3,6-Dianhydrohexite Als Bausteine Für Polymere. *J. für Prakt. Chemie/Chemiker-Zeitung* **1992**, *334*, 298–310. https://doi.org/10.1002/prac.19923340403.
(34) Laanesoo, S.; Bonjour, O.; Parve, J.; Parve, O.; Matt, L.; Vares, L.; Jannasch, P. Poly(Alkanoyl Isosorbide Methacrylate)s: From Amorphous to Semicrystalline and Liquid Crystalline Biobased Materials. *Biomacromolecules* **2021**, *22*, 640–648. https://doi.org/10.1021/acs.biomac.0c01474.
(35) Laanesoo, S.; Bonjour, O.; Sedrik, R.; Tamsalu, I.; Jannasch, P.; Vares, L. Combining Isosorbide and Lignin-Related Benzoic Acids for High-Tg Polymethacrylates. *Eur. Polym. J.* **2024**, *202*, 112595. https://doi.org/10.1016/j.eurpolymj.2023.112595.
(36) Nonque, F.; Benlahoues, A.; Audourenc, J.; Sahut, A.; Saint-Loup, R.; Woisel, P.; Potier, J. Study on Polymerization of Bio-Based Isosorbide Monomethacrylate for the Formation of Low-T and High-T Sustainable Polymers. *Eur. Polym. J.* **2021**, *160*, 110799. https://doi.org/10.1016/j.eurpolymj.2021.110799.
(37) Gallagher, J. J.; Hillmyer, M. A.; Reineke, T. M. Isosorbide-Based Polymethacrylates. *ACS Sustain. Chem. Eng.* **2015**, *3*, 662–667. https://doi.org/10.1021/sc5008362.
(38) *Lignin and Lignans: Advances in Chemistry*; Heitner, C., Dimmel, D., Schmidt, J., Eds.; CRC Press, 2016. https://doi.org/10.1201/EBK1574444865.
(39) Strassberger, Z.; Tanase, S.; Rothenberg, G. The Pros and Cons of Lignin Valorisation in an Integrated Biorefinery. *RSC Adv.* **2014**, *4*, 25310–25318. https://doi.org/10.1039/c4ra04747h.
(40) Wang, C.; Kelley, S. S.; Venditti, R. A. Lignin-Based Thermoplastic Materials. *ChemSusChem* **2016**, *9*, 770–783. https://doi.org/10.1002/cssc.201501531.
(41) Sun, Z.; Fridrich, B.; De Santi, A.; Elangovan, S.; Barta, K. Bright Side of Lignin Depolymerization: Toward New Platform Chemicals. *Chem. Rev.* **2018**, *118*, 614–678. https://doi.org/10.1021/acs.chemrev.7b00588.
(42) Wan, Z.; Zhang, H.; Guo, Y.; Li, H. Advances in Catalytic Depolymerization of Lignin. *ChemistrySelect* **2022**, *7*. https://doi.org/10.1002/slct.202202582.
(43) Xu, C.; Arancon, R. A. D.; Labidi, J.; Luque, R. Lignin Depolymerisation Strategies: Towards Valuable Chemicals and Fuels. *Chem. Soc. Rev.* **2014**, *43*, 7485–7500. https://doi.org/10.1039/c4cs00235k.
(44) Bass, G. F.; Epps, T. H. Recent Developments towards Performance-Enhancing Lignin-Based Polymers. *Polym. Chem.* **2021**, *12*, 4130–4158. https://doi.org/10.1039/d1py00694k.
(45) Laurichesse, S.; Avérous, L. Chemical Modification of Lignins: Towards Biobased Polymers. *Prog. Polym. Sci.* **2014**, *39*, 1266–1290. https://doi.org/10.1016/j.progpolymsci.2013.11.004.
(46) Kun, D.; Pukánszky, B. Polymer/Lignin Blends: Interactions, Properties, Applications. *Eur. Polym. J.* **2017**, *93*, 618–641. https://doi.org/10.1016/j.eurpolymj.2017.04.035.
(47) Holmberg, A. L.; Reno, K. H.; Nguyen, N. A.; Wool, R. P.; Epps, T. H. Syringyl Methacrylate, a Hardwood Lignin-Based Monomer for High-Tg Polymeric Materials. *ACS Macro Lett.* **2016**, *5*, 574–578. https://doi.org/10.1021/acsmacrolett.6b00270.
(48) Wang, S.; Shuai, L.; Saha, B.; Vlachos, D. G.; Epps, T. H. From Tree to Tape: Direct Synthesis of Pressure Sensitive Adhesives from Depolymerized Raw Lignocellulosic Biomass. *ACS Cent. Sci.* **2018**, *4*, 701–708. https://doi.org/10.1021/acscentsci.8b00140.

(49) Holmberg, A. L.; Nguyen, N. A.; Karavolias, M. G.; Reno, K. H.; Wool, R. P.; Thomas H. Epps, I. Softwood Lignin-Based Methacrylate Polymers with Tunable Thermal and Viscoelastic Properties. *Macromolecules* **2016**, *49*, 1286–1295. https://doi.org/10.1021/acs.macromol.5b02316.

(50) Bonjour, O.; Nederstedt, H.; Arcos-Hernandez, M. V.; Laanesoo, S.; Vares, L.; Jannasch, P. Lignin-Inspired Polymers with High Glass Transition Temperature and Solvent Resistance from 4-Hydroxybenzonitrile, Vanillonitrile, and Syringonitrile Methacrylates. *ACS Sustain. Chem. Eng.* **2021**, *9*, 16874–16880. https://doi.org/10.1021/acssuschemeng.1c07048.

(51) Zhou, J.; Zhang, H.; Deng, J.; Wu, Y. High Glass-Transition Temperature Acrylate Polymers Derived from Biomasses, Syringaldehyde, and Vanillin. *Macromol. Chem. Phys.* **2016**, *217*, 2402–2408. https://doi.org/10.1002/macp.201600305.

(52) Wan, Y.; Zhao, W.; Zhao, H.; Zhou, M.; He, J.; Zhang, Y. Living/Controlled Polymerization of Renewable Lignin-Based Monomers by Lewis Pairs. *Macromolecules* **2023**, *56*, 7763–7770. https://doi.org/10.1021/acs.macromol.3c01538.

(53) Xu, L.; Yao, Q.; Deng, J.; Han, Z.; Zhang, Y.; Fu, Y.; Huber, G. W.; Guo, Q. Renewable N-Heterocycles Production by Thermocatalytic Conversion and Ammonization of Biomass over ZSM-5. *ACS Sustain. Chem. Eng.* **2015**, *3*, 2890–2899. https://doi.org/10.1021/acssuschemeng.5b00841.

(54) Thadathil, A.; Pradeep, H.; Joshy, D.; Ismail, Y. A.; Periyat, P. Polyindole and Polypyrrole as a Sustainable Platform for Environmental Remediation and Sensor Applications. *Mater. Adv.* **2022**, *3*, 2990–3022. https://doi.org/10.1039/d2ma00022a.

(55) Mindt, M.; Beyraghdar Kashkooli, A.; Suarez-Diez, M.; Ferrer, L.; Jilg, T.; Bosch, D.; Martins dos Santos, V.; Wendisch, V. F.; Cankar, K. Production of Indole by Corynebacterium Glutamicum Microbial Cell Factories for Flavor and Fragrance Applications. *Microb. Cell Fact.* **2022**, *21*, 1–17. https://doi.org/10.1186/s12934-022-01771-y.

(56) Yamamoto, Y.; Sato, Y.; Ebina, T.; Yokoyama, C.; Takahasi, S.; Mito, Y.; Tanabe, H.; Nishiguchi, N.; Nagaoka, K. Separation of High Purity Indole from Coal Tar by High Pressure Crystallization. *Fuel* **1991**, *70*, 565–566. https://doi.org/10.1016/0016-2361(91)90039-D.

(57) Dunn, M. F. Allosteric Regulation of Substrate Channeling and Catalysis in the Tryptophan Synthase Bienzyme Complex. *Arch. Biochem. Biophys.* **2012**, *519*, 154–166. https://doi.org/10.1016/j.abb.2012.01.016.

(58) Mülhaupt, R. Hermann Staudinger and the Origin of Macromolecular Chemistry. *Angew. Chemie – Int. Ed.* **2004**, *43*, 1054–1063. https://doi.org/10.1002/ANIE.200330070.

(59) Odian, G. *Principles of Polymerization*, Fourth Edi.; John Wiley and Sons, Inc.: Hoboken, New Jersey, 2004. https://doi.org/10.1002/047147875X.

(60) *Compendium of Polymer Terminology and Nomenclature*; Jones, R. G., Wilks, E. S., Metanomski, W. V., Kahovec, J., Hess, M., Stepto, R., Kitayama, T., Eds.; Royal Society of Chemistry: Cambridge, **2009**; Vol. 42. https://doi.org/10.1039/9781847559425.

(61) Moad, G.; Solomon, D. H. *The Chemistry of Radical Polymerization*, 2nd ed.; Elsevier, **2006**. https://doi.org/10.1016/B978-0-08-044288-4.X5015-8.

(62) Carraher Jr., C. E. *Introduction to Polymer Chemistry*, 4th ed.; CRC Press, 2017. https://doi.org/10.1201/9781315369488.

(63) Truong, N. P.; Jones, G. R.; Bradford, K. G. E.; Konkolewicz, D.; Anastasaki, A. A Comparison of RAFT and ATRP Methods for Controlled Radical Polymerization. *Nat. Rev. Chem.* **2021**, *5*, 859–869. https://doi.org/10.1038/s41570-021-00328-8.

(64) Chiefari, J.; Chong, Y. K. (Bill); Ercole, F.; Krstina, J.; Jeffery, J.; Le, T. P. T.; Mayadunne, R. T. A.; Meijs, G. F.; Moad, C. L.; Moad, G.; Rizzardo, E.; Thang, S. H. Living Free-Radical Polymerization by Reversible Addition−Fragmentation Chain Transfer: The RAFT Process. *Macromolecules* **1998**, *31*, 5559–5562. https://doi.org/10.1021/ma9804951.

(65) Wang, J. S.; Matyjaszewski, K. Controlled/"Living" Radical Polymerization. Atom Transfer Radical Polymerization in the Presence of Transition-Metal Complexes. *J. Am. Chem. Soc.* **1995**, *117*, 5614–5615. https://doi.org/10.1021/ja00125a035.

(66) Hoyle, C. E.; Bowman, C. N. Thiol-Ene Click Chemistry. *Angew. Chemie - Int. Ed.* **2010**, *49*, 1540–1573. https://doi.org/10.1002/anie.200903924.

(67) Cramer, N. B.; Reddy, S. K.; O'Brien, A. K.; Bowman, C. N. Thiol – Ene Photopolymerization Mechanism and Rate Limiting Step Changes for Various Vinyl Functional Group Chemistries. *Macromolecules* **2003**, *36*, 7964–7969. https://doi.org/10.1021/ma034667s.

(68) Hoyle, C. E.; Lee, T. Y.; Roper, T. Thiol–Enes: Chemistry of the Past with Promise for the Future. *J. Polym. Sci. Part A Polym. Chem.* **2004**, *42*, 5301–5338. https://doi.org/10.1002/pola.20366.

(69) Summonte, S.; Racaniello, G. F.; Lopedota, A.; Denora, N.; Bernkop-Schnürch, A. Thiolated Polymeric Hydrogels for Biomedical Application: Cross-Linking Mechanisms. *J. Control. Release* **2021**, *330*, 470–482. https://doi.org/10.1016/J.JCONREL.2020.12.037.

(70) Rydholm, A. E.; Held, N. L.; Benoit, D. S. W.; Bowman, C. N.; Anseth, K. S. Modifying Network Chemistry in Thiol-Acrylate Photopolymers through Post-polymerization Functionalization to Control Cell-Material Interactions. *J. Biomed. Mater. Res. – Part A* **2008**, *86*, 23–30. https://doi.org/10.1002/jbm.a.31526.

(71) Moon, N. G.; Mazzini, F.; Pekkanen, A. M.; Wilts, E. M.; Long, T. E. Sugar-Derived Poly(β-Thioester)s as a Biomedical Scaffold. *Macromol. Chem. Phys.* **2018**, *219*, 1–9. https://doi.org/10.1002/macp.201800177.

(72) Baldwin, A. D.; Kiick, K. L. Reversible Maleimide-Thiol Adducts Yield Glutathione-Sensitive Poly(Ethylene Glycol)-Heparin Hydrogels. *Polym. Chem.* **2013**, *4*, 133–143. https://doi.org/10.1039/c2py20576a.

(73) Vandenbergh, J.; Ranieri, K.; Junkers, T. Synthesis of (Bio) -Degradable Poly (β -Thioester) s via Amine Catalyzed Thiol − Ene Click Polymerization. *Macromol. Chem. Phys.* **2012**, 2611–2617. https://doi.org/doi.org/10.1002/macp.201200470.

(74) Chan, J. W.; Hoyle, C. E.; Lowe, A. B.; Bowman, M. Nucleophile-Initiated Thiol-Michael Reactions: Effect of Organocatalyst, Thiol, and Ene. *Macromolecules* **2010**, *43*, 6381–6388. https://doi.org/10.1021/ma101069c.

(75) Koo, S. P. S.; Stamenović, M. M.; Arun Prasath, R.; Inglis, A. J.; Prez, F. E. D. U.; Barner-Kowollik, C.; Van Camp, W. I. M.; Junkers, T. Limitations of Radical Thiol-Ene Reactions for Polymer-Polymer Conjugation. *J. Polym. Sci. Part A Polym. Chem.* **2010**, *48*, 1699–1713. https://doi.org/10.1002/pola.23933.

(76) Vandenbergh, J.; Peeters, M.; Kretschmer, T.; Wagner, P.; Junkers, T. Cross-Linked Degradable Poly(β-Thioester) Networks via Amine-Catalyzed Thiol-Ene Click Polymerization. *Polymer (Guildf).* **2014**, *55*, 3525–3532. https://doi.org/10.1016/j.polymer.2014.05.043.
(77) Tillet, G.; Boutevin, B.; Ameduri, B. Chemical Reactions of Polymer Crosslinking and Post-Crosslinking at Room and Medium Temperature. *Progress in Polymer Science (Oxford)*. February **2011**, pp 191–217. https://doi.org/10.1016/j.progpolymsci.2010.08.003.
(78) Nielsen, L. E. Cross-Linking–Effect on Physical Properties of Polymers. *J. Macromol. Sci. Part C* **1969**, *3*, 69–103. https://doi.org/10.1080/15583726908545897.
(79) Goodyear, C. *Gum-Elastic and Its Varieties : With a Detailed Account of Its Applications and Uses, and of the Discovery of Vulcanization*; Published for the author: New Haven, Conn., **1853**. https://doi.org/10.5962/bhl.title.62544.
(80) Kloxin, C. J.; Scott, T. F.; Adzima, B. J.; Bowman, C. N. Covalent Adaptable Networks (CANs): A Unique Paradigm in Cross-Linked Polymers. *Macromolecules* **2010**, *43*, 2643–2653. https://doi.org/10.1021/ma902596s.
(81) Liu, Y.; Yu, Z.; Wang, B.; Li, P.; Zhu, J.; Ma, S. Closed-Loop Chemical Recycling of Thermosetting Polymers and Their Applications: A Review. *Green Chem.* **2022**, *24*, 5691–5708. https://doi.org/10.1039/D2GC00368F.
(82) Wojtecki, R. J.; Meador, M. A.; Rowan, S. J. Using the Dynamic Bond to Access Macroscopically Responsive Structurally Dynamic Polymers. *Nat. Mater. 2011 101* **2010**, *10*, 14–27. https://doi.org/10.1038/nmat2891.
(83) European Chemicals Agency. Adipohydrazide https://echa.europa.eu/et/substance-information/-/substanceinfo/100.012.727 (accessed 2024 -09 -03).
(84) Schyns, Z. O. G.; Shaver, M. P. Mechanical Recycling of Packaging Plastics: A Review. *Macromol. Rapid Commun.* **2021**, *42*, 1–27. https://doi.org/10.1002/marc.202000415.
(85) Plastics Europe. *The Circular Economy for Plastics - A European Analysis*; 2024.
(86) Liu, Y.; Shi, J.; Jin, H.; Guo, L. Chemical Recycling Methods for Managing Waste Plastics: A Review. *Environ. Chem. Lett.* **2024**, *22*, 149–169. https://doi.org/10.1007/s10311-023-01664-5.
(87) Kosloski-Oh, S. C.; Wood, Z. A.; Manjarrez, Y.; De Los Rios, J. P.; Fieser, M. E. Catalytic Methods for Chemical Recycling or Upcycling of Commercial Polymers. *Mater. Horizons* **2021**, *8*, 1084–1129. https://doi.org/10.1039/d0mh01286f.
(88) Payne, J.; Jones, M. D. The Chemical Recycling of Polyesters for a Circular Plastics Economy: Challenges and Emerging Opportunities. *ChemSusChem* **2021**, *14*, 4041–4070. https://doi.org/10.1002/cssc.202100400.
(89) Ge, M.; Miao, J.-T.; Zhang, K.; Wu, Y.; Zheng, L.; Wu, L. Building Biobased, Degradable, Flexible Polymer Networks from Vanillin via Thiol–Ene "Click" Photopolymerization. *Polym. Chem.* **2020**, *12*, 564–571. https://doi.org/10.1039/d0py01407a.
(90) Lingier, S.; Spiesschaert, Y.; Dhanis, B.; De Wildeman, S.; Du Prez, F. E. Rigid Polyurethanes, Polyesters, and Polycarbonates from Renewable Ketal Monomers. *Macromolecules* **2017**, *50*, 5346–5352. https://doi.org/10.1021/acs.macromol.7b00899.

(91) Hufendiek, A.; Lingier, S.; Du Prez, F. E. Thermoplastic Polyacetals: Chemistry from the Past for a Sustainable Future? *Polym. Chem.* **2019**, *10*, 9–33. https://doi.org/10.1039/c8py01219a.
(92) Hu, H.; Tian, Y.; Kong, Z.; Ying, W. Bin; Chen, C.; Li, F.; Zhang, R.; Zhu, J. A High Performance Copolyester with "Locked" Biodegradability: Solid Stability and Controlled Degradation Enabled by Acid-Labile Acetal. *ACS Sustain. Chem. Eng.* **2021**, *9*, 2280–2290. https://doi.org/10.1021/acssuschemeng.0c08274.
(93) Ciuffi, B.; Fratini, E.; Rosi, L. Plastic Pretreatment: The Key for Efficient Enzymatic and Biodegradation Processes. *Polym. Degrad. Stab.* **2024**, *222*, 110698. https://doi.org/10.1016/j.polymdegradstab.2024.110698.
(94) Tournier, V.; Topham, C. M.; Gilles, A.; David, B.; Folgoas, C.; Moya-Leclair, E.; Kamionka, E.; Desrousseaux, M.-L.; Texier, H.; Gavalda, S.; Cot, M.; Guémard, E.; Dalibey, M.; Nomme, J.; Cioci, G.; Barbe, S.; Chateau, M.; André, I.; Duquesne, S.; Marty, A. An Engineered PET Depolymerase to Break down and Recycle Plastic Bottles. *Nature* **2020**, *580*, 216–219. https://doi.org/10.1038/s41586-020-2149-4.
(95) Gavankar, S.; Suh, S.; Keller, A. A. The Role of Scale and Technology Maturity in Life Cycle Assessment of Emerging Technologies: A Case Study on Carbon Nanotubes. *J. Ind. Ecol.* **2015**, *19*, 51–60. https://doi.org/10.1111/JIEC.12175.
(96) Hatti-Kaul, R.; Törnvall, U.; Gustafsson, L.; Börjesson, P. Industrial Biotechnology for the Production of Bio-Based Chemicals – a Cradle-to-Grave Perspective. *Trends Biotechnol.* **2007**, *25*, 119–124. https://doi.org/10.1016/J.TIBTECH.2007.01.001.
(97) Moni, S. M.; Mahmud, R.; High, K.; Carbajales-Dale, M. Life Cycle Assessment of Emerging Technologies: A Review. *J. Ind. Ecol.* **2020**, *24*, 52–63. https://doi.org/10.1111/jiec.12965.
(98) van der Giesen, C.; Cucurachi, S.; Guinée, J.; Kramer, G. J.; Tukker, A. A Critical View on the Current Application of LCA for New Technologies and Recommendations for Improved Practice. *J. Clean. Prod.* **2020**, *259*, 120904. https://doi.org/10.1016/j.jclepro.2020.120904.
(99) Cucurachi, S.; Van Der Giesen, C.; Guinée, J. Ex-Ante LCA of Emerging Technologies. *Procedia CIRP* **2018**, *69*, 463–468. https://doi.org/10.1016/J.PROCIR.2017.11.005.
(100) Thonemann, N.; Schulte, A.; Maga, D. How to Conduct Prospective Life Cycle Assessment for Emerging Technologies? A Systematic Review and Methodological Guidance. *Sustain.* **2020**, *12*, 1–23. https://doi.org/10.3390/su12031192.
(101) Thonemann, N.; Schulte, A. From Laboratory to Industrial Scale: A Prospective LCA for Electrochemical Reduction of CO2 to Formic Acid. *Environ. Sci. Technol.* **2019**, *53*, 12320–12329. https://doi.org/10.1021/acs.est.9b02944.
(102) Tufvesson, L. M.; Tufvesson, P.; Woodley, J. M.; Börjesson, P. Life Cycle Assessment in Green Chemistry: Overview of Key Parameters and Methodological Concerns. *Int. J. Life Cycle Assess.* **2013**, *18*, 431–444. https://doi.org/10.1007/s11367-012-0500-1.
(103) Benavides, P. T.; Lee, U.; Zarè-Mehrjerdi, O. Life Cycle Greenhouse Gas Emissions and Energy Use of Polylactic Acid, Bio-Derived Polyethylene, and Fossil-Derived Polyethylene. *J. Clean. Prod.* **2020**, *277*, 124010. https://doi.org/10.1016/j.jclepro.2020.124010.

(104) Suarez, A.; Ford, E.; Venditti, R.; Kelley, S.; Saloni, D.; Gonzalez, R. Is Sugarcane-Based Polyethylene a Good Alternative to Fight Climate Change? *J. Clean. Prod.* **2023**, *395*, 136432. https://doi.org/10.1016/j.jclepro.2023.136432.
(105) Ventura, S. P. M.; De Morais, P.; Coelho, J. A. S.; Sintra, T.; Coutinho, J. A. P.; Afonso, C. A. M. Evaluating the Toxicity of Biomass Derived Platform Chemicals. *Green Chem.* **2016**, *18*, 4733–4742. https://doi.org/10.1039/C6GC01211F.
(106) Zimmermann, L.; Dierkes, G.; Ternes, T. A.; Vö, C.; Wagner, M. Benchmarking the in Vitro Toxicity and Chemical Composition of Plastic Consumer Products. **2019**. https://doi.org/10.1021/acs.est.9b02293.
(107) Anastas, P. T.; Warner, J. C. *Green Chemistry: Theory and Practice*; Oxford University Press: Oxford [England], **1998**.
(108) Bonjour, O.; Liblikas, I.; Pehk, T.; Khai-Nghi, T.; Rissanen, K.; Vares, L.; Jannasch, P.; Jannasch, P. Rigid Biobased Polycarbonates with Good Processability Based on a Spirocyclic Diol Derived from Citric Acid. *Green Chem.* **2020**, *22*, 3940–3951. https://doi.org/10.1039/d0gc00849d.
(109) Kaljurand, I.; Kütt, A.; Sooväli, L.; Rodima, T.; Mäemets, V.; Leito, I.; Koppel, I. A. Extension of the Self-Consistent Spectrophotometric Basicity Scale in Acetonitrile to a Full Span of 28 PKa Units: Unification of Different Basicity Scales. *J. Org. Chem.* **2005**, *70*, 1019–1028. https://doi.org/10.1021/jo048252w.
(110) Allaoua, I.; Goi, B. E.; Obadia, M. M.; Debuigne, A.; Detrembleur, C.; Drockenmuller, E. (Co)Polymerization of Vinyl Levulinate by Cobalt-Mediated Radical Polymerization and Functionalization by Ketoxime Click Chemistry. *Polym. Chem.* **2014**, *5*, 2973–2979. https://doi.org/10.1039/C3PY01505J.
(111) Yakovleva, M. P.; Mingaleeva, G. R.; Denisova, K. S.; Ishmuratova, N. M.; Ishmuratov, G. Y. Synthesis of Optically Active Macrolides from L-Menthol. *Chem. Nat. Compd.* **2018**, *54*, 889–892. https://doi.org/10.1007/S10600-018-2505-X/METRICS.
(112) Ishmuratov, G. Y.; Vydrina, V. A.; Denisova, K. S.; Yakovleva, M. P.; Gazetdinov, R. R.; Vyrypaev, E. M.; Tolstikov, A. G. Synthesis from (-)-α-Pinene of an Optically Active Macrocyclic Diesterdihydrazide with 2,6-Pyridinedicarboxylic and Adipic Acid Moities. *Chem. Nat. Compd.* **2017**, *53*, 63–65. https://doi.org/10.1007/S10600-017-1912-8/METRICS.
(113) Clarke, C. J.; Tu, W. C.; Levers, O.; Bröhl, A.; Hallett, J. P. Green and Sustainable Solvents in Chemical Processes. *Chem. Rev.* **2018**, *118*, 747–800. https://doi.org/10.1021/acs.chemrev.7b00571.
(114) Roelfsema, M.; van Soest, H. L.; Harmsen, M.; van Vuuren, D. P.; Bertram, C.; den Elzen, M.; Höhne, N.; Iacobuta, G.; Krey, V.; Kriegler, E.; Luderer, G.; Riahi, K.; Ueckerdt, F.; Després, J.; Drouet, L.; Emmerling, J.; Frank, S.; Fricko, O.; Gidden, M.; Humpenöder, F.; Huppmann, D.; Fujimori, S.; Fragkiadakis, K.; Gi, K.; Keramidas, K.; Köberle, A. C.; Aleluia Reis, L.; Rochedo, P.; Schaeffer, R.; Oshiro, K.; Vrontisi, Z.; Chen, W.; Iyer, G. C.; Edmonds, J.; Kannavou, M.; Jiang, K.; Mathur, R.; Safonov, G.; Vishwanathan, S. S. Taking Stock of National Climate Policies to Evaluate Implementation of the Paris Agreement. *Nat. Commun. 2020 111* **2020**, *11*, 1–12. https://doi.org/10.1038/s41467-020-15414-6.
(115) Sacchi, R.; Terlouw, T.; Siala, K.; Dirnaichner, A.; Bauer, C.; Cox, B.; Mutel, C.; Daioglou, V.; Luderer, G. PRospective EnvironMental Impact AsSEment (Premise): A Streamlined Approach to Producing Databases for Prospective Life Cycle Assessment Using Integrated Assessment Models. *Renew. Sustain. Energy Rev.* **2022**, *160*, 112311. https://doi.org/10.1016/j.rser.2022.112311.

(116) *IPCC, 2013: Summary for Policymakers. In Climate Change 2013: The Physical Science Basis. Contribution of Working Group I to the Fifth Assessment Report of the Intergovernmental Panel on Climate Change*; Stocker, T. F., Qin, D., Plattner, G.-K., Tignor, M., Allen, S. K., Boschung, J., Nauels, A., Xia, Y., Bex, V., Midgley, P. M., Eds.; Cambridge University Press: Cambridge, United Kingdom and New York, NY, USA, 2014.
(117) Huijbregts, M. A. J.; Steinmann, Z. J. N.; Elshout, P. M. F.; Stam, G.; Verones, F.; Vieira, M.; Zijp, M.; Hollander, A.; van Zelm, R. ReCiPe2016: A Harmonised Life Cycle Impact Assessment Method at Midpoint and Endpoint Level. *Int. J. Life Cycle Assess.* **2017**, *22*, 138–147. https://doi.org/10.1007/s11367-016-1246-y.
(118) Nakajima, R.; Ogino, T.; Yokoshima, S.; Fukuyama, T. Total Synthesis of (-)-Mersicarpine. *J. Am. Chem. Soc.* **2010**, *132*, 1236–1237. https://doi.org/10.1021/ja9103233.

APPENDIX

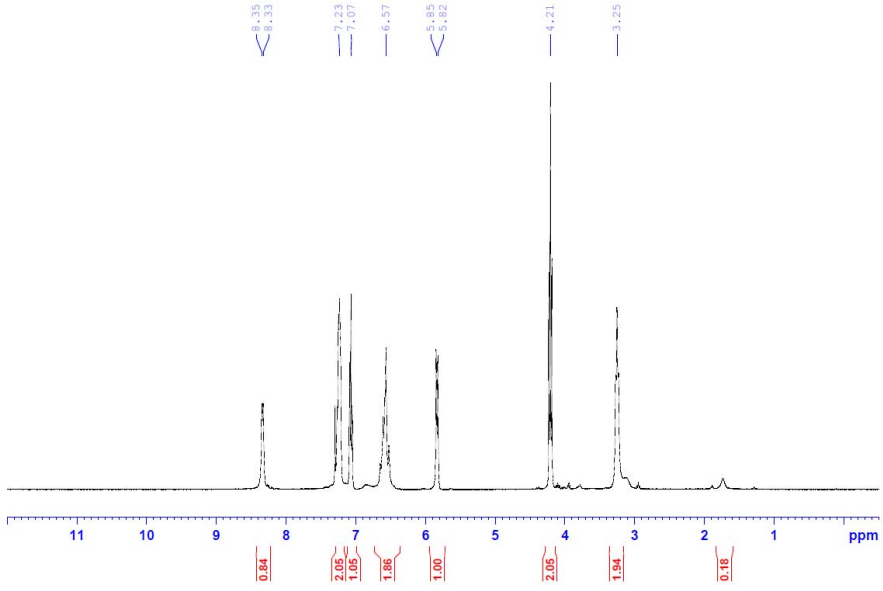

Figure A1. ^{1}H NMR spectrum of indoline acrylate measured in $CDCl_3$.

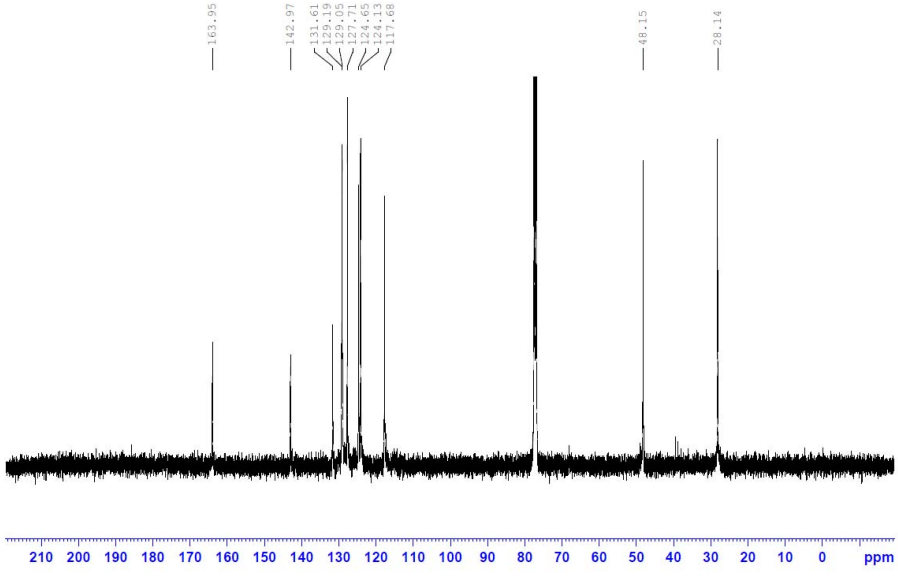

Figure A2. ^{13}C NMR spectrum of indoline acrylate measured in $CDCl_3$.

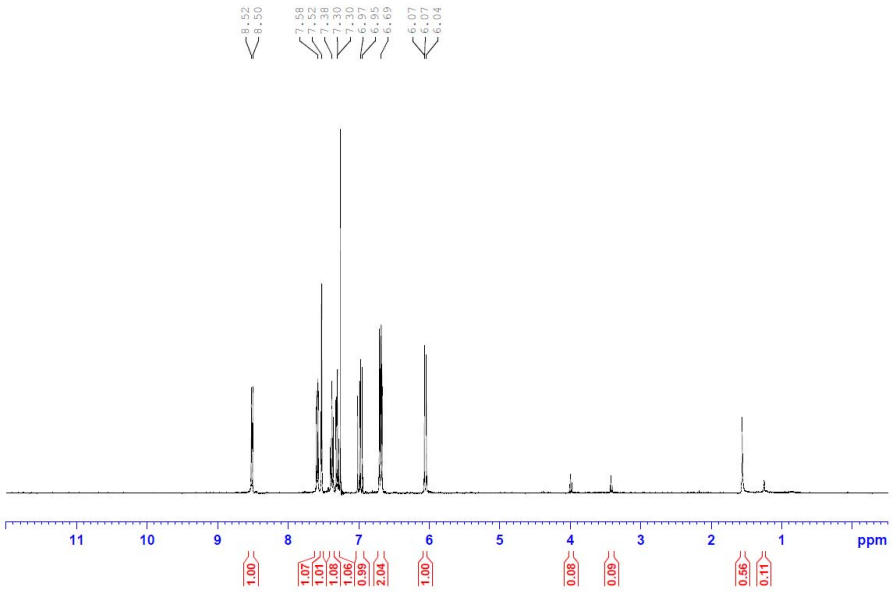

Figure A3. ^{1}H NMR spectrum of indole acrylate measured in $CDCl_3$.

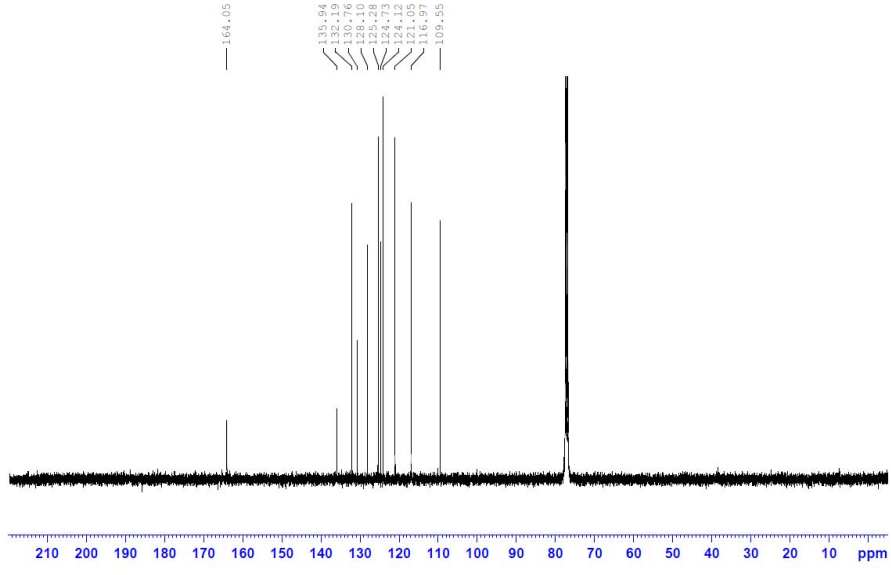

Figure A4. ^{13}C NMR spectrum of indole acrylate measured in $CDCl_3$.

ACKNOWLEDGEMENT

I would like to thank both of my supervisors, Lauri Vares and Patric Jannasch, for their continued support and advice through my years of PhD studies. We have had many insightful talks and meetings, where countless problems have been solved, which have helped me reach the end goal of graduation. Also, I would like to thank my previous supervisor Uno Mäeorg, who first introduced me to Lauri and was also involved with some projects during my PhD. Additionally, I would like to thank everyone who has been in the group during my time. This includes Siim, who helped me start out in the lab when I first started and who we worked together on my first article. I am also grateful for the help of Livia, Ilme and Alina, who I have collaborated with in articles and who have given good advice in general.

I would also like to thank everyone from Lund University who I had the opportunity to work with during my short time there. A special thanks goes to Olivier who helped me settle in in Lund, taught me to use the analysis apparatus and measured my countless samples during my PhD studies. Thanks to everyone else I have worked with or collaborated with, most notably Narie, who introduced me to LCA and helped us figure out the hotspots for our processes.

Finally, I would like to thank my family and friends for their support throughout the years and finding time for activities to get my mind off from writing articles when needed. Now you can stop asking when I am defending. I am especially grateful for the support of Elli who has seen up close what it is like to try and get to the defense of my PhD.

Thank you all!

PUBLICATIONS

CURRICULUM VITAE

Name: Rauno Sedrik
Date of birth: 11th September 1994
Citizenship: Estonian
Contact: Institute of Technology, University of Tartu
Nooruse 1, 50411, Tartu, Estonia
E-mail: rauno.sedrik@ut.ee

Education:

2019–…	University of Tartu, PhD studies in engineering and technology
2017–2019	University of Tartu, MSc in materials science
2013–2017	University of Tartu, BSc in materials science
2001–2013	Käina Gymnasium, Secondary education

Language skills:

Estonian	native language
English	excellent in speech and writing
Russian	intermediate in speech and writing

Professional employment:

2020–2024	University of Tartu, Institute of Technology, Junior Research Fellow in Polymer Chemistry

Scientific publications:

1. **Sedrik, R.**; Bonjour, O.; Laanesoo, S.; Liblikas, I.; Pehk, T.; Jannasch, P.; Vares, L. Chemically Recyclable Poly(β-Thioether Ester)s Based on Rigid Spirocyclic Ketal Diols Derived from Citric Acid. *Biomacromolecules* **2022**, 23, 2685–2696.
2. Matt, L.; **Sedrik, R.**; Bonjour, O.; Vasiliauskaité, M.; Jannasch, P.; Vares, L. Covalent Adaptable Polymethacrylate Networks by Hydrazide Crosslinking Via Isosorbide Levulinate Side Groups. *ACS Sustain. Chem. Eng.* **2023**, 11, 8294–8307.
3. de Souza, N. R. D.; Matt, L.; **Sedrik, R.**; Vares, L.; Cherubini, F. Integrating Ex-Ante and Prospective Life-Cycle Assessment for Advancing the Environmental Impact Analysis of Emerging Bio-Based Technologies. *Sustain. Prod. Consum.* **2023**, 43, 319–332.
4. Laanesoo, S.; Bonjour, O.; **Sedrik, R.**; Tamsalu, I.; Jannasch, P.; Vares, L. Combining Isosorbide and Lignin-Related Benzoic Acids for High-T_g Polymethacrylates. *Eur. Polym. J.* **2024**, 202, 112595.

5. **Sedrik, R.**; Bonjour, O.; de Souza, N. R. D.; Ismagilova, A.; Tamsalu, I.; Kisand, V.; Cherubini, F.; Jannasch, P.; Vares, L. Aromatic Polymethacrylates from Lignin-Based Feedstock: Synthesis, Thermal Properties, Life-Cycle Assessment and Toxicity. *ChemSusChem* **2024**, e202401239.
6. Tarasova, E.; Savale, N.; Trifonova, L.; Krasnou, I.; Reile, I.; Kudrjašova, M.; Mere, A.; Kaljuvee, T.; Mikli, V.; **Sedrik, R.**; Krumme, A. Effect of Green Co-Solvents on Properties and Synthesis of Cellulose Esters in Superbase Ionic Liquid. *Cellulose* **2024**, 31.

Research grants and scholarships:

2022 Dora Plus mobility grant for doctoral student mobility by Archimedes (for laboratory work in Lund University)

Additional scientific activities:

2022 Mar.–May

Visiting PhD student at Polymer Science and Technology group (supervisor prof. Patric Jannasch), Lund University, Lund, Sweden

ELULOOKIRJELDUS

Nimi: Rauno Sedrik
Sünniaeg: 11. september 1994
Kodakondsus: Eesti
Kontakt: Tehnoloogiainstituut, Tartu Ülikool
Nooruse 1, 50411, Tartu, Eesti
E-mail: rauno.sedrik@ut.ee

Haridus:

2019–…	Tartu Ülikool, doktorantuur (tehnika ja tehnoloogia)
2017–2019	Tartu Ülikool, magistriõpe (materjaliteadus)
2013–2017	Tartu Ülikool, bakalaureuseõpe (materjaliteadus)
2001–2013	Käina Gümnaasium, keskharidus

Keeleoskus:

eesti keel	emakeel
inglise keel	väga hea kõnes ja kirjas
vene keel	kesktase kõnes ja kirjas

Teenistuskäik:

2018–2024	Tartu Ülikool, Tehnoloogiainstituut, nooremteadur

Teaduspublikatsioonid ja patendiavaldused:

1. **Sedrik, R.**; Bonjour, O.; Laanesoo, S.; Liblikas, I.; Pehk, T.; Jannasch, P.; Vares, L. Chemically Recyclable Poly(β-Thioether Ester)s Based on Rigid Spirocyclic Ketal Diols Derived from Citric Acid. *Biomacromolecules* **2022**, 23, 2685–2696.
2. Matt, L.; **Sedrik, R.**; Bonjour, O.; Vasiliauskaité, M.; Jannasch, P.; Vares, L. Covalent Adaptable Polymethacrylate Networks by Hydrazide Crosslinking Via Isosorbide Levulinate Side Groups. *ACS Sustain. Chem. Eng.* **2023**, 11, 8294–8307.
3. de Souza, N. R. D.; Matt, L.; **Sedrik, R.**; Vares, L.; Cherubini, F. Integrating Ex-Ante and Prospective Life-Cycle Assessment for Advancing the Environmental Impact Analysis of Emerging Bio-Based Technologies. *Sustain. Prod. Consum.* **2023**, 43, 319–332.
4. Laanesoo, S.; Bonjour, O.; **Sedrik, R.**; Tamsalu, I.; Jannasch, P.; Vares, L. Combining Isosorbide and Lignin-Related Benzoic Acids for High-T_g Polymethacrylates. *Eur. Polym. J.* **2024**, 202, 112595.

5. **Sedrik, R.**; Bonjour, O.; de Souza, N. R. D.; Ismagilova, A.; Tamsalu, I.; Kisand, V.; Cherubini, F.; Jannasch, P.; Vares, L. Aromatic Polymethacrylates from Lignin-Based Feedstock: Synthesis, Thermal Properties, Life-Cycle Assessment and Toxicity. *ChemSusChem* **2024**, e202401239.
6. Tarasova, E.; Savale, N.; Trifonova, L.; Krasnou, I.; Reile, I.; Kudrjašova, M.; Mere, A.; Kaljuvee, T.; Mikli, V.; **Sedrik, R.**; Krumme, A. Effect of Green Co-Solvents on Properties and Synthesis of Cellulose Esters in Superbase Ionic Liquid. *Cellulose* **2024**, 31.

Tunnustused ja stipendiumid:

2022 Dora Pluss doktorantide mobiilsusgrant (laboripraktikaks Lundi Ülikoolis), väljaandja SA Archimedes

Muu teadustegevus:

2022 märts – mai
Külalisdoktorant *Polymer Science and Technology* uurimisgrupis (juhendaja professor Patric Jannasch), Lundi Ülikool, Lund, Rootsi

DISSERTATIONES TECHNOLOGIAE UNIVERSITATIS TARTUENSIS

1. **Imre Mäger**. Characterization of cell-penetrating peptides: Assessment of cellular internalization kinetics, mechanisms and bioactivity. Tartu 2011, 132 p.
2. **Taavi Lehto**. Delivery of nucleic acids by cell-penetrating peptides: application in modulation of gene expression. Tartu 2011, 155 p.
3. **Hannes Luidalepp**. Studies on the antibiotic susceptibility of *Escherichia coli*. Tartu 2012, 111 p.
4. **Vahur Zadin**. Modelling the 3D-microbattery. Tartu 2012, 149 p.
5. **Janno Torop**. Carbide-derived carbon-based electromechanical actuators. Tartu 2012, 113 p.
6. **Julia Suhorutšenko**. Cell-penetrating peptides: cytotoxicity, immunogenicity and application for tumor targeting. Tartu 2012, 139 p.
7. **Viktoryia Shyp**. G nucleotide regulation of translational GTPases and the stringent response factor RelA. Tartu 2012, 105 p.
8. **Mardo Kõivomägi**. Studies on the substrate specificity and multisite phosphorylation mechanisms of cyclin-dependent kinase Cdk1 in *Saccharomyces cerevisiae*. Tartu, 2013, 157 p.
9. **Liis Karo-Astover**. Studies on the Semliki Forest virus replicase protein nsP1. Tartu, 2013, 113 p.
10. **Piret Arukuusk**. NickFects–novel cell-penetrating peptides. Design and uptake mechanism. Tartu, 2013, 124 p.
11. **Piret Villo**. Synthesis of acetogenin analogues. Asymmetric transfer hydrogenation coupled with dynamic kinetic resolution of α-amido-β-keto esters. Tartu, 2013, 151 p.
12. **Villu Kasari**. Bacterial toxin-antitoxin systems: transcriptional cross-activation and characterization of a novel *mqsRA* system. Tartu, 2013, 108 p.
13. **Margus Varjak**. Functional analysis of viral and host components of alphavirus replicase complexes. Tartu, 2013, 151 p.
14. **Liane Viru**. Development and analysis of novel alphavirus-based multifunctional gene therapy and expression systems. Tartu, 2013, 113 p.
15. **Kent Langel**. Cell-penetrating peptide mechanism studies: from peptides to cargo delivery. Tartu, 2014, 115 p.
16. **Rauno Temmer**. Electrochemistry and novel applications of chemically synthesized conductive polymer electrodes. Tartu, 2014, 206 p.
17. **Indrek Must**. Ionic and capacitive electroactive laminates with carbonaceous electrodes as sensors and energy harvesters. Tartu, 2014, 133 p.
18. **Veiko Voolaid**. Aquatic environment: primary reservoir, link, or sink of antibiotic resistance? Tartu, 2014, 79 p.
19. **Kristiina Laanemets**. The role of SLAC1 anion channel and its upstream regulators in stomatal opening and closure of *Arabidopsis thaliana.* Tartu, 2015, 115 p.

20. **Kalle Pärn**. Studies on inducible alphavirus-based antitumour strategy mediated by site-specific delivery with activatable cell-penetrating peptides. Tartu, 2015, 139 p.
21. **Anastasia Selyutina**. When biologist meets chemist: a search for HIV-1 inhibitors. Tartu, 2015, 172 p.
22. **Sirle Saul**. Towards understanding the neurovirulence of Semliki Forest virus. Tartu, 2015, 136 p.
23. **Marit Orav**. Study of the initial amplification of the human papillomavirus genome. Tartu, 2015, 132 p.
24. **Tormi Reinson**. Studies on the Genome Replication of Human Papillomaviruses. Tartu, 2016, 110 p.
25. **Mart Ustav Jr**. Molecular Studies of HPV-18 Genome Segregation and Stable Replication. Tartu, 2016, 152 p.
26. **Margit Mutso**. Different Approaches to Counteracting Hepatitis C Virus and Chikungunya Virus Infections. Tartu, 2016, 184 p.
27. **Jelizaveta Geimanen**. Study of the Papillomavirus Genome Replication and Segregation. Tartu, 2016, 168 p.
28. **Mart Toots**. Novel Means to Target Human Papillomavirus Infection. Tartu, 2016, 173 p.
29. **Kadi-Liis Veiman**. Development of cell-penetrating peptides for gene delivery: from transfection in cell cultures to induction of gene expression *in vivo*. Tartu, 2016, 136 p.
30. **Ly Pärnaste**. How, why, what and where: Mechanisms behind CPP/cargo nanocomplexes. Tartu, 2016, 147 p.
31. **Age Utt**. Role of alphavirus replicase in viral RNA synthesis, virus-induced cytotoxicity and recognition of viral infections in host cells. Tartu, 2016, 183 p.
32. **Veiko Vunder**. Modeling and characterization of back-relaxation of ionic electroactive polymer actuators. Tartu, 2016, 154 p.
33. **Piia Kivipõld**. Studies on the Role of Papillomavirus E2 Proteins in Virus DNA Replication. Tartu, 2016, 118 p.
34. **Liina Jakobson**. The roles of abscisic acid, CO_2, and the cuticle in the regulation of plant transpiration. Tartu, 2017, 162 p.
35. **Helen Isok-Paas**. Viral-host interactions in the life cycle of human papillomaviruses. Tartu, 2017, 158 p.
36. **Hanna Hõrak**. Identification of key regulators of stomatal CO_2 signalling via O_3-sensitivity. Tartu, 2017, 260 p.
37. **Jekaterina Jevtuševskaja**. Application of isothermal amplification methods for detection of *Chlamydia trachomatis* directly from biological samples. Tartu, 2017, 96 p.
38. **Ülar Allas**. Ribosome-targeting antibiotics and mechanisms of antibiotic resistance. Tartu, 2017, 152 p.
39. **Anton Paier**. Ribosome Degradation in Living Bacteria. Tartu, 2017, 108 p.
40. **Vallo Varik**. Stringent Response in Bacterial Growth and Survival. Tartu, 2017, 101 p.

41. **Pavel Kudrin**. In search for the inhibitors of *Escherichia coli* stringent response factor RelA. Tartu, 2017, 138 p.
42. **Liisi Henno**. Study of the human papillomavirus genome replication and oligomer generation. Tartu, 2017, 144 p.
43. **Katrin Krõlov**. Nucleic acid amplification from crude clinical samples exemplified by *Chlamydia trachomatis* detection in urine. Tartu, 2018, 118 p.
44. **Eve Sankovski**. Studies on papillomavirus transcription and regulatory protein E2. Tartu, 2018, 113 p.
45. **Morteza Daneshmand**. Realistic 3D Virtual Fitting Room. Tartu, 2018, 233 p.
46. **Fatemeh Noroozi**. Multimodal Emotion Recognition Based Human-Robot Interaction Enhancement. Tartu, 2018, 113 p.
47. **Krista Freimann**. Design of peptide-based vector for nucleic acid delivery in vivo. Tartu, 2018, 103 p.
48. **Rainis Venta**. Studies on signal processing by multisite phosphorylation pathways of the *S. cerevisiae* cyclin-dependent kinase inhibitor Sic1. Tartu, 2018, 155 p.
49. **Inga Põldsalu**. Soft actuators with ink-jet printed electrodes. Tartu, 2018, 85 p.
50. **Kadri Künnapuu**. Modification of the cell-penetrating peptide PepFect14 for targeted tumor gene delivery and reduced toxicity. Tartu, 2018, 114 p.
51. **Toomas Mets**. RNA fragmentation by MazF and MqsR toxins of *Escherichia coli.* Tartu, 2019, 119 p.
52. **Kadri Tõldsepp**. The role of mitogen-activated protein kinases MPK4 and MPK12 in CO_2-induced stomatal movements. Tartu, 2019, 259 p.
53. **Pirko Jalakas**. Unravelling signalling pathways contributing to stomatal conductance and responsiveness. Tartu, 2019, 120 p.
54. **S. Sunjai Nakshatharan**. Electromechanical modelling and control of ionic electroactive polymer actuators. Tartu, 2019, 165 p.
55. **Eva-Maria Tombak**. Molecular studies of the initial amplification of the oncogenic human papillomavirus and closely related nonhuman primate papillomavirus genomes. Tartu, 2019, 150 p.
56. **Meeri Visnapuu**. Design and physico-chemical characterization of metal-containing nanoparticles for antimicrobial coatings. Tartu, 2019, 138 p.
57. **Jelena Beljantseva**. Small fine-tuners of the bacterial stringent response – a glimpse into the working principles of Small Alarmone Synthetases. Tartu, 2020, 104 p.
58. **Egon Urgard**. Potential therapeutic approaches for modulation of inflammatory response pathways. Tartu, 2020, 120 p.
59. **Sofia Raquel Alves Oliveira**. HPLC analysis of bacterial alarmone nucleotide (p)ppGpp and its toxic analogue ppApp. Tartu, 2020, 122 p.
60. **Mihkel Örd**. Ordering the phosphorylation of cyclin-dependent kinase Cdk1 substrates in the cell cycle. Tartu, 2021, 228 p.
61. **Fred Elhi**. Biocompatible ionic electromechanically active polymer actuator based on biopolymers and non-toxic ionic liquids. Tartu, 2021, 140 p.

62. **Liisi Talas**. Reconstructing paleo-diversity, dynamics and response of eukaryotes to environmental change over the Late-Glacial and Holocene period in lake Lielais Svētiņu using sedaDNA. Tartu, 2021, 118 p.
63. **Livia Matt**. Novel isosorbide-based polymers. Tartu, 2021, 118 p.
64. **Koit Aasumets**. The dynamics of human mitochondrial nucleoids within the mitochondrial network. Tartu, 2021, 104 p.
65. **Faiza Summer**. Development and optimization of flow electrode capacitor technology. Tartu, 2022, 109 p.
66. **Olavi Reinsalu**. Cancer-testis antigen MAGE-A4 is incorporated into extracellular vesiclesand is exposed to the surface. Tartu, 2022, 130 p.
67. **Tetiana Brodiazhenko**. RelA-SpoT Homolog enzymes as effectors of Toxin-Antitoxin systems. Tartu, 2022, 132 p.
68. **Georg-Marten Lanno**. Development of novel antibacterial drug delivery systems as wound scaffolds using electrospinning technology. Tartu, 2022, 175 p.
69. **Liubov Cherkashchenko**. New insights into alphaviral nsP2 functions. Tartu, 2023, 171 p.
70. **Kristina Kiisholts**. Peptide-based drug carriers and preclinical nanomedicine applications for endometriosis treatment. Tartu, 2023, 138 p.
71. **Kai Rausalu**. Alphaviral nsP2 protease: From requirements for functionality to inhibition. Tartu, 2023, 175 p.
72. **Laura Sandra Lello**. Unraveling the intricate nature of the alphavirus RNA replicase. Tartu, 2023, 219 p.
73. **Houman Masnavi**. Visibility Aware Navigation. Tartu, 2023, 180 p.
74. **Kadir Aktas**. Cosmic Ray Tomography based Object Reconstruction and Recognition. Tartu, 2023, 104 p.
75. **Egils Avots**. Brain abnormality detection using statistical analysis of individual structural connectivity networks and EEG signals. Tartu, 2023, 223 p.
76. **Sainan Wang**. Structure-guided insights into the functions of CHIKV nsP2. Tartu, 2024, 154 p.
77. **Anneli Samel**. Unveiling the characteristics of cancer-testis antigen MAGEA10. Tartu, 2024, 136 p.
78. **Ikechukwu Ofodile**. Fault tolerant attitude control for nanosatellites: ESTCube-2 case. Tartu, 2024, 130 p.
79. **Olena Zamora**. Impacts of plant hormones on controlling stomatal conductance. Tartu, 2024, 166 p.
80. **Mariliis Hinnu**. *In vitro* methods for studying the mechanisms of ribosome-targeting antibiotics. Tartu, 2024, 143 p.
81. **Chung-Yueh Yeh**. Characterization of MPK and HT1 kinases in CO_2-induced stomatal movements. Tartu, 2024, 118 p.
82. **Iman Dadras**. Low power neural network-based control and actuation solutions for insect-scale robots. Tartu, 2024, 149 p.
83. **Fatemeh Rastgar**. Towards reliable real-time trajectory optimization. Tartu, 2024, 158 p.

84. **Maria Maloverjan**. Optimizing cell-penetrating peptide-based nanoparticles for delivery of nucleic acid therapeutics. Tartu, 2024, 172 p.
85. **Joonas Merisalu**. Resistive switching in memristor structures with multilayer dielectrics. Tartu, 2024, 149 p.
86. **Siim Laanesoo**. Novel high-performance biomass-based polymers. Tartu, 2024, 117 p.
87. **Henri Ingelman**. Systems-level characterisation and improvement of *Clostridium autoethanogenum* metabolism. Tartu, 2024, 164 p.
88. **Mailis Laht**. Using the One Health approach for mapping the spread of antibiotic resistant bacteria in Estonia. Tartu, 2024, 188 p.
89. **Ingrid Rebane**. Structure-property relationships of moldable silicone foams. Tartu, 2024, 164 p.
90. **Robert Valner**. Design of TeMoto, a software framework for dependable, adaptive, and collaborative autonomous robots. Tartu, 2024, 182 p.
91. **Kristiina Kurg**. Exploring the potential of a liquid biopsy approach for melanoma diagnostics and the role of extracellular vesicles in atherosclerosis development. Tartu, 2025, 201 p.